Date of issue: November 24, 2010

The Mextram Bipolar Transistor Model

level 504.9

R. van der Toorn, J.C.J. Paasschens, and W.J. Kloosterman

Mextram definition document

Authors' address data: R. van der Toorn;
e-mail: R.vanderToorn@tudelft.nl
http://mextram.ewi.tudelft.nl

Keywords: Mextram, compact modelling, bipolar transistors, large-signal modelling, distortion modelling, circuit simulation, semiconductor technology, integrated circuits

Abstract: This document presents the definition of the CMC world stardard model Mextram, for vertical bipolar transistors.

The goal of this document is to present the full definition of the model, including the parameter set, the equivalent circuit and all the equations for currents, charges and noise sources.

Apart from the definition also an introduction into the physical background is given. We have given also a very basic parameter extraction procedure. Both the background and the parameter extraction are documented separately in dedicated documents.

The transition from Mextram 503 to Mextram 504 is described, to enable the translation of a 503 parameter-set to a 504 parameter-set. At last we have given some numerical examples that can act as a test of implementation.

Preface

October 2004 The Mextram bipolar transistor model has been put in the public domain in Januari 1994. At that time level 503, version 1 of Mextram was used within Koninklijke Philips Electronics N.V. In June 1995 version 503.2 was released which contained some improvements.

Mextram level 504 contains a complete review of the Mextram model. The preliminary version has been completed in June 2000. This report documents version 504.5.

October 2004, J.P.

March 2005 In the fall of 2004, Mextram was elected as a world standard transistor model by the *Compact Model Council (CMC)*, a consortium of representatives from over 20 major semiconductor manufacturers.

This report documents version 504.6.

March 2005, RvdT.

Spring 2008 In 2007, the notion of flexible topology was introduced by the community of compact model developers and model implementation specialists. In the spring 2008 release of Mextram, this was used to extend the topology of Mextram and add the distribution of the collector resistance in a backwards compatible manner.

This report documents version 504.7.

Spring 2008, RvdT.

Q4 2008, Q1 2009 This document presents version 504.8, which adds a model for Zener tunneling currents in the Emitter base junction.

Q4 2009 – Q1 2010 This document presents version 504.9, which extends collector-substrate modelling capabilities.

2009 – 2010, RvdT.

History of model and documentation

June 2000 : Release of Mextram level 504 (preliminary version)
Complete review of the model compared to Mextram level 503

April 2001 : Release of Mextram 504, version 0 (504.0)
Small fixes:
– Parameters R_{th} and C_{th} added to MULT-scaling
– Expression for α in Eq. (4.219) fixed
Changes w.r.t. June 2000 version:
– Addition of overlap capacitances C_{BEO} and C_{BCO}

– Change in temperature scaling of diffusion voltages
– Change in neutral base recombination current (4.178)
– Addition of numerical examples with self-heating

September 2001 : Release of Mextram 504, version 1 (504.1)
Lower bound on $\mathsf{R_{th}}$ is now $0°\mathrm{C/W}$
Small changes in F_{ex} (4.166) and $Q_{B_1B_2}$ (4.173) to enhance robustness

March 2002 : Release of Mextram 504, version 2 (504.2)
Numerical stability improvement of x_i/W_{epi} at small $\mathcal{V}_{\mathrm{C_1C_2}}$, p. 48
Numerical stability improvement of p_0^*, Eq. (4.201)

December 2002 : Minor changes in documentation, not in model

October 2003 : Release of Mextram 504, version 3 (504.3)
MULT has been moved in list of parameters
Lower clipping value of $\mathsf{T_{ref}}$ changed to $-273°\mathrm{C}$
Added I_C, I_B and β_{dc} to operating point information

April 2004 : Release of Mextram 504, version 4 (504.4)
Noise of collector epilayer has been removed [originally Eq. (4.183)].

October 2004 : Release of Mextram 504, version 5 (504.5)
Addition of temperature dependence of thermal resistance
Addition of noise due to avalanche current

March 2005 : Release of Mextram 504, version 6 (504.6)
Added parameter $\mathsf{dA_{Is}}$ for fine tuning of temp. dep. of $\mathsf{I_{sT}}$; eqn. (4.37)
"$G_{\mathrm{EM}} = 0$" added to equation (4.68)
Upper clipping value 1.0 of $\mathsf{K_{avl}}$ introduced

March 2008 : Release of Mextram 504, version 7 (504.7)
Added resistances of buried layer $\mathsf{R_{Cblx}}$and $\mathsf{R_{Cbli}}$, and their temperature scaling parameter $\mathsf{A_{Cbl}}$.
Lower clipping value of resistances $\mathsf{R_E}$, $\mathsf{R_{BC}}$, $\mathsf{R_{BV}}$, $\mathsf{R_{Cc}}$, $\mathsf{R_{Cv}}$, $\mathsf{SCR_{Cv}}$ increased to $1\mathrm{m}\Omega$
Bug fix high temperature limit B_{nT} .

June 2009 : Release of Mextram 504, version 8 (504.8),
Zener tunneling current in emitter-base junction:
– Sections: 2.1.4, 3, 4.8.5, 4.16
– Parameters: $\mathsf{I_{zEB}}$, $\mathsf{N_{zEB}}$
– Material constants, implemented as parameters: $\mathsf{V_{gzEB}}$, $\mathsf{A_{VgEB}}$, T_{VgEB}
– Equations: (4.51b) to (4.51e), (4.117a), (4.185), (4.193)
– OP-info: $g_{\pi,x}$, I_{ztEB}

Q2 2010 : Release of Mextram 504, version 9 (504.9),
Small Fix w.r.t. 504.8:
– added lower clip value to parameter T_{VgEB} (§4.3)
Added to operating point information:
– external terminal voltages V_{BE}, V_{BC}, V_{CE}, V_{SE}, V_{BS}, V_{SC}
– external terminal currents I_E, I_S
Collector-substrate model:
– Parameters: $\mathsf{I_{CSs}}$, $\mathsf{A_{sub}}$
– physics based temperature scaling ideal collector-substrate current
– See: § 2.3.5, § 2.6.1, § 4.6, Eqns. (4.44), (4.64)

Contents

1 Introduction

Mextram is an advanced compact model for the description of bipolar transistors. It contains many features that the widely-used Gummel-Poon model lacks. Mextram can be used for advanced processes like double-poly or even SiGe transistors, for high-voltage power devices, and even for uncommon situations like lateral NPN-transistors in LDMOS technology.

Mextram level 503 has been put in the public domain [1] by Koninklijke Philips Electronics N.V. in 1994. Since the model update of 1995 it had been unchanged. A successor, Mextram level 504, was developed in the late nineties of the 20th century for several reasons, the main ones being the need for even better description of transistor characteristics and the need for an easier parameter extraction. In the fall of 2004, Mextram was elected as a world standard transistor model by the *Compact Model Council (CMC)*, a consortium of representatives from over 20 major semiconductor manufacturers.

The goal of this document is to give the model definition of Mextram 504. Since especially section 4 is also meant as an implementation guide, the structure of our presentation will be more along the lines of implemented code than structured in a didactical way. But we have also added an introduction of the physics behind the model and an introduction to the parameter extraction. These latter two are more extensively documented in separate reports [2, 3]. An introduction into the usage of Mextram 504 can be found in Ref. [4].

The improved description of transistor characteristics of Mextram 504 compared to Mextram 503 were achieved by changing some of the formulations of the model. For instance Mextram 504 contains the Early voltages as separate parameters, whereas in Mextram 503 they were calculated from other parameters. This is needed for the description of SiGe processes and improves the parameter extraction (and hence the description) in the case of normal transistors. An even more important improvement is the description of the epilayer. Although the physical description has not changed, the order in which some of the equations are used to get compact model formulations has been modified. The result is a much smoother behaviour of the model characteristics, i.e. the model formulations are now such that the first and higher-order derivatives are better. This is important for the output-characteristics and cut-off frequency, but also for (low-frequency) third order harmonic distortion. For the same reason of smoothness some other formulations, like that of the depletion capacitances, have been changed.

In Mextram almost all of the parameters have a physical meaning. This has been used in Mextram 503 to relate different parts of the model to each other by using the same parameters. Although this is the most physical way to go, it makes it difficult to do parameter extraction, since some parameters have an influence on more than one physical effect. Therefore we tried in Mextram 504 to remove as much of this interdependence as possible, without losing the physical basis of the model. To do this we added some extra parameters. At the same time we removed some parameters of Mextram 503 that were introduced long ago but which had a limited influence on the characteristics, and were therefore difficult to extract.

The complete Mextram model has been thoroughly revised. Many of the formulations

have been changed although not all changes where large. Also the documentation of the model is being extended. In this document an overview is given of the various features of the level 504 version of the Mextram model.

In Sec. 2 an introduction is given of the physical basis of the model. The transistor parameters are discussed in the relevant sections. More information about the usage of Mextram can be found in Ref. [4] More information about the physical background is given in Ref. [2].

Most of the parameters can be extracted from capacitance, DC and S-parameter measurements and are process and transistor layout (geometry) dependent. Initial/predictive parameter sets can be computed from process and layout data. Parameter extraction is shortly discussed in Sec. 3. More information can be found in Ref. [3]. The translation of Mextram 503 parameters to Mextram 504 parameters is discussed in Sec. 5.

The precise model description is given in Sec. 4. The model equations are all explicit functions of internal branch voltages and therefore no internal quantities have to be solved iteratively. As a help for the implementation, numerical examples are given in Sec. 6.

1.1 Survey of modelled effects

Mextram contains descriptions for the following effects:

- Bias-dependent Early effect
- Low-level non-ideal base currents
- High-injection effects
- Ohmic resistance of the epilayer
- Velocity saturation effects on the resistance of the epilayer
- Hard and quasi-saturation (including Kirk effect)
- Weak avalanche in the collector-base junction (optionally including snap-back behaviour)
- Zener-tunneling current in the emitter-base junction
- Charge storage effects
- Split base-collector and base-emitter depletion capacitance
- Substrate effects and parasitic PNP
- Explicit modelling of inactive regions
- Current crowding and conductivity modulation of the base resistance
- First order approximation of distributed high frequency effects in the intrinsic base (high-frequency current crowding and excess phase-shift)
- Recombination in the base (meant for SiGe transistors)
- Early effect in the case of a graded bandgap (meant for SiGe transistors)

- Temperature scaling
- Self-heating
- Thermal noise, shot noise and $1/f$-noise

Mextram does not contain extensive geometrical or process scaling rules (only a multiplication factor to put transistors in parallel). The model is well scalable, however, especially since it contains descriptions for the various intrinsic and extrinsic regions of the transistor.

Some parts of the model are optional and can be switched on or off by setting flags. These are the extended modelling of reverse behaviour, the distributed high-frequency effects, and the increase of the avalanche current when the current density in the epilayer exceeds the doping level.

Besides the NPN transistor also a PNP model description is available. Both three-terminal devices (discrete transistors) and four-terminal devices (IC-processes which also have a substrate) can be described.

2 Physical description of the model

In this section we introduce the physical origins of the Mextram model. Extensive documentation is given in Ref. [2]. Some experience with the Gummel-Poon model [5] will help, since we are not able to give all the basic derivations. Even then, for some parts of the model we can only give an idea of where the equations come from, without giving a detailed overview.

Mextram, as any other bipolar compact model, describes the various currents and charges that form the equivalent circuit, given in Fig. 1 on page 35. In tables 1 and 2 we have given a list of the currents and charges of this equivalent circuit. For every current and charge in this equivalent circuit we will give a description. We will first describe the active transistor. This is the intrinsic part of the transistor, which is also modelled by the Gummel-Poon model. Next we will discuss the extrinsic regions.

To improve the clarity of the different formulas we used different typografic fonts. For parameters we use a sans-serif font, e.g. $\mathsf{V_{dE}}$ and $\mathsf{R_{Cv}}$. A list of all parameters is given in section 4.3. For the node-voltages as given by the circuit simulator we use a calligrafic $\mathcal{V}$, e.g. $\mathcal{V}_{\mathrm{B_2E_1}}$ and $\mathcal{V}_{\mathrm{B_2C_2}}$. All other quantities are in normal (italic) font, like $I_{C_1C_2}$ and $V^*_{B_2C_2}$.

2.1 Active transistor

2.1.1 Main current

In the Mextram model the generalisation of the Moll-Ross relation [6, 7], better known as the integral charge control relation (ICCR) [8], is used to take into account the influence of the depletion charges Q_{t_E} and Q_{t_C} and the diffusion charges Q_{BE} and Q_{BC} on the main current. The basic relation is*

$$I_N = \mathsf{I_s}\left(e^{\mathcal{V}_{\mathrm{B_2E_1}}/V_T} - e^{V^*_{B_2C_2}/V_T}\right)\frac{1}{q_B}. \tag{2.1}$$

The thermal voltage is as always $V_T = kT/q$. (In table 3 we have given a list of various physical transistor quantities.) The normalized base charge is something like

$$q_B = \frac{Q_{B0} + Q_{t_E} + Q_{t_C} + Q_{BE} + Q_{BC}}{Q_{B0}}, \tag{2.2}$$

where Q_{B0} is the base charge at zero bias. This normalized base charge can be given as a product of the Early effect (describing the variation of the base width given by the depletion charges) and a term which includes high injection effects. The Early effect term is

$$q_1 = \frac{Q_{B0} + Q_{t_E} + Q_{t_C}}{Q_{B0}} = 1 + \frac{V_{t_E}(\mathcal{V}_{\mathrm{B_2E_1}})}{\mathsf{V_{er}}} + \frac{V_{t_C}(\mathcal{V}_{\mathrm{B_2C_1}}, I_{C_1C_2})}{\mathsf{V_{ef}}}. \tag{2.3}$$

*Note that $V^*_{B_2C_2}$ is a calculated quantity and not the node voltage $\mathcal{V}_{\mathrm{B_2C_2}}$. For its interpretation the difference is not very important, but for the smoothness of the model it is. See Sec. 2.2.

Table 1: *The currents of the equivalent circuit given in Fig. 1 on page 35.*

Currents	
I_N	Main current
$I_{C_1C_2}$	Epilayer current
$I_{B_1B_2}$	Pinched-base current
$I^S_{B_1}$	Ideal side-wall base current
I_{B_1}	Ideal forward base current
I_{B_2}	Non-ideal forward base current
I_{B_3}	Non-ideal reverse base current
$I_{\rm avl}$	Avalanche current
$I_{\rm ex}$	Extrinsic reverse base current
$XI_{\rm ex}$	Extrinsic reverse base current
$I_{\rm sub}$	Substrate current
$XI_{\rm sub}$	Substrate current
$I_{\rm Sf}$	Substrate failure current

The voltages V_{t_E} and V_{t_C} describe the curvature of the depletion charges as function of junction biases, but not their magnitude: $Q_{t_E} = (1 - \mathsf{XC_{jE}}) \cdot \mathsf{C_{jE}} \cdot V_{t_E}$ and $Q_{t_C} = \mathsf{XC_{jc}} \cdot \mathsf{C_{jc}} \cdot V_{t_C}$ (see section 2.1.5 and 2.1.6). The total normalized base charge is

$$q_B = q_1 \, (1 + \tfrac{1}{2} n_0 + \tfrac{1}{2} n_B), \tag{2.4}$$

where n_0 and n_B are the electron densities in the base at the emitter edge and at the collector edge. Both are normalized to the (average) base doping. These densities directly depend on the internal junction voltages $\mathcal{V}_{\rm B_2E_1}$ and $V^*_{B_2C_2}$, and can be found by considering the pn product at both junctions. They also include high injection effects in the base for which we have a single knee current $\mathsf{I_k}$.

The following parameters are involved:

$\mathsf{I_s}$	The transistor main saturation current
$\mathsf{I_k}$	The knee current for high injection effects in the base
$\mathsf{V_{ef}}$ and $\mathsf{V_{er}}$	The forward and reverse Early voltages

The parameters for the charges will be discussed later.

2.1.2 Ideal forward base current

The ideal forward base current is defined in the usual way. The total base current has a bottom and a sidewall contribution. The separation is given by the factor $\mathsf{XI_{B_1}}$. This factor can be determined by analysing the maximum current gain of transistors with different geometries.

$$I_{B_1} = (1 - \mathsf{XI_{B_1}}) \, \frac{\mathsf{I_s}}{\mathsf{\beta_f}} \, \left(e^{\mathcal{V}_{\rm B_2E_1}/V_T} - 1 \right), \tag{2.5}$$

$$I^S_{B_1} = \mathsf{XI_{B_1}} \, \frac{\mathsf{I_s}}{\mathsf{\beta_f}} \, \left(e^{\mathcal{V}_{\rm B_1E_1}/V_T} - 1 \right). \tag{2.6}$$

Table 2: *The charges of the equivalent circuit given in Fig. 1 on page 35.*

Charges	
Q_{BEO}	Base-emitter overlap charge
Q_{BCO}	Base-collector overlap charge
Q_E	Emitter charge or emitter neutral charge
Q_{t_E}	Base-emitter depletion charge
$Q_{t_E}^S$	Sidewall base-emitter depletion charge
Q_{BE}	Base-emitter diffusion charge
Q_{BC}	Base-collector diffusion charge
Q_{t_C}	Base-collector depletion charge
$Q_{\rm epi}$	Epilayer diffusion charge
$Q_{B_1B_2}$	AC current crowding charge
$Q_{\rm tex}$	Extrinsic base-collector depletion charge
$XQ_{\rm tex}$	Extrinsic base-collector depletion charge
$Q_{\rm ex}$	Extrinsic base-collector diffusion charge
$XQ_{\rm ex}$	Extrinsic base-collector diffusion charge
Q_{t_S}	Collector-substrate depletion charge

Table 3: *A list of some of the physical quantities used to describe the transistor.*

q	Unit charge
V_T	Thermal voltage kT/q
$L_{\rm em}$	Emitter length
$H_{\rm em}$	Emitter width
$A_{\rm em}$	Emitter surface $H_{\rm em}\,L_{\rm em}$
Q_{B0}	Base (hole) charge at zero bias
n_i	Intrinsic electron and hole density.
n_0	Normalized electron density in the base at the emitter edge
n_B	Normalized electron density in the base at the collector edge
$n_{B\rm ex}$	Normalized electron density in the extrinsic base at the collector edge
p_0	Normalized hole density in the collector epilayer at the base edge
p_W	Normalized hole density in the collector epilayer at the buried layer edge
$W_{\rm epi}$	Width the collector epilayer
$N_{\rm epi}$	Doping level of the collector epilayer
ε	Dielectric constant
$v_{\rm sat}$	Saturated drift velocity
μ	Mobility

The parameters are:

β_f	Ideal forward current gain
$\mathsf{XI}_{\mathsf{B}_1}$	Fraction of ideal base current that belongs to the sidewall

2.1.3 Non-ideal forward base current

The non-ideal forward base current originates from the recombination in the depleted base-emitter region and from many surface effects. A general formulation with a non-ideality factor is used:

$$I_{B_2} = \mathsf{I}_{\mathsf{Bf}} \left(e^{\mathcal{V}_{\mathrm{B_2E_1}}/\mathsf{m}_{\mathsf{Lf}} V_T} - 1 \right). \tag{2.7}$$

When recombination is the main contribution we have $\mathsf{m}_{\mathsf{Lf}} = 2$.

I_{Bf}	Saturation current of the non-ideal forward base current
m_{Lf}	Non-ideality factor of the non-ideal base current

2.1.4 Zener tunneling current in the emitter base junction

Mextram 504.8 adopted a model of Zener tunneling current in the emitter-base junction.

The Mextram 504.8 formulation is based on analytical formulations as documented in the semiconductor device physics literature [9], [10], [11]. which describe a Zener tunneling current as it flows in the emitter-base junction when the junction is forced in *reverse* bias ($V_{EB} > 0$).

In Mextram, in the *forward* bias regime it is assumed that the Zener tunneling current can always be negelected. This is implemented by formally setting the value of the Zener tunneling current identically equal to zero in forward bias and gives the computational advantage that Zener current does not need to be evaluated in forward bias.

It follows that all derivatives of the Zener current with respect to bias are identically equal to zero for $0 < V_{be}$ and hence in the limit $V_{be} \downarrow 0$. Smoothness of the tunneling current at zero bias then implies that *all* derivatives of the Zener current with respect to bias should vanish in the limit $V_{be} \uparrow 0$ at zero bias. This concerns the actual formulation of the Zener current in reverse bias and has been addressed as follows.

The Zener tunneling current depends on a factor commonly denoted by "D" [9], which takes degrees of occupation of conduction and valence bands into account. In the Mextram formulation of tunneling current, we adopt an advanced formulation [11] of D which furthermore takes effects of direction of electron momentum into account. It turns out that continuity at zero bias of current with respect to bias, up to and including the first derivative, is then automatically established. Subsequently, by dedicated adjustment of the description of the electric field, as applied in the D factor, continuity of *all* derivatives of current with respect to voltage has been established.

The temperature scaling of the model is fully physics based, which brings the advantage that the parameters of the temperature scaling model are material (bandgap) parameters.

Values for these, for given semiconductor material, can be found in the literature. Since the Zener effect is not very sensitive to temperature in the first place, we expect that literature values for these parameters will in general suffice so that no dedicated parameter extraction will be needed in this respect.

The two remaining parameters, $\mathsf{I_{zEB}}$ and $\mathsf{N_{zEB}}$ of the Zener current model have been chosen with care so as to minimize their interdependence.

Regarding noise, we follow the JUNCAP2 [12] model and assume that the Zener tunneling current exhibits full shot noise.

2.1.5 Base-emitter depletion charge

The depletion charges are modelled in the classical way, using a grading coefficient. Since this classical formulation contains a singularity (it becomes infinite when the forward bias equals the built-in voltage) we have modified it: beyond the built-in voltage the capacitance becomes constant. This maximum value is the zero-bias capacitance times a pre-defined factor (3.0 for the base-emitter depletion charge, 2.0 for the other depletion charges).

The base-emitter depletion capacitance is partitioned in a bottom and a sidewall component by the parameter $\mathsf{XC_{jE}}$

$$C_{t_E} = \frac{\mathrm{d}Q_{t_E}}{\mathrm{d}\mathcal{V}_{\mathrm{B_2E_1}}} = (1 - \mathsf{XC_{jE}})\ \frac{\mathsf{C_{jE}}}{(1 - \mathcal{V}_{\mathrm{B_2E_1}}/\mathsf{V_{dE}})^{\mathsf{pE}}}, \tag{2.8}$$

$$C^S_{t_E} = \frac{\mathrm{d}Q^S_{t_E}}{\mathrm{d}\mathcal{V}_{\mathrm{B_1E_1}}} = \mathsf{XC_{jE}}\ \frac{\mathsf{C_{jE}}}{(1 - \mathcal{V}_{\mathrm{B_1E_1}}/\mathsf{V_{dE}})^{\mathsf{pE}}}. \tag{2.9}$$

The model parameters are:

$\mathsf{C_{jE}}$	Zero bias emitter base depletion capacitance
$\mathsf{V_{dE}}$	Emitter base built-in voltage
pE	Emitter base grading coefficient
$\mathsf{XC_{jE}}$	The fraction of the BE depletion capacitance *not* under the emitter (sidewall fraction)

2.1.6 Base-collector depletion charge

The base-collector depletion capacitance C_{t_C} underneath the emitter takes into account the finite thickness of the epilayer and current modulation:

$$C_{t_C} = \frac{\mathrm{d}Q_{t_C}}{\mathrm{d}V_{\mathrm{junc}}} = \mathsf{XC_{jC}}\ \mathsf{C_{jC}}\ \left((1 - \mathsf{X_p})\frac{f(I_{C_1C_2})}{(1 - V_{\mathrm{junc}}/\mathsf{V_{dC}})^{\mathsf{pC}}} + \mathsf{X_p}\right), \tag{2.10}$$

$$f(I_{C_1C_2}) = \left(1 - \frac{I_{C_1C_2}}{I_{C_1C_2} + \mathsf{I_{hc}}}\right)^{\mathsf{mC}}. \tag{2.11}$$

The capacitance depends on the junction voltage $V_{\rm junc}$ that is calculated using the external base-collector bias minus the voltage drop over the epilayer, as if there were no injection. The current modulation (Kirk effect) has its own 'grading' coefficient $\mathsf{m_C}$ and uses the parameter $\mathsf{I_{hc}}$ from the epilayer model.

$\mathsf{C_{jc}}$	Zero bias collector-base depletion capacitance
$\mathsf{V_{dc}}$	Collector-base built-in voltage
$\mathsf{p_C}$	Collector-base grading coefficient
$\mathsf{XC_{jc}}$	The fraction of the BC depletion capacitance under the emitter.
$\mathsf{X_p}$	Ratio of depletion layer thickness at zero bias and epilayer thickness
$\mathsf{m_C}$	Collector current modulation coefficient [$\mathsf{m_C} \simeq 0.5\ (1 - \mathsf{X_p})$].

2.1.7 Emitter diffusion charge

The emitter diffusion charge Q_E is given by:

$$Q_E = \tau_{\mathsf{E}}\ \mathsf{I_s}\left(e^{\mathcal{V}_{\mathrm{B_2E_1}}/\mathsf{m}_{\tau}\,V_T} - 1\right)\ \left(\frac{\mathsf{I_s}}{\mathsf{I_k}}\right)^{1/\mathsf{m}_{\tau}-1}. \tag{2.12}$$

The actual transit time corresponding to this charge is a function of the current. When $\mathsf{m}_{\tau} > 1$ it has a minimum which for a transistor without quasi-saturation occurs at $I_c \simeq \mathsf{I_k}$. The formulation above is such that the minimum is approximately given by τ_{E}, independent of m_{τ}. Note that this charge Q_E is not a part of the collector current description, in contrast to the (normalized) depletion and base diffusion charges.

τ_{E}	Minimum delay time of emitter diffusion charge
m_{τ}	Non-ideality factor of the emitter diffusion charge

2.1.8 Base diffusion charges

The diffusion charges are given in terms of the normalized electron densities n_0 and n_B discussed earlier. The base transit time determines the zero bias base charge $Q_{B0} = \tau_{\mathsf{B}}\ \mathsf{I_k}$. Also the Early effect is included via q_1:

$$Q_{BE} = \tfrac{1}{2} q_1\ Q_{B0}\ n_0, \tag{2.13}$$

$$Q_{BC} = \tfrac{1}{2} q_1\ Q_{B0}\ n_B. \tag{2.14}$$

Note that n_0 and n_B are almost proportional to $I_C/\mathsf{I_k}$. The diffusion charges are therefore almost independent of the knee current, and so is the transit time.

τ_{B}	The base transit time

2.1.9 Base-charge partitioning

Distributed high-frequency effects [13] are modelled, in first order approximation, both in lateral direction (high-frequency current-crowding) and in vertical direction (excess

phase-shift). The distributed effects are an optional feature of the Mextram model and can be switched on and off by flag EXPHI

Excess phase shift can only be modelled accurately when all the charges and resistances, especially in the extrinsic transistor and in the interconnect, are modelled properly. Even then the intrinsic transistor can have a (small) influence. This is modelled in Mextram using base-charge partitioning. For simplicity it is only implemented for the forward base charge (Q_{BE}) and with a single partitioning factor, based on high-level injection. The previously calculated diffusion charges are changed according to:

$$Q_{BC} \rightarrow \tfrac{1}{3}\, Q_{BE} + Q_{BC}, \tag{2.15}$$
$$Q_{BE} \rightarrow \tfrac{2}{3}\, Q_{BE}. \tag{2.16}$$

In lateral direction (current crowding) a charge is added parallel to the intrinsic base resistance

$$Q_{B_1B_2} = \tfrac{1}{5}\, \mathcal{V}_{\mathrm{B_1B_2}}\ \left(C_{t_E} + C_{BE} + C_E\right). \tag{2.17}$$

2.2 Modelling of the epilayer current and charges

In this subsection the modelling of the epilayer resistance and charge will be discussed. This resistance is modelled as a current source $I_{C_1C_2}$, but it is also sometimes loosely denoted as R_{Cv}, the variable part of the collector resistance. The resistance depends on the supplied collector voltage and the collector current, imposed primarily by the base-emitter voltage. The effective resistance of the epilayer is strongly voltage- and current-dependent for the following reasons:

- In the forward mode of operation the internal base-collector junction voltage $\mathcal{V}_{\mathrm{B_2C_2}}$ may become forward-biased at high collector-currents (quasi-saturation). A region in the collector near the base will then be injected by carriers from the base. This injection region with thickness x_i has a low resistance.
- In the reverse mode of operation, both the external and internal base-collector junctions are forward biased. The whole epitaxial layer is then flooded with carriers and, consequently, has a low resistance.
- The current flow in the highly resistive region is Ohmic if the carrier density n is low ($n \ll N_{\mathrm{epi}}$) and space-charge limited if the carrier density exceeds the doping level N_{epi}. In the latter case the carriers move with the saturated drift velocity v_{sat} (hot-carrier current-flow).
- Current spreading in the epilayer reduces the resistance and is of special importance if the carrier density exceeds N_{epi}.

A compact model formulation of quasi-saturation is given by Kull et al. [14]. The model of Kull is only valid if the collector current is below the critical current for hot carriers:

$$\mathsf{I_{hc}} = qN_{\mathrm{epi}}v_{\mathrm{sat}}A_{\mathrm{em}}. \tag{2.18}$$

The Kull formulation has served as a basis for the epilayer model in Mextram. In the next section the model of Kull will be summarized and extended with hot carrier current flow (see also [15, 16, 17]).

2.2.1 Collector epilayer resistance model

The model of Kull is based on charge neutrality ($p + N_{\rm epi} \simeq n$) and gives the current $I_{C_1C_2}$ through the epilayer as a function of the internal and external base-collector biases. These biases are given by the solution vector of the circuit simulator. The final equations of the Kull formulation are [14]

$$I_{C_1C_2} = \frac{E_c + \mathcal{V}_{\rm C_1C_2}}{\mathsf{R_{Cv}}}, \tag{2.19a}$$

$$E_c = V_T \left[2\,p_0 - 2\,p_W - \ln\left(\frac{p_0+1}{p_W+1}\right)\right], \tag{2.19b}$$

$$p_0 = \tfrac{1}{2}\sqrt{1 + 4\,\exp[(\mathcal{V}_{\rm B_2C_2} - \mathsf{V_{dC}})/V_T]} - \tfrac{1}{2}, \tag{2.19c}$$

$$p_W = \tfrac{1}{2}\sqrt{1 + 4\,\exp[(\mathcal{V}_{\rm B_2C_1} - \mathsf{V_{dC}})/V_T]} - \tfrac{1}{2}. \tag{2.19d}$$

The voltage source E_c takes into account the decrease in resistance due to carriers injected from the base into the collector epilayer. If both junctions are reverse biased ($\mathcal{V}_{\rm B_2C_2} < \mathsf{V_{dC}}$ and $\mathcal{V}_{\rm B_2C_1} < \mathsf{V_{dC}}$) then E_c is zero and we have a simple constant resistance $\mathsf{R_{Cv}}$. Therefore this model does not take into account the hot-carrier behaviour (carriers moving with the saturated drift-velocity) in the lightly-doped collector epilayer.

The model is valid if the transistor operates in reverse mode, which means negative collector current $I_{C_1C_2}$. Normally this happens when the base-emitter junction is reverse biased and the base-collector junction is forward biased. The entire epilayer then gets filled with carriers and therefore a space-charge region will not exist.

In forward mode we have to change the formulation to include velocity saturation effects. The effective resistance for higher currents then becomes the space-charge resistance $\mathsf{SCR_{Cv}}$. Furthermore, the Kull model as described above, is not smooth enough (higher derivatives contain spikes) [16]. Mextram uses the following scheme in forward mode.

- Calculate $I_{C_1C_2}$ from the Kull model, Eq. (2.19), using the junction biases $\mathcal{V}_{\rm B_2C_2}$ and $\mathcal{V}_{\rm B_2C_1}$ given by the circuit simulator.
- Calculate the thickness $x_i/W_{\rm epi}$ of the injection region from the current, now including both Ohmic voltage drop and space-charge limited voltage drop

  $$I_{C_1C_2} = \frac{\mathsf{V_{dC}} - \mathcal{V}_{\rm B_2C_1}}{\mathsf{SCR_{Cv}}\,(1 - x_i/W_{\rm epi})^2} \times \frac{\mathsf{V_{dC}} - \mathcal{V}_{\rm B_2C_1} + \mathsf{SCR_{Cv}}\,\mathsf{I_{hc}}(1 - x_i/W_{\rm epi})}{\mathsf{V_{dC}} - \mathcal{V}_{\rm B_2C_1} + \mathsf{R_{Cv}}\,\mathsf{I_{hc}}}. \tag{2.20}$$

  The resulting thickness x_i will be different from that of the Kull model alone. In the implemented formulation we made sure that the equation does not lead to negative $x_i/W_{\rm epi}$, by using a smoothing function with parameter $\mathsf{a_{x_i}}$.

- The Kull model is perfectly valid in the injection region. For this region we have the following equation

$$\frac{x_i}{W_{\rm epi}}\, I_{C_1C_2}\, \mathsf{R_{Cv}} = E_c \simeq 2\, V_T\, (p_0^* - p_W)\, \frac{p_0^* + p_W + 1}{p_0^* + p_W + 2}. \tag{2.21}$$

  The approximation is such that both for very small and for very large p_0^* and p_W it gives the correct results, while in the intermediate regime it is off by maximally 5%. From $x_i/W_{\rm epi}$, $I_{C_1C_2}$, and p_W we can therefore calculate p_0^*, the hole density at the internal base-collector junction. The * is used to denote the difference between p_0^* calculated here and p_0 from the Kull model, calculated in Eq. (2.19).

- From p_0^* we can calculate the physical value of the internal base-collector bias $V^*_{B_2C_2}$.

- This physical internal bias is smooth and contains all effects we want to include. It can therefore be used for the main current I_N in Eq. (2.1), for the diffusion charge Q_{BC} and for the epilayer charge $Q_{\rm epi}$.

Summarizing, the epilayer resistance model takes into account:

- Ohmic current flow at low current densities.

- Space-charge limited current flow at high current densities.

- The decrease in resistance due to carriers injected from the base if only the internal base-collector junction is forward biased (quasi-saturation) and if both the internal and external base-collector junctions are forward biased (reverse mode of operation).

We have used a different formulation for reverse mode ($I_{C_1C_2} < 0$) and forward mode ($I_{C_1C_2} > 0$). This does not give discontinuities in the first and second derivative. The third derivative however is discontinuous. This is no real problem since normally the transistor is not biased in this region.

The model parameters are:

$\mathsf{V_{dc}}$	Built-in voltage of the base-collector junction (also used in the depletion capacitance Q_{t_C})
$\mathsf{I_{hc}}$	Critical current for hot carrier behaviour
$\mathsf{R_{Cv}}$	Ohmic resistance of the total epilayer
$\mathsf{SCR_{Cv}}$	Space-charge resistance of the epilayer
$\mathsf{a_{x_i}}$	Smoothing parameter for the onset of quasi-saturation

The model parameters can be given in physical quantities. Note that this is not part of the model itself, but rather of the scaling one should perform around the model. It is important to take current spreading into account [15]. Therefore we present the scaling

formula here for the parameters of the epilayer model. Other parameters need to be scaled too of course. (See table 3 for the meaning of some of the quantities.)

$$\mathsf{V_{dC}} = V_T \ \ln\left(N_{\rm epi}^2/n_i^2\right), \tag{2.22}$$

$$\mathsf{I_{hc}} = qN_{\rm epi}A_{\rm em}v_{\rm sat}\ (1+S_{fL})^2, \tag{2.23}$$

$$\mathsf{R_{Cv}} = \frac{W_{\rm epi}}{qN_{\rm epi}\mu A_{\rm em}}\ \frac{1}{(1+S_{fL})^2}, \tag{2.24}$$

$$\mathsf{SCR_{Cv}} = \frac{W_{\rm epi}^2}{2\varepsilon v_{\rm sat}A_{\rm em}}\ \frac{1}{(1+S_{fH})^2}. \tag{2.25}$$

The emitter area and the low and high-current spreading factors can be given as function of the emitter length $L_{\rm em}$ and width $H_{\rm em}$:

$$A_{\rm em} = H_{\rm em}L_{\rm em}, \tag{2.26}$$

$$S_{fL} = \tan(\alpha_l)\ W_{\rm epi}\ \left(\frac{1}{H_{\rm em}}+\frac{1}{L_{\rm em}}\right), \tag{2.27}$$

$$S_{fH} = \tfrac{2}{3}\ \tan(\alpha_h)\ W_{\rm epi}\ \left(\frac{1}{H_{\rm em}}+\frac{1}{L_{\rm em}}\right). \tag{2.28}$$

Here α_l is the spreading angle at low current levels ($I_{C_1C_2} < \mathsf{I_{hc}}$) and α_h is the spreading angle at high current levels ($I_{C_1C_2} > \mathsf{I_{hc}}$). Note that S_{fH} is in principle equal to the current spreading factor $\mathsf{S_{fH}}$ used in the high-current avalanche model.

2.2.2 Diffusion charge of the epilayer

The diffusion charge of the epilayer can be derived easily by applying the ICCR [7] to the injection region only:

$$I_{C_1C_2} = \mathsf{I_s}\ \left(e^{V^*_{B_2C_2}/V_T} - e^{\mathcal{V}_{\rm B_2C_1}/V_T}\right)\ \frac{Q_{B0}}{Q_{\rm epi}}. \tag{2.29}$$

Using the expressions from the epilayer current model this can be rewritten to

$$Q_{\rm epi} = \boldsymbol{\tau}_{\mathsf{epi}}\ \frac{2\,V_T}{\mathsf{R_{Cv}}}\ \frac{x_i}{W_{\rm epi}}\ (p_0^* + p_W + 2). \tag{2.30}$$

The transit time can also be given in terms of other quantities.

$$\boldsymbol{\tau}_{\mathsf{epi}} = \frac{W_{\rm epi}^2}{4\,D_n} = \mathsf{I_s}\ Q_{B0}\ \left(\frac{\mathsf{R_{Cv}}}{2\,V_T}\right)^2\ e^{\mathsf{V_{dC}}/V_T}. \tag{2.31}$$

This can be used as an initial guess in the parameter extraction (and was implicitely used in Mextram 503).

$\boldsymbol{\tau}_{\mathsf{epi}}$ Transit time of the epilayer

2.2.3 Avalanche multiplication model

Due to the high-electric field in the space-charge region avalanche currents will be generated. This generation of avalanche currents strongly depends on the maximum electric field. For low currents the maximum of the electric field will be at the base-collector junction. In the model of Ref. [18] the avalanche current is only a function of the electric field at the internal base-collector junction. Therefore the validity of this model is restricted to low current densities ($I_{C_1C_2} < \mathsf{I_{hc}}$). Our avalanche model [19] is based on Ref. [18], but does take this current dependence into account.

As an optional feature (using the flag EXAVL) the model is extended to current levels exceeding $\mathsf{I_{hc}}$, taking into account that the maximum of the electric field might reside at the buried layer. Snap-back behaviour is then modelled as well, which gives a better physical description. For these high current densities current spreading in the collector region changes the electric-field distribution and decreases the maximum electric-field. Because the generation of avalanche current is very sensitive to the maximum electric-field it is difficult to make an accurate and still simple model for high collector current densities, so we have chosen an emperical solution [19]. Because this operating area (high voltages, high current levels) is not of very practical interest (due to power dissipation) and, more importantly, the convergency behaviour of the model degrades considerably (the output resistance can become negative), we have made it an optional feature. Without using the extended model the output resistance can be very small but it is always positive.

The generation of avalanche current is based on Chynoweth's empirical law for the ionization coefficient [20]. The probability P_n of the generation of an electron-hole pair per unit of length is

$$P_n = A_n \ \exp\left(\frac{-B_n}{|E|}\right). \tag{2.32}$$

Because only weak-avalanche multiplication is considered, the generated avalanche current is proportional with the main current $I_{C_1C_2}$ through the epilayer

$$I_{\text{avl}} = I_{C_1C_2} \int_{x=0}^{x=x_d} A_n \ \exp\left(\frac{-B_n}{|E(x)|}\right) \ \mathrm{d}x, \tag{2.33}$$

where x_d is the boundary of the space-charge region. To calculate the avalanche current we have to evaluate the integral of Eq. (2.33) in the space-charge region. This integral is strongly determined by the maximum electric field. We make a suitable approximation around this maximum electric field

$$E(x) \simeq E_M \ \left(1 - \frac{x}{\lambda}\right) \simeq \frac{E_M}{1 + x/\lambda}, \tag{2.34}$$

where λ is the point where the extrapolation of the electric-field is zero. The generated avalanche current becomes:

$$\frac{I_{\text{avl}}}{I_{C_1C_2}} = \frac{A_n}{B_n} \ E_m \ \lambda \ \left\{\exp\left[\frac{-B_n}{E_M}\right] - \exp\left[\frac{-B_n}{E_M} \ \left(1 + \frac{x_d}{\lambda}\right)\right]\right\}. \tag{2.35}$$

The maximum electric field E_M, the depletion layer thickness x_d, and the intersection point λ are calculated using the simple model for the capacitance of an abrupt junction. In the high current model also quasi-saturation and the Kirk effect are included.

The parameters are

$\mathsf{W_{avl}}$	The effective thickness of the epilayer for avalanche
$\mathsf{V_{avl}}$	A voltage describing the derivative of the electric field at low currents
$\mathsf{S_{fH}}$	High current spreading factor [see Eq. (2.28); used only when EXAVL=1]

2.3 Extrinsic regions

2.3.1 Reverse base current

The reverse base current, similar to I_{B_1}, is affected by high injection and partitioned over the two external base-collector branches (with parameter $\mathsf{X_{ext}}$). It uses the electron density $n_{B\mathrm{ex}}$ in the external region of the base

$$I_{\mathrm{ex}} = \frac{1}{\beta_{\mathsf{ri}}} \left[\tfrac{1}{2}\, \mathsf{I_k}\; n_{B\mathrm{ex}}(\mathcal{V}_{\mathrm{B_1C_4}}) - \mathsf{I_s}\right]. \tag{2.36}$$

The current XI_{ex} is calculated in a similar way using the density $Xn_{B\mathrm{ex}}(\mathcal{V}_{\mathrm{BC_3}})$. As the convergency may be affected by this partitioning, it is an optional feature (with flag EXMOD).

β_{ri} Ideal reverse current gain
$\mathsf{X_{ext}}$ Partitioning factor of the extrinsic regions

2.3.2 Non-ideal reverse base current

The non-ideal reverse base current originates from the recombination in the depleted base-collector region:

$$I_{B_3} = \mathsf{I_{Br}}\, \frac{e^{\mathcal{V}_{\mathrm{B_1C_4}}/V_T} - 1}{e^{\mathcal{V}_{\mathrm{B_1C_4}}/2V_T} + e^{\mathsf{V_{Lr}}/2V_T}}. \tag{2.37}$$

The formulation of this non-ideal base current differs from the Gummel-Poon model. It is meant to describe a transition from ideality factor 1 ($\mathcal{V}_{\mathrm{B_1C_4}} < \mathsf{V_{Lr}}$) to ideality factor 2 ($\mathcal{V}_{\mathrm{B_1C_4}} > \mathsf{V_{Lr}}$).

$\mathsf{I_{Br}}$ Saturation current of the non-ideal reverse base current.
$\mathsf{V_{Lr}}$ Cross-over voltage of the non-ideal reverse base current.

2.3.3 Extrinsic base-collector depletion capacitance

The base-collector depletion capacitance of the extrinsic region is divided over the external-base node (charge: XQ_{tex}), and the internal-base node B_1 (charge: Q_{tex}). The partitioning is important for the output conductance Y_{12} at high frequencies. The model formulation is obtained by omitting the current modulation term in the formulation of Q_{t_C} in Eq. (2.10)

$$C_{\mathrm{tex}} = \frac{\mathrm{d}Q_{\mathrm{tex}}}{\mathrm{d}\mathcal{V}_{\mathrm{B_1C_4}}} = (1-\mathsf{X_{ext}})(1-\mathsf{XC_{jc}})\mathsf{C_{jc}} \left(\frac{1-\mathsf{X_p}}{(1-\mathcal{V}_{\mathrm{B_1C_4}}/\mathsf{V_{dc}})^{\mathsf{pc}}} + \mathsf{X_p}\right), \tag{2.38}$$

$$XC_{\mathrm{tex}} = \frac{\mathrm{d}XQ_{\mathrm{tex}}}{\mathrm{d}\mathcal{V}_{\mathrm{BC_3}}} = \mathsf{X_{ext}}\,(1-\mathsf{XC_{jc}})\,\mathsf{C_{jc}} \left(\frac{1-\mathsf{X_p}}{(1-\mathcal{V}_{\mathrm{BC_3}}/\mathsf{V_{dc}})^{\mathsf{pc}}} + \mathsf{X_p}\right). \tag{2.39}$$

Parameter used:

$\mathsf{X_{ext}}$ Partitioning factor for the extrinsic region

2.3.4 Diffusion charge of the extrinsic region

These charges are formulated in the same way as Q_{BC} and $Q_{\rm epi}$, and depend on the biases $\mathcal{V}_{\rm B_1C_4}$ and $\mathcal{V}_{\rm BC_3}$. The corresponding transit time should be the sum of $\tau_{\rm B}$ and $\tau_{\rm epi}$ multiplied by the ratio of the corresponding surfaces.

$\tau_{\rm R}$ Reverse transit time of the extrinsic regions

2.3.5 Parasitic PNP

The description of the substrate current of the parasitic PNP takes into account high injection

$$I_{\rm sub} = \frac{2\,{\rm I_{SsT}}\,\left(e^{\mathcal{V}_{\rm B_1C_4}/V_T}-1\right)}{1+\sqrt{1+4\,\dfrac{\rm I_{sT}}{\rm I_{ksT}}\,e^{\mathcal{V}_{\rm B_1C_4}/V_T}}}. \tag{2.40}$$

When $\mathsf{EXMOD} = 1$ the substrate current is partitioned over the constant base resistance, just as $I_{\rm ex}$.

Up until and including Mextram 504.8, the reverse behaviour of the parasitic PNP was not modelled. Only the simple diode current $I_{\rm Sf}$ used to be present that was meant to act as a signal to designers. Therefore in backwards compatibility mode, when $\mathsf{I_{CSs}}$ has its default value -1.0, the collector-substrate junction current model reduces to this mode. From level 504.9 onwards, for physical values of $\mathsf{I_{CSs}}$, $\mathsf{I_{CSs}} \geq 0$, the substrate-collector junction is modeled by an ideal diode current $I_{\rm Sf}$; this model has a physics-based temperature scaling with a mobility temperature scaling parameter $\mathsf{A_{sub}}$.

$\mathsf{I_{Ss}}$ Substrate saturation current.
$\mathsf{I_{ks}}$ Knee in the substrate current, projected on $\mathsf{I_s}$
$\mathsf{I_{CSs}}$ Collector-substrate ideal saturation current
$\mathsf{A_{sub}}$ Temperature coefficient of $\mathsf{I_{CSs}}$

2.3.6 Collector-substrate depletion capacitance.

The collector-substrate capacitance C_{t_S} is modelled in the usual way

$$C_{t_S} = \frac{{\rm d}Q_{t_S}}{{\rm d}\mathcal{V}_{\rm SC_1}} = \frac{\mathsf{C_{js}}}{(1-\mathcal{V}_{\rm SC_1}/\mathsf{V_{ds}})^{\mathsf{ps}}}. \tag{2.41}$$

The parameters used are

$\mathsf{C_{js}}$ Zero bias collector-substrate depletion capacitance
$\mathsf{V_{ds}}$ Collector-substrate built-in voltage
$\mathsf{p_S}$ Collector-substrate grading coefficient.

2.3.7 Constant overlap capacitances

The model has two constant overlap capacitances.

$\mathsf{C_{BEO}}$	Base-emitter overlap capacitance
$\mathsf{C_{BCO}}$	Base-collector overlap capacitance

2.4 Resistances

2.4.1 Constant series resistances

The model contains constant, though temperature dependent, series resistors at the base, emitter and collector terminals. The resistances of the burried layer underneath the transistor are represented by two constant, temperature dependent resistances $\mathsf{R_{Cblx}}$and $\mathsf{R_{Cbli}}$; see also ref. [21] . Note that the substrate resistance is not incorporated in the model itself but should be added in a macro model or sub-circuit since it depends on the layout.

$\mathsf{R_E}$	Constant emitter resistance
$\mathsf{R_{Bc}}$	Constant base resistance
$\mathsf{R_{Cc}}$	Collector Contact resistance
$\mathsf{R_{Cblx}}$	Resistance Collector Buried Layer: extrinstic part
$\mathsf{R_{Cbli}}$	Resistance Collector Buried Layer: intrinstic part

The buried layer resistances were introduced in Mextram 504.7, in a backwards compatibe way. This implies that the default values of these resistances is zero. Because values of $0\,\Omega$ thus are allowed for resistances $\mathsf{R_{Cblx}}$ and $\mathsf{R_{Cbli}}$, the lower clipping value of the resistances is zero and very small values of the resistances $\mathsf{R_{Cblx}}$ and $\mathsf{R_{Cbli}}$ are formally allowed. Resistance values very close to zero are known to form a potential threat to convergence however. In order to exclude the possibility that the resistances of the buried layer take such small values during the convergence process due to temperature effects, the lower clipping value for the temperature coefficient $\mathsf{A_{Cbl}}$ of the resistances $\mathsf{R_{Cblx}}$ and $\mathsf{R_{Cbli}}$ has been set to zero.

In case one of both of the $\mathsf{R_{Cblx}}$ and $\mathsf{R_{Cbli}}$ resistances vanish, the corresponding node (C_3 and or C_4) effectively disappears from the equivalent circuit. Hence the circuit topology depends on parameter values. Special attention has to be paid to this in implementation of the model.

2.4.2 Variable base resistance

The base resistance is divided in a constant part $\mathsf{R_{Bc}}$ (see previous section) and a variable part, loosely denoted by R_{Bv} but formally given by $I_{B_1B_2}$. The parameter $\mathsf{R_{Bv}}$ is the resistance of the variable part at zero base-emitter and base-collector bias. The variable (bias-dependent) part is modulated by the base width variation (Early effect) and at high current densities it decreases due to the diffusion charges Q_{BE} and Q_{BC}, just as the main current:

$$R_b = \mathsf{R_{Bv}}/q_B. \tag{2.42}$$

The resistance model also takes into account DC current crowding. The resistances decreases at high base currents when $\mathcal{V}_{\mathrm{B_1B_2}}$ is positive and it increases when $\mathcal{V}_{\mathrm{B_1B_2}}$ is negative (reversal of the base current):

$$I_{B_1B_2} = \frac{2\,V_T}{3\,R_b}\,\left(e^{\mathcal{V}_{\mathrm{B_1B_2}}/V_T} - 1\right) + \frac{\mathcal{V}_{\mathrm{B_1B_2}}}{3\,R_b}. \tag{2.43}$$

The AC current crowding is an optional feature of the model ($\mathsf{EXPHI} = 1$) and has been described earlier.

$\mathsf{R_{Bv}}$ zero bias value of the variable base resistance

2.5 Modelling of SiGe and possibly other HBT's

The most important difference between SiGe and pure-Si transistors is the difference between the total base hole charge (used for charges and for R_{Bv}) and the Gummel number (used in the main current). Its precise behaviour is important when the gradient of the bandgap is non-zero. In that case we have a different normalized base 'charge' q_B^I for the current:

$$q_B^I = \frac{\exp\left(\left[\frac{V_{t_E}}{\mathsf{V_{er}}} + 1\right]\,\frac{\mathsf{dE_g}}{V_T}\right) - \exp\left(\frac{-V_{t_C}}{\mathsf{V_{ef}}}\,\frac{\mathsf{dE_g}}{V_T}\right)}{\exp\left(\frac{\mathsf{dE_g}}{V_T}\right) - 1}. \tag{2.44}$$

Normally one would write $\mathsf{dE_g}/kT$ in these formulas. However, the value of $\mathsf{dE_g}$ is given in electron-Volt. This means we need to correct with q, the unity charge. It is then correct (at least in value) to divide $\mathsf{dE_g}$ by V_T.

In some cases SiGe transistors show neutral-base recombination. This means that the base current is dependent on the base-collector voltage. We have added a formulation that describes this effect and also the increase of the base current in quasi-saturation, due to Auger recombination. The ideal base current then is:

$$\begin{aligned} I_{B_1} = {} & \frac{\mathsf{I_s}}{\beta_{\mathsf{f}}}\,(1 - \mathsf{XI_{B_1}})\,\Bigg[(1 - \mathsf{X_{rec}})\;\left(e^{\mathcal{V}_{\mathrm{B_2E_1}}/V_T} - 1\right) \\ & + \mathsf{X_{rec}}\,\left(e^{\mathcal{V}_{\mathrm{B_2E_1}}/V_T} + e^{V^*_{B_2C_2}/V_T} - 2\right)\,\left(1 + \frac{V_{t_C}}{\mathsf{V_{ef}}}\right)\Bigg]. \end{aligned} \tag{2.45}$$

Note that the parameter $\mathsf{X_{rec}}$ can be larger than 1.

$\mathsf{dE_g}$ Gradient of the bandgap in the intrinsic base times its width
$\mathsf{X_{rec}}$ Pre-factor of the recombination part of the ideal base current

2.6 Miscellaneous

2.6.1 Temperature scaling rules

The Mextram model contains extensive temperature scaling rules (see section 4.7). The parameters in the temperature scaling rules are:

V_{g_B}, V_{g_C}, V_{g_S}, V_{g_j}, $dV_{g\beta f}$, $dV_{g\beta r}$, $dV_{g\tau_E}$	Bandgap voltages or differences
A_E, A_B, A_{epi}, A_{ex}, A_C, A_{Cbl}, A_S, A_{sub}	Mobility exponents
$A_{Q_{B0}}$	Exponent of zero bias base charge
A_{th}	Exponent of thermal resistance

The temperature rules are applied to the avalanche constant B_n and to the following parameters:

Saturation and knee currents	I_s, I_{Ss}, I_{CSs}, I_k, I_{ks}
Gain modelling	β_f, β_{fi}, V_{er}, V_{ef}, I_{Bf}, I_{Br}
Resistances	R_E, R_{Bc}, R_{Bv}, R_{Cc}, R_{Cblx}, R_{Cbli}, R_{Cv}
Capacitances	C_{j_E}, C_{j_C}, C_{j_S}, V_{d_E}, V_{d_C}, V_{d_S}, X_p
Transit times	τ_E, τ_B, τ_{epi}, τ_R
Thermal resistance	R_{th}

2.6.2 Self-heating

Self-heating is part of the model (see section 4.14). It is defined in the usual way by adding a self-heating network containing a current source describing the dissipated power and both a thermal resistance and a thermal capacitance. The total dissipated power is a sum of the dissipated power of each branch of the equivalent circuit.

Note that the effect of the parameter DTA and dynamic selfheating are independent. This is discussed in Ref. [4]. The local ambient temperature is increased as:

$$T_{\text{local ambient}} = T_{\text{global ambient}} + \mathrm{DTA}.$$

Dynamic self-heating gives an extra and independent contribution:

$$T_{\text{device}} = T_{\text{local ambient}} + (\Delta T)_{\text{dynamic heating}},$$

where $(\Delta T)_{\text{dynamic heating}}$ is given by $\mathcal{V}_{\mathrm{dT}}$, the voltage at the temperature node of the self-heating network shown in Fig. 2.

The temperature dependence of the thermal resistance is taken into account. At large dissipation, the relation between dissipation and temperature increase becomes non-linear. This can be implemented in a sub-circuit [22].

R_{th}	Thermal resistance
C_{th}	Thermal capacitance

2.6.3 Noise model

Noise is included in various branches of the model:

Thermal noise	:	resistances $\mathsf{R_E}$, $\mathsf{R_{Bc}}$, $\mathsf{R_{Cc}}$, $\mathsf{R_{Cblx}}$, $\mathsf{R_{Cbli}}$, and variable resistance R_{Bv} [23]
Shot noise	:	I_N, I_{B_1}, $I_{B_1}^S$, I_{B_2}, I_{B_3}, $I_{\rm ex}$, $XI_{\rm ex}$, $I_{\rm sub}$, and $XI_{\rm sub}$
$1/f$ noise [24]	:	I_{B_1}, $I_{B_1}^S$, I_{B_2}, I_{B_3}, $I_{\rm ex}$ and $XI_{\rm ex}$

Avalanche multiplication (due to impact-ionization) also adds noise [25]. This effect can be switched on or off by using the parameter $\mathsf{K_{avl}}$. Physically, it should be on: $\mathsf{K_{avl}} = 1$. For increased flexibility $\mathsf{K_{avl}}$ is allowed to have other values between 0 and 1; values greater than 1 are excluded because those could lead to a noise-correlation coefficient, for collector and base current noise, greater than 1.

$\mathsf{A_f}$	Exponent of the current dependence of the $1/f$ noise
$\mathsf{K_f}$	Pre-factor of the $1/f$ noise
$\mathsf{K_{fN}}$	Pre-factor of the $1/f$ noise in the non-ideal base current
$\mathsf{K_{avl}}$	Pre-factor (switch) for the noise due to avalanche

2.6.4 Number of transistor parameters

The parameters used in the Mextram model can be divided in:

Forward current modelling	:	28
Reverse current modelling (including PNP)	:	8
Extra parameters used only in charge modelling	:	14
Temperature scaling model	:	19
Self-heating	:	2
Noise model	:	4
HBT options	:	2
General parameters (level, flags, reference temperature)	:	7
Total	:	79

Of the total parameters mentioned above 4 parameters ($\mathsf{XC_{jE}}$, $\mathsf{XC_{jC}}$, $\mathsf{XI_{B_1}}$, and $\mathsf{X_{ext}}$) are specially dedicated to geometrical scaling (other parameters scale too of course). A scaling model itself, however, is not part of Mextram.

2.7 Comments about the Mextram model

2.7.1 Convergency and computation time

Mextram is a more complex model than Gummel-Poon. Therefore, the computing time is larger, especially when self-heating is included. For the same reason the convergency will be less, although we cannot give any quantitative comparison. The computation time of Mextram 504 is comparable to that of Mextram 503. However, tests show that Mextram

504 has better convergency than Mextram 503. This is probably mainly due to improved smoothness of the model.

2.7.2 Not modelled within the model

Mextram does not contain a substrate resistance. We know that this substrate resistance can have an influence on transistor characteristics. This is mainly seen in the real part of Y_{22}. For optimimum flexibility we did not make it a part of the model itself, because in the technology it is also not part of the transistor itself. It depends very much on the layout. The layout in a final design might be different from the layout used in parameter extraction. Also complicated substrate resistance/capacitance networks are sometimes needed. Therefore we chose to let the substrate resistance not be part of the model.

2.7.3 Possible improvements

The forward current of the parasitic PNP transistor is modelled. Mextram, however, does not contain a full description of the reverse current of the PNP since we believe that this is not important for designers.

The output conductance $\mathrm{d}I_C/\mathrm{d}\mathcal{V}_{\mathrm{CE}}$ at the point where hard saturation starts seems to be too abrupt for high current levels, compared to measurements. At present it is not possible to improve this, without losing some of the other features of the model.

The clarity of the extrinsic current model describing XI_{ex} and XI_{sub} could be improved by adding an extra node and an extra contact base resistance. Since the quality of the description does not improve, the parameter extraction would be more difficult, and the model topology would become dependent on a parameter (EXMOD) we choose not to do this.

3 Introduction to parameter extraction

The accuracy of circuit simulation depends not only on the performance of the transistor model itself, but also on the model parameters used. The use of a very sophisticated model with poorly determined parameters will result in an inaccurate simulation of the electronic circuit. The determination of the model-parameter extraction methodology is an important task in the development of a compact model. A strong correlation between model parameters hampers unambiguous determination of individual parameters. Most parameters are extracted directly from measured data. Therefore we need depletion capacitance (CV), terminal currents versus voltages (DC) and high-frequency measurements (S-parameters). Important is that these measurements are done over a large range of collector, base and emitter biasing conditions. This greatly improves the accuracy of the parameters. The number of data points in an interval is of minor importance.

To extract Mextram model parameters the model is implemented in the characterization and analysis program ICCAP of Agilent. Previous work on parameter extraction methodology has shown that accurate extraction of all Mextram parameters is feasible without evaluation of the full model equations in a circuit simulator [26]. This method greatly enhances the efficiency and user-friendliness of parameter extraction.

The general extraction strategy [26] is to put the parameters in small groups (typical 1–3) and extract these parameters simultaneously out of measured data sensitive to these parameters. The composition of each individual group depends on the technology. However, it is possible to give general guide lines. A more thorough documentation on parameter extraction for Mextram 504, including temperature and geometric scaling, is given in Ref. [3].

A typical grouping of Mextram parameters is given in the following table:

Base-emitter capacitance	:	$\mathsf{C_{jE}}$, $\mathsf{V_{d_E}}$, $\mathsf{p_E}$
Base-collector capacitance	:	$\mathsf{C_{jC}}$, $\mathsf{p_C}$, $\mathsf{X_p}$
Collector-substrate capacitance	:	$\mathsf{C_{js}}$, $\mathsf{V_{d_S}}$, $\mathsf{p_S}$
Zener tunneling current parameters: reverse biased EB junction, $V_{CB} = 0$	:	$\mathsf{I_{zEB}}$, $\mathsf{N_{zEB}}$
Avalanche at small collector currents, high V_{CB}	:	$\mathsf{W_{avl}}$, $\mathsf{V_{avl}}$
Reverse Early effect	:	$\mathsf{V_{er}}$
Forward Early effect	:	$\mathsf{V_{ef}}$
Forward Gummel plot small V_{BE}	:	$\mathsf{I_s}$
Substrate current small V_{BC}	:	$\mathsf{I_{Ss}}$, $\mathsf{I_{CSs}}$
Forward current gain up to medium current levels	:	β_f, $\mathsf{I_{Bf}}$, $\mathsf{m_{Lf}}$
Reverse current gain up to medium current levels	:	β_ri, $\mathsf{I_{Br}}$, $\mathsf{V_{Lr}}$, $\mathsf{I_{ks}}$
Giacoletto method	:	$\mathsf{R_E}$
From forward Gummel plot at large V_{BE},		

Y-parameters, or scaling	:	$\mathsf{R_{Bc}}$, $\mathsf{R_{Bv}}$
Substrate current in hard saturation	:	$\mathsf{R_{Cc}}$
Geometry scaling	:	$\mathsf{XC_{jE}}$, $\mathsf{XC_{jC}}$, $\mathsf{XI_{B_1}}$
Temperature scaling	:	Temperature parameters.
Decrease of V_{BE} for constant I_B at high V_{CE}	:	$\mathsf{R_{th}}$
Collector current up to high V_{CE}	:	$\mathsf{I_k}$
From the fall-of of h_{fe} and f_T at high currents	:	$\mathsf{R_{Cv}}$, $\mathsf{V_{dc}}$
From the f_T vs. I_C	:	$\mathsf{SCR_{Cv}}$, $\mathsf{I_{hc}}$, τ_{E}, τ_{B}, τ_{epi}, ($\mathsf{m}_{\boldsymbol{\tau}}$, $\mathsf{m_C}$, $\mathsf{a_{x_i}}$)
Reverse Gummel plot at large V_{BC}	:	$\mathsf{X_{ext}}$
Output conductance as function of frequency	:	$\mathsf{C_{th}}$

The first step in the determination of parameters is to generate an initial parameter set. An accurate calculation of the epilayer related parameters [see Eqs. (2.22)–(2.28)] prevents a lot of trouble and improves the convergency of the parameter extraction.

It is not possible to extract all the Mextram model parameters from one measured transistor. For example the scaling parameters $\mathsf{XC_{jE}}$, $\mathsf{XC_{jC}}$ and $\mathsf{XI_{B_1}}$ are determined from geometrical scaling rules. The same is true for the overlap capacitances $\mathsf{C_{BEO}}$ and $\mathsf{C_{BCO}}$.

It helps if the parameters are extracted in the sequence given in the table given above.

The extraction of the emitter and base resistances will give only satisfactory results when the current gain in this region is accurately modelled. It is nearly impossible to get accurate results for the variable part of the base resistance from DC measurements. Therefore either $\mathsf{R_{Bv}}$ is calculated from scaling information, or the resistances are extracted from S-parameters [27].

At high collector currents and voltages the measurements often become distorted by rise of the device temperature due to self heating. This complicates the extraction of $\mathsf{R_{Cv}}$, $\mathsf{SCR_{Cv}}$, $\mathsf{I_{hc}}$, $\mathsf{I_k}$ and the transit time parameters. Self-heating should therefore be included. When doing this, the temperature scaling parameters should be known or estimated. First $\mathsf{I_k}$ is extracted from the collector current at high $\mathcal{V}_{CE}$ in the output characteristic (I_C versus $\mathcal{V}_{CE}$ at constant I_B). At sufficient high $\mathcal{V}_{CE}$ the transistor comes out of quasi-saturation and therefore the epilayer resistance is of minor importance at these bias points. Next at small values of $\mathcal{V}_{CE}$ the DC current gain is optimised by extracting $\mathsf{R_{Cv}}$ and $\mathsf{V_{dc}}$. We can use the measured output characteristics or I_C and I_B from the Gummel plot of the S-parameter measurement setup. The latter has the advantage that the high current parameters and transit times parameters are extracted from the same device. In the final step $\mathsf{SCR_{Cv}}$, $\mathsf{I_{hc}}$ and the transit times parameters are extracted from f_T. The hot-carrier current $\mathsf{I_{hc}}$ should be the collector current beyond the top of the f_T. The spacing between the different maxima of the f_T curves for currents around $\mathsf{I_{hc}}$ is determined by $\mathsf{R_{Cv}}$ and $\mathsf{SCR_{Cv}}$. These three extraction steps have to be repeated once or twice to get a stable parameter set.

To extract S_{fH} one needs to measure the avalanche effect at high currents (at least I_{hc}) and voltages and fit the model to the measurements. It is very important to take self-heating into account.

The reverse transit time can only be accurately determined from reverse high-frequency measurements. These are not normally done, since they need dedicated structures. As an alternative one can use the forward high-frequency measurements in or close to hard saturation ($\mathcal{V}_{CE} = 0.2\,\mathrm{V}$), or one can calculate it according to Eq. (5.41).

The two SiGe parameters can be determined as follows. The bandgap difference dE_g in the base between collector-edge and emitter-edge can be estimated from the process. The Early-effect on the base-current in the forward Early measurement can be used to determine X_{rec}.

Zener tunneling current model The model for Zener tunneling current in the emitter base junction shares a model for the electric field with the emitter base depletion capacitance model. Therefore the Zener tunneling current has dedicated parameters I_{zEB} and N_{zEB}, but shares the parameters V_{d_E}, p_E with the depletion capacitance model. Depletion capacitance parameters should therefore be extracted before extraction of the dedicated Zener tunneling current parameters I_{zEB} and N_{zEB}.

4 Formal model formulation

In this section the formal definition of the model is given. We have given the description that includes a substrate node and self-heating. It is also possible to use Mextram without the substrate node, self-heating or both.

We will start with the structural elements of Mextram, the notation, the parameters and the equivalent circuit. Then a few model constants are defined and the temperature rules are given. The major part of this section consists of the description of the currents and of the charges. Then some extra modelling features are discussed, such as the extended modelling of the reverse current gain, the distributed high-frequency effects and heterjunction features. The noise model, MULT-scaling and self-heating are next. At last some implementation issues, the embedding of PNP transistors and operating point information are discussed.

4.1 Structural elements of Mextram

Mextram has the following somewhat independent parts.

Parameters The set of parameters consists of the following classes: the model-definition parameters like LEVEL and the three flags; the electrical parameters; the temperature scaling parameters; the noise parameters; and the self-heating parameters.

The model-definition parameters determine exactly which model is used. For some parts of the model we provide some extended features. These can be included or excluded using the three flags. The main part of the model is the description of currents and charges. For this description we need a set of electrical parameters. These parameters vary with temperature. In the parameter set itself only the values of the electrical parameters at the reference temperature are given. The temperature scaling parameters are used to calculate the actual values of the electrical parameters from their value at the reference temperature. This temperature scaling can in general be performed in preprocessing. The noise parameters are extra parameters use to calculate the various noise-sources.

Geometric scaling is not part of the model. The parameter MULT gives the possibility of putting several transistors in parallel. In this sense it is a very simple geometric scaling parameter. The model parameters can be scaling dependent (some are even especially made for this purpose, like the X-parameters). The scaling itself has to be done outside the model.

Self-heating Self-heating increases the local temperature of the transistor w.r.t. the ambient temperature. This is due to power dissipation of the transistor itself. When taking self-heating into account (this is an optional feature) the actual temperature depends on the actual bias conditions. This means that temperature scaling must be performed at every bias-point, and not only in preprocessing.

Clipping After temperature-scaling it is possible that some parameters are outside a physically realistic range, or in a range that might create difficulties in the numerical evaluation of the model, for example a division by zero. In order to prevent this, some parameters are limited to a pre-specified range directly after scaling. This procedure is called clipping.

Equivalent circuit The equivalent circuit describes how the various circuit elements of the model (currents, charges and noise-sources) are connected to each other. From the equivalent circuit and all the electrical equations it is also possible to derive a small-signal equivalent circuit.

Current and charge equations The current and charge equations are the main part of the model. They are needed to calculate the various currents and charges defined in the equivalent circuit. The currents are those through common resistances, diode-like currents or more complicated voltage controlled current sources. The charges are the various depletion charges and diffusion charges in the model. The charges are only needed in AC and transient simulation, but not in DC simulations. Therefore some parameters have no influence on the DC model. However a part of the charge formulation is needed in the DC model, e.g. the curvature of the depletion charges determines the bias-dependent Early effect.

Noise equations The noise equations describe the current noise sources that are parallel to some of the equivalent circuit elements. Only shot-noise, thermal noise and $1/f$-noise is modelled.

Operating point information When the transistor is biased in a certain way, it is sometimes convenient to gain some insight in the internal state of the model. This is possible via the operating point information. This information contains all the internal biases, currents and charges, all the elements of the complete small-signal circuit, the elements of a very simplified small-signal circuit, and some characteristic values like f_T.

Embedding for PNP transistors All the equations that will be given are for NPN transistors. For PNP transistors the same equations can be used after some embedding. This only consists of changing signs of biases before currents and charges are calculated and changing signs of currents and charges afterwards.

4.2 Notation

We used different fonts for different kind of quantities to clarify the structure of the equations:

$\mathsf{V_{d_E}}$, $\mathsf{R_{Cv}}$	Parameters
$\mathsf{V_{d_ET}}$, $\mathsf{R_{CvT}}$	Parameters after temperature scaling
$\mathcal{V}_{\mathrm{B_2E_1}}$, $\mathcal{V}_{\mathrm{B_2C_2}}$	Node voltages as given by the circuit simulator
$I_{C_1C_2}$, $V^*_{B_2C_2}$	Calculated quantities

When a previously calculated quantity needs to be changed this is denoted as

$$(\text{new value}) \rightarrow (\text{expression using previous values}) \tag{4.1}$$

4.3 Parameters

The following table gives all the parameters of Mextram. This includes the extra parameters needed when a substrate is present and the extra parameters needed when using a version with self-heating. The table contains the parameter name as used in the implementation as well as the symbol used in the formulas. Furthermore the unit of the parameter and a short description are given. The parameters are sorted in a logical way. First we have some general parameters like the level and the flags. Next the current parameters of the basic model, the parameters of the avalanche model, the resistances and epilayer parameters, the parameters of the depletion capacitances and the transit times are given. Then we have the parameters for the SiGe model features, followed by those of the temperature model (mobility exponents and bandgap voltages) and the noise parameters. The parameters specific for the four-terminal device are next. At last we have the self-heating parameters.

The parameters denoted with a '$*$' are not used in the DC model.

#	symbol	name	units	description
1	LEVEL	LEVEL	—	Model level, must be set to 504
2	$\mathsf{T_{ref}}$	TREF	°C	Reference temperature. Default is $25°\mathrm{C}$
3	DTA	DTA	°C	Difference between the local ambient and global ambient temperatures: $T_{\text{local ambient}} = T_{\text{global ambient}} + \mathsf{DTA}$
4	EXMOD	EXMOD	—	Flag for extended modelling of the reverse current gain
5	EXPHI	EXPHI	—	$*$Flag for the distributed high-frequency effects in transient
6	EXAVL	EXAVL	—	Flag for extended modelling of avalanche currents

#	symbol	name	units	description
7	I_s	IS	A	Collector-emitter saturation current
8	I_k	IK	A	Collector-emitter high injection knee current
9	V_{er}	VER	V	Reverse Early voltage
10	V_{ef}	VEF	V	Forward Early voltage
11	β_f	BF	—	Ideal forward current gain
12	I_{Bf}	IBF	A	Saturation current of the non-ideal forward base current
13	m_{Lf}	MLF	—	Non-ideality factor of the non-ideal forward base current
14	XI_{B_1}	XIBI	—	Part of ideal base current that belongs to the sidewall
15	I_{zEB}	IZEB	A	Pre-factor of emitter-base Zener tunneling current
16	N_{zEB}	NZEB	—	Coefficient of emitter-base Zener tunneling current
17	β_{ri}	BRI	—	Ideal reverse current gain
18	I_{Br}	IBR	A	Saturation current of the non-ideal reverse base current
19	V_{Lr}	VLR	V	Cross-over voltage of the non-ideal reverse base current
20	X_{ext}	XEXT	—	Part of $I_{\rm ex}$, $Q_{\rm tex}$, $Q_{\rm ex}$ and $I_{\rm sub}$ that depends on $\mathcal{V}_{\rm BC_3}$ instead of $\mathcal{V}_{\rm B_1C_4}$
21	W_{avl}	WAVL	m	Epilayer thickness used in weak-avalanche model
22	V_{avl}	VAVL	V	Voltage determining curvature of avalanche current
23	S_{fH}	SFH	—	Current spreading factor of avalanche model (when $\mathsf{EXAVL} = 1$)
24	R_E	RE	Ω	Emitter resistance
25	R_{Bc}	RBC	Ω	Constant part of the base resistance
26	R_{Bv}	RBV	Ω	Zero-bias value of the variable part of the base resistance
27	R_{Cc}	RCC	Ω	Collector Contact resistance
28	R_{Cblx}	RCBLX	Ω	Resistance of the Collector Buried Layer: eXtrinsic part
29	R_{Cbli}	RCBLI	Ω	Resistance of the Collector Buried Layer: Intrinsic part
30	R_{Cv}	RCV	Ω	Resistance of the un-modulated epilayer
31	SCR_{Cv}	SCRCV	Ω	Space charge resistance of the epilayer
32	I_{hc}	IHC	A	Critical current for velocity saturation in the epilayer
33	a_{x_i}	AXI	—	Smoothness parameter for the onset of quasi-saturation
34	C_{j_E}	CJE	F	$*$Zero-bias emitter-base depletion capacitance
35	V_{d_E}	VDE	V	Emitter-base diffusion voltage
36	p_E	PE	—	Emitter-base grading coefficient
37	XC_{j_E}	XCJE	—	$*$Fraction of the emitter-base depletion capacitance that belongs to the sidewall
38	C_{BEO}	CBEO	—	$*$Emitter-base overlap capacitance
39	C_{jC}	CJC	F	$*$Zero-bias collector-base depletion capacitance
40	V_{d_C}	VDC	V	Collector-base diffusion voltage
41	p_C	PC	—	Collector-base grading coefficient
42	X_p	XP	—	Constant part of C_{jC}
43	m_C	MC	—	Coefficient for the current modulation of the collector-base depletion capacitance
44	XC_{j_C}	XCJC	—	$*$Fraction of the collector-base depletion capacitance under the emitter
45	C_{BCO}	CBCO	—	$*$Collector-base overlap capacitance

#	symbol	name	units	description
46	m_τ	MTAU	—	∗Non-ideality factor of the emitter stored charge
47	τ_E	TAUE	s	∗Minimum transit time of stored emitter charge
48	τ_B	TAUB	s	∗Transit time of stored base charge
49	τ_{epi}	TEPI	s	∗Transit time of stored epilayer charge
50	τ_R	TAUR	s	∗Transit time of reverse extrinsic stored base charge
51	dE_g	DEG	eV	Bandgap difference over the base
52	X_{rec}	XREC	—	Pre-factor of the recombination part of I_{B_1}
53	$A_{Q_{B0}}$	AQBO	—	Temperature coefficient of the zero-bias base charge
54	A_E	AE	—	Temperature coefficient of the resistivity of the emitter
55	A_B	AB	—	Temperature coefficient of the resistivity of the base
56	A_{epi}	AEPI	—	Temperature coefficient of the resistivity of the epilayer
57	A_{ex}	AEX	—	Temperature coefficient of the resistivity of the extrinsic base
58	A_C	AC	—	Temperature coefficient of the resistivity of the collector contact
59	A_{Cbl}	ACBL	—	Temperature coefficient of the resistivity of the collector buried layer
60	dA_{I_s}	DAIS	—	Parameter for fine tuning of temperature dependence of collector-emitter saturation current
61	$dV_{g\beta f}$	DVGBF	V	Band-gap voltage difference of forward current gain
62	$dV_{g\beta r}$	DVGBR	V	Band-gap voltage difference of reverse current gain
63	V_{g_B}	VGB	V	Band-gap voltage of the base
64	V_{g_C}	VGC	V	Band-gap voltage of the collector
65	V_{g_j}	VGJ	V	Band-gap voltage recombination emitter-base junction
66	V_{gzEB}	VGZEB	V	Band-gap at reference temperature relevant to the Zener effect in the emitter-base junction
67	A_{VgEB}	AVGEB	$\mathrm{V/K}$	Temperature scaling coefficient of emitter-base Zener tunneling current
68	T_{VgEB}	TVGEB	K	Temperature scaling coefficient of emitter-base Zener tunneling current
69	$dV_{g\tau_E}$	DVGTE	V	∗Band-gap voltage difference of emitter stored charge

#	symbol	name	units	description
70	A_f	AF	—	∗Exponent of the Flicker-noise
71	K_f	KF	—	∗Flicker-noise coefficient of the ideal base current
72	K_{fN}	KFN	—	∗Flicker-noise coefficient of the non-ideal base current
73	K_{avl}	KAVL	—	∗Switch for white noise contribution due to avalanche
74	I_{Ss}	ISS	A	Base-substrate saturation current
75	I_{CSs}	ICSS	A	Collector-substrate ideal saturation current
76	I_{ks}	IKS	A	Base-substrate high injection knee current
77	C_{js}	CJS	F	∗Zero-bias collector-substrate depletion capacitance
78	V_{ds}	VDS	V	∗Collector-substrate diffusion voltage
79	p_S	PS	—	∗Collector-substrate grading coefficient
80	V_{gs}	VGS	V	Band-gap voltage of the substrate
81	A_S	AS	—	For a closed buried layer: $A_S = A_C$, and for an open buried layer: $A_S = A_{epi}$
82	A_{sub}	ASUB	—	Temperature coefficient for mobility of minorities in the substrate
83	R_{th}	RTH	°C/W	Thermal resistance
84	C_{th}	CTH	J/°C	∗Thermal capacitance
85	A_{th}	ATH	—	Temperature coefficient of the thermal resistance
86	MULT	MULT	—	Multiplication factor

The following table gives the default values and the clipping values of the parameters. These values should not be circuit simulator dependent. The default values come from a realistic transistor and are therefore a good indication of typical values.

#	symbol	name	default	clip low	clip high
1	LEVEL	LEVEL	504	–	–
2	T_{ref}	TREF	25.0	−273	–
3	DTA	DTA	0.0	–	–
4	EXMOD	EXMOD	1.0	0.0	1.0
5	EXPHI	EXPHI	1.0	0.0	1.0
6	EXAVL	EXAVL	0.0	0.0	1.0
7	I_s	IS	$22.0 \cdot 10^{-18}$	0.0	–
8	I_k	IK	0.1	$1.0 \cdot 10^{-12}$	–
9	V_{er}	VER	2.5	0.01	–
10	V_{ef}	VEF	44.0	0.01	–
11	β_f	BF	215.0	$1.0 \cdot 10^{-4}$	–
12	I_{Bf}	IBF	$2.7 \cdot 10^{-15}$	0.0	–
13	m_{Lf}	MLF	2.0	0.1	–
14	XI_{B_1}	XIBI	0.0	0.0	1.0
15	I_{zEB}	IZEB	0.0	0.0	–
16	N_{zEB}	NZEB	22.0	0.0	–
17	β_{ri}	BRI	7.0	$1.0 \cdot 10^{-10}$	–
18	I_{Br}	IBR	$1.0 \cdot 10^{-15}$	0.0	–
19	V_{Lr}	VLR	0.2	–	–
20	X_{ext}	XEXT	0.63	0.0	1.0
21	W_{avl}	WAVL	$1.1 \cdot 10^{-6}$	$1.0 \cdot 10^{-9}$	–
22	V_{avl}	VAVL	3.0	0.01	–
23	S_{fH}	SFH	0.3	0.0	–
24	R_E	RE	5.0	$1.0 \cdot 10^{-3}$	–
25	R_{Bc}	RBC	23.0	$1.0 \cdot 10^{-3}$	–
26	R_{Bv}	RBV	18.0	$1.0 \cdot 10^{-3}$	–
27	R_{Cc}	RCC	12.0	$1.0 \cdot 10^{-3}$	–
28	R_{Cblx}	RCBLX	0.0	0.0	–
29	R_{Cbli}	RCBLI	0.0	0.0	–
30	R_{Cv}	RCV	150.0	$1.0 \cdot 10^{-3}$	–
31	SCR_{Cv}	SCRCV	1250.0	$1.0 \cdot 10^{-3}$	–
32	I_{hc}	IHC	$4.0 \cdot 10^{-3}$	$1.0 \cdot 10^{-12}$	–
33	a_{x_i}	AXI	0.3	0.02	–
34	C_{j_E}	CJE	$73.0 \cdot 10^{-15}$	0.0	–
35	V_{d_E}	VDE	0.95	0.05	–
36	p_E	PE	0.4	0.01	0.99
37	XC_{j_E}	XCJE	0.4	0.0	1.0
38	C_{BEO}	CBEO	0.0	0.0	–

#	symbol	name	default	clip low	clip high
39	C_{jc}	CJC	$78.0 \cdot 10^{-15}$	0.0	–
40	V_{d_C}	VDC	0.68	0.05	–
41	p_C	PC	0.5	0.01	0.99
42	X_p	XP	0.35	0.0	0.99
43	m_C	MC	0.5	0.0	1.0
44	XC_{jc}	XCJC	$32.0 \cdot 10^{-3}$	0.0	1.0
45	C_{BCO}	CBCO	0.0	0.0	–
46	m_τ	MTAU	1.0	0.1	–
47	τ_E	TAUE	$2.0 \cdot 10^{-12}$	0.0	–
48	τ_B	TAUB	$4.2 \cdot 10^{-12}$	0.0	–
49	τ_{epi}	TEPI	$41.0 \cdot 10^{-12}$	0.0	–
50	τ_R	TAUR	$520.0 \cdot 10^{-12}$	0.0	–
51	dE_g	DEG	0.0	–	–
52	X_{rec}	XREC	0.0	0.0	–
53	$A_{Q_{B0}}$	AQBO	0.3	–	–
54	A_E	AE	0.0	–	–
55	A_B	AB	1.0	–	–
56	A_{epi}	AEPI	2.5	–	–
57	A_{ex}	AEX	0.62	–	–
58	A_C	AC	2.0	–	–
59	A_{Cbl}	ACBL	2.0	0.0	–
60	dA_{I_s}	DAIS	0.0	–	–
61	$dV_{g\beta f}$	DVGBF	$50.0 \cdot 10^{-3}$	–	–
62	$dV_{g\beta r}$	DVGBR	$45.0 \cdot 10^{-3}$	–	–
63	V_{g_B}	VGB	1.17	0.1	–
64	V_{g_C}	VGC	1.18	0.1	–
65	V_{g_j}	VGJ	1.15	0.1	–
66	$V_{g_{ZEB}}$	VGZEB	1.15	0.1	–
67	A_{VgEB}	AVGEB	$4.73 \cdot 10^{-4}$	–	–
68	T_{VgEB}	TVGEB	636.0	0.0	–
69	$dV_{g\tau_E}$	DVGTE	0.05	–	–

#	symbol	name	default	clip low	clip high
70	A_f	AF	2.0	0.01	–
71	K_f	KF	$20.0 \cdot 10^{-12}$	0.0	–
72	K_{fN}	KFN	$20.0 \cdot 10^{-12}$	0.0	–
73	K_{avl}	KAVL	0.0†	0.0†	1.0
74	I_{Ss}	ISS	$48.0 \cdot 10^{-18}$	0.0	–
75	I_{CSs}	ICSS	-1.0‡	–	–
76	I_{ks}	IKS	$250.0 \cdot 10^{-6}$	$1.0 \cdot 10^{-12}$	–
77	C_{js}	CJS	$315.0 \cdot 10^{-15}$	0.0	–
78	V_{ds}	VDS	0.62	0.05	–
79	p_S	PS	0.34	0.01	0.99
80	V_{gs}	VGS	1.20	0.1	–
81	A_S	AS	1.58	–	–
82	A_{sub}	ASUB	2.0	–	–
83	R_{th}	RTH	300.0	0.0	–
84	C_{th}	CTH	$3.0 \cdot 10^{-9}$	0.0§	–
85	A_{th}	ATH	0.0	–	–
86	MULT	MULT	1.0	0.0	–

†The physical and therefore recommended value is $K_{avl} = 1$.
‡For $I_{CSs} < 0$ (default), the substrate-collector current I_{Sf} reduces to backwards compatibility mode.
§Please note that a value of $C_{th} = 0$ often leads to incorrect results, see Sec. 4.14.

4.4 Equivalent circuit

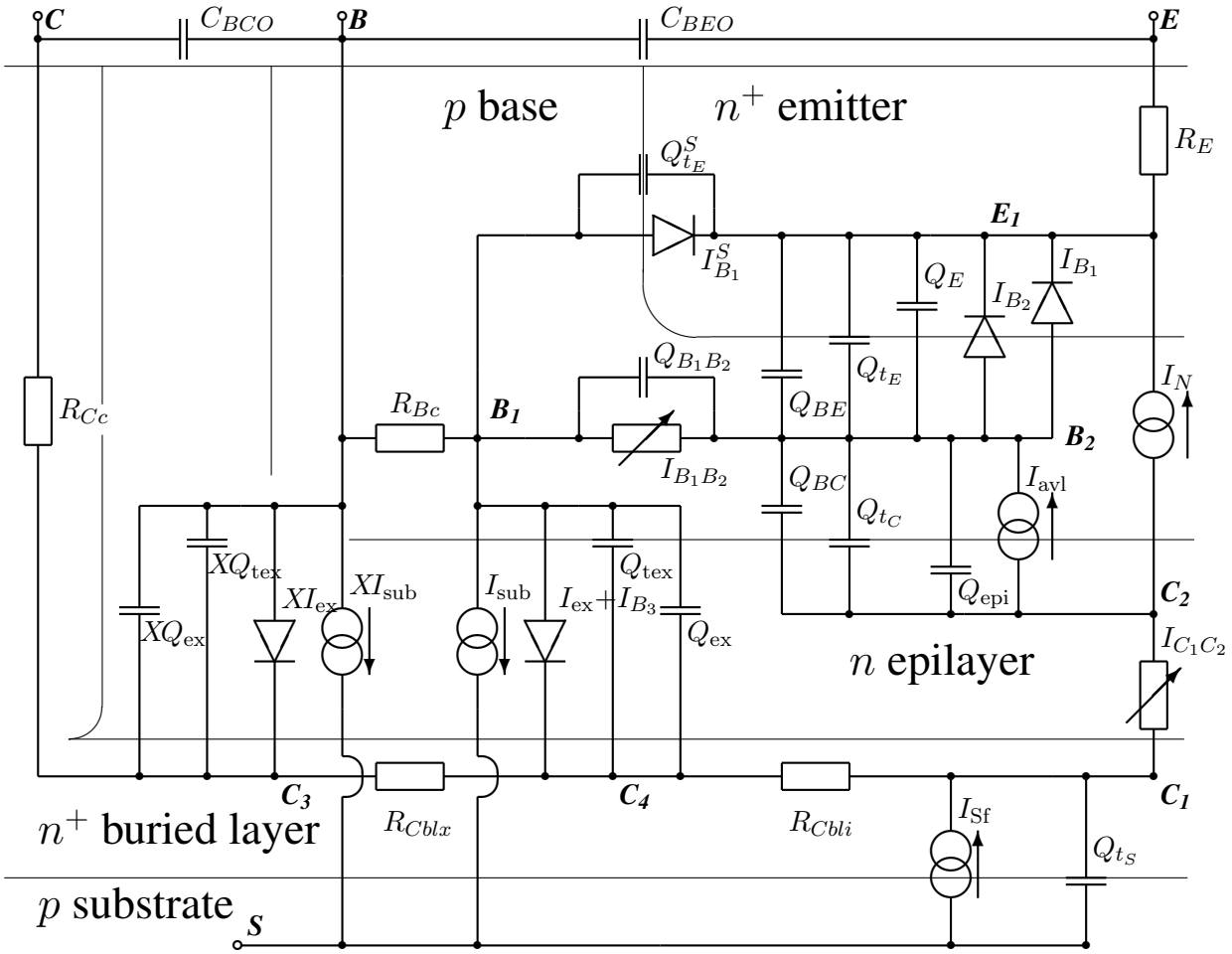

Figure 1: *The full Mextram equivalent circuit for the vertical NPN transistor. Schematically the different regions of the physical transistor are shown. The current $I_{B_1B_2}$ describes the variable base resistance and is therefore sometimes called R_{Bv}. The current $I_{C_1C_2}$ describes the variable collector resistance (or epilayer resistance) and is therefore sometimes called R_{Cv}. The extra circuit for self-heating is discussed in Sec. 4.14.*

4.5 Model constants

$$k = 1.3806226 \cdot 10^{-23}\,\mathrm{JK}^{-1} \tag{4.2}$$
$$q = 1.6021918 \cdot 10^{-19}\,\mathrm{C} \tag{4.3}$$
$$\left(\frac{k}{q}\right) = 0.86171 \cdot 10^{-4}\,\mathrm{V/K} \tag{4.4}$$
$$G_{\min} = 1.0 \cdot 10^{-13}\,\mathrm{A/V} \tag{4.5a}$$
$$V_{\mathrm{d,low}} = 0.05\,\mathrm{V} \tag{4.5b}$$
$$a_{j_E} = 3.0 \tag{4.6}$$
$$a_{j_C} = 2.0 \tag{4.7}$$
$$a_{j_S} = 2.0 \tag{4.8}$$

Constants A_n and B_n for impact ionization depend on the transistor type:
For NPN:

$$A_n = 7.03 \cdot 10^{7}\,\mathrm{m}^{-1} \tag{4.9}$$

$$B_n = 1.23 \cdot 10^{8}\,\mathrm{V\,m}^{-1} \tag{4.10}$$

For PNP:

$$A_n = 1.58 \cdot 10^{8}\,\mathrm{m}^{-1} \tag{4.11}$$

$$B_n = 2.04 \cdot 10^{8}\,\mathrm{V\,m}^{-1} \tag{4.12}$$

The default reference temperature $\mathsf{T_{ref}}$ for parameter determination is $25\,^{\circ}\mathrm{C}$.

4.6 MULT-scaling

The parameter MULT may be used to put several transistors in parallel. This means that all currents, charges, and noise-current sources should be multiplied by MULT. It is however much easier to implement this by scaling some of the parameters up front. MULT is allowed to be non-integer for increased flexibility. To scale the geometry of a transistor the use of a process-block is preferable over using this feature.

The following parameters are multiplied by MULT

$$\begin{array}{llllllllll} \mathsf{I_s}, & \mathsf{I_k}, & \mathsf{I_{Bf}}, & \mathsf{I_{Br}}, & \mathsf{I_{hc}}, & \mathsf{I_{Ss}}, & \mathsf{I_{CSs}}, & \mathsf{I_{ks}}, & \mathsf{I_{zEB}} \\ \mathsf{C_{jE}}, & \mathsf{C_{jC}}, & \mathsf{C_{jS}}, & \mathsf{C_{BEO}}, & \mathsf{C_{BCO}}, & \mathsf{C_{th}} \end{array} \tag{4.13}$$

The following parameters are divided by MULT

$$\mathsf{R_E},\quad \mathsf{R_{Bc}},\quad \mathsf{R_{Bv}},\quad \mathsf{R_{Cc}},\quad \mathsf{R_{Cblx}},\quad \mathsf{R_{Cbli}},\quad \mathsf{R_{Cv}},\quad \mathsf{SCR_{Cv}},\quad \mathsf{R_{th}} \tag{4.14}$$

The flicker-noise coefficients are scaled as

$$\mathsf{K_f} \rightarrow \mathsf{K_f} \cdot \mathsf{MULT}^{1-\mathsf{A_f}} \tag{4.15}$$

$$\mathsf{K_{fN}} \rightarrow \mathsf{K_{fN}} \cdot \mathsf{MULT}^{1-[2(\mathsf{m_{Lf}}-1)+\mathsf{A_f}(2-\mathsf{m_{Lf}})]} \tag{4.16}$$

4.7 Temperature scaling

The actual simulation temperature is denoted by TEMP (in $^\circ$C). The temperature at which the parameters are determined is $\mathsf{T_{ref}}$ (also in $^\circ$C).

Conversion to Kelvin Note the addition of the voltage $\mathcal{V}_{\rm dT}$ of the thermal node (see Sec. 4.14).

$$T_K = \mathsf{TEMP} + \mathsf{DTA} + 273.15 + \mathcal{V}_{\rm dT} \tag{4.17a}$$

$$T_{\rm amb} = \mathsf{TEMP} + \mathsf{DTA} + 273.15 \tag{4.17b}$$

$$T_{RK} = \mathsf{T_{ref}} + 273.15 \tag{4.18}$$

$$t_N = \frac{T_K}{T_{RK}} \tag{4.19}$$

Thermal voltage

$$V_T = \left(\frac{k}{q}\right)\, T_K \tag{4.20}$$

$$V_{T_R} = \left(\frac{k}{q}\right)\, T_{RK} \tag{4.21}$$

$$\frac{1}{V_{\Delta T}} = \frac{1}{V_T} - \frac{1}{V_{T_R}} \tag{4.22}$$

Depletion capacitances The junction diffusion voltages $\mathsf{V_{d_E}}$, $\mathsf{V_{d_C}}$, and $\mathsf{V_{d_S}}$ with respect to temperature are

$$U_{d_E T} = -3\,V_T\ \ln t_N + \mathsf{V_{d_E}}\ t_N + (1 - t_N)\ \mathsf{V_{g_B}} \tag{4.23a}$$

$$\mathsf{V_{d_E T}} = U_{d_E T} + V_T \ln\{1 + \exp[(V_{\mathrm{d,low}} - U_{d_E T})/V_T]\} \tag{4.23b}$$

$$U_{d_C T} = -3\,V_T\ \ln t_N + \mathsf{V_{d_C}}\ t_N + (1 - t_N)\ \mathsf{V_{g_C}} \tag{4.24a}$$

$$\mathsf{V_{d_C T}} = U_{d_C T} + V_T \ln\{1 + \exp[(V_{\mathrm{d,low}} - U_{d_C T})/V_T]\} \tag{4.24b}$$

$$U_{d_S T} = -3\,V_T\ \ln t_N + \mathsf{V_{d_S}}\ t_N + (1 - t_N)\ \mathsf{V_{g_S}} \tag{4.25a}$$

$$\mathsf{V_{d_S T}} = U_{d_S T} + V_T \ln\{1 + \exp[(V_{\mathrm{d,low}} - U_{d_S T})/V_T]\} \tag{4.25b}$$

The zero-bias capacitances scale with temperature as

$$\mathsf{C_{j_E T}} = \mathsf{C_{j_E}}\ \left(\frac{\mathsf{V_{d_E}}}{\mathsf{V_{d_E T}}}\right)^{\mathsf{p_E}} \tag{4.26}$$

$$\mathsf{C_{j_S T}} = \mathsf{C_{j_S}}\ \left(\frac{\mathsf{V_{d_S}}}{\mathsf{V_{d_S T}}}\right)^{\mathsf{p_S}} \tag{4.27}$$

The collector depletion capacitance is divided in a variable and a constant part. The constant part is temperature independent.

$$\mathsf{C_{j_C T}} = \mathsf{C_{j_C}}\ \left[(1 - \mathsf{X_p})\ \left(\frac{\mathsf{V_{d_C}}}{\mathsf{V_{d_C T}}}\right)^{\mathsf{p_C}} + \mathsf{X_p}\right] \tag{4.28}$$

$$\mathsf{X_{pT}} = \mathsf{X_p}\ \left[(1 - \mathsf{X_p})\ \left(\frac{\mathsf{V_{d_C}}}{\mathsf{V_{d_C T}}}\right)^{\mathsf{p_C}} + \mathsf{X_p}\right]^{-1} \tag{4.29}$$

Resistances The various parameters A describe the mobility of the corresponding regions: $\mu \propto t_N^{-\mathsf{A}}$. The temperature dependence of the zero-bias base charge goes as $Q_{B0\mathrm{T}}/Q_{B0} = t_N^{\mathsf{A_{Q_{B0}}}}$.

$$\mathsf{R_{ET}} = \mathsf{R_E}\; t_N^{\mathsf{A_E}} \tag{4.30}$$

$$\mathsf{R_{BvT}} = \mathsf{R_{Bv}}\; t_N^{\mathsf{A_B}-\mathsf{A_{Q_{B0}}}} \tag{4.31}$$

$$\mathsf{R_{BcT}} = \mathsf{R_{Bc}}\; t_N^{\mathsf{A_{ex}}} \tag{4.32}$$

$$\mathsf{R_{CvT}} = \mathsf{R_{Cv}}\; t_N^{\mathsf{A_{epi}}} \tag{4.33}$$

$$\mathsf{R_{CcT}} = \mathsf{R_{Cc}}\; t_N^{\mathsf{A_C}} \tag{4.34a}$$

$$\mathsf{R_{CblxT}} = \mathsf{R_{Cblx}}\; t_N^{\mathsf{A_{Cbl}}} \tag{4.34b}$$

$$\mathsf{R_{CbliT}} = \mathsf{R_{Cbli}}\; t_N^{\mathsf{A_{Cbl}}} \tag{4.34c}$$

Conductances With the parasitic collector resistances, conductances are associated. These are to be used in the noise model and for the calculation of dissipated power. For those contexts, for the cases in which one or more of the resistances is zero, the appropriate value for the corresponding conductance is zero. In cases of vanishing resistance values, the topology of the equiavalent circuit is effectively changed. This is to be taken into account in implementations of the model.

$$\begin{array}{lll} \text{if} & \mathsf{R_{Cc}} > 0 & \text{then} \quad \mathsf{G_{CcT}} = 1/\mathsf{R_{CcT}} \;\; , \\ & & \text{else} \quad \mathsf{G_{CcT}} = 0 \;\; . \end{array} \tag{4.34d}$$

$$\begin{array}{lll} \text{if} & \mathsf{R_{Cblx}} > 0 & \text{then} \quad \mathsf{G_{CblxT}} = 1/\mathsf{R_{CblxT}} \;\; , \\ & & \text{else} \quad \mathsf{G_{CblxT}} = 0 \;\; . \end{array} \tag{4.34e}$$

$$\begin{array}{lll} \text{if} & \mathsf{R_{Cbli}} > 0 & \text{then} \quad \mathsf{G_{CbliT}} = 1/\mathsf{R_{CbliT}} \;\; , \\ & & \text{else} \quad \mathsf{G_{CbliT}} = 0 \;\; . \end{array} \tag{4.34f}$$

Current gains

$$\beta_{fT} = \beta_f \; t_N^{A_E - A_B - A_{Q_{B0}}} \; \exp[-dV_{g\beta f}/V_{\Delta T}] \tag{4.35}$$

$$\beta_{riT} = \beta_{ri} \; \exp[-dV_{g\beta r}/V_{\Delta T}] \tag{4.36}$$

Currents and voltages

$$I_{sT} = I_s \; t_N^{4 - A_B - A_{Q_{B0}} + dA_{I_s}} \; \exp[-V_{g_B}/V_{\Delta T}] \tag{4.37}$$

$$I_{kT} = I_k \; t_N^{1 - A_B} \tag{4.38}$$

$$I_{BfT} = I_{Bf} \; t_N^{(6 - 2m_{Lf})} \; \exp[-V_{g_j}/m_{Lf} \; V_{\Delta T}] \tag{4.39}$$

$$I_{BrT} = I_{Br} \; t_N^2 \; \exp[-V_{g_C}/2V_{\Delta T}] \tag{4.40}$$

$$V_{efT} = V_{ef} \; t_N^{A_{Q_{B0}}} \; \left[(1 - X_p) \; \left(\frac{V_{d_C}}{V_{d_C T}} \right)^{p_C} + X_p \right]^{-1} \tag{4.41}$$

$$V_{erT} = V_{er} \; t_N^{A_{Q_{B0}}} \; \left(\frac{V_{d_E}}{V_{d_E T}} \right)^{-p_E} \tag{4.42}$$

The temperature dependence of I_{Ss} and I_{ks} is given by A_S and V_{g_S}.
A_S equals A_C for a closed buried layer (BN) and A_S equals A_{epi} for an open buried layer.

$$I_{SsT} = I_{Ss} \; t_N^{4 - A_S} \; \exp[-V_{g_S}/V_{\Delta T}] \tag{4.43}$$

$$I_{CSsT} = I_{CSs} \; t_N^{3.5 - 0.5A_{sub}} \; \exp[-V_{g_S}/V_{\Delta T}] \tag{4.44}$$

$$I_{ksT} = I_{ks} \; t_N^{1 - A_S} \; \frac{I_{sT}}{I_s} \; \frac{I_{Ss}}{I_{SsT}} \tag{4.45}$$

When either $I_s = 0$ or $I_{SsT} = 0$ we take $I_{ksT} = I_{ks} \; t_N^{1 - A_S}$.

Transit times

$$\tau_{\mathrm{ET}} = \tau_{\mathsf{E}}\ t_N^{(\mathsf{A_B}-2)}\ \exp[-\mathsf{dV_{g\tau_E}}/V_{\Delta T}] \tag{4.46}$$

$$\tau_{\mathrm{BT}} = \tau_{\mathsf{B}}\ t_N^{\mathsf{A_{Q_{B0}}}+\mathsf{A_B}-1} \tag{4.47}$$

$$\tau_{\mathsf{epi}\mathrm{T}} = \tau_{\mathsf{epi}}\ t_N^{\mathsf{A_{epi}}-1} \tag{4.48}$$

$$\tau_{\mathrm{RT}} = \tau_{\mathsf{R}}\ \frac{\tau_{\mathrm{BT}} + \tau_{\mathsf{epi}\mathrm{T}}}{\tau_{\mathsf{B}} + \tau_{\mathsf{epi}}} \tag{4.49}$$

Avalanche constant Note that this temperature rule is independent of $\mathsf{T_{ref}}$ since we take B_n as a material constant. For $T_K < 525.0K$ we have

$$B_{n\mathrm{T}} = B_n\ [1 + 7.2 \cdot 10^{-4}\ (T_K - 300) - 1.6 \cdot 10^{-6}\ (T_K - 300)^2] \tag{4.50a}$$

whereas for $T_K \geq 525.0K$

$$B_{n\mathrm{T}} = B_n\ * 1.081 \tag{4.50b}$$

Heterojunction features

$$\mathsf{dE_{g}}_{\mathrm{T}} = \mathsf{dE_g}\ t_N^{\mathsf{A_{Q_{B0}}}} \tag{4.51a}$$

EB Zener tunneling current model Temperature scaling of the Zener tunneling current model for the emitter-base junction is partially based on the following well-known temperature dependence of the bandgap:

$$\mathsf{V_{gz0K}} = \max{}_{\mathtt{logexp}}(\mathsf{V_{gzEB}} + \frac{\mathsf{A_{VgEB}} * T_{RK}^2}{T_{RK} + T_{\mathsf{VgEB}}}, 0.05; 0.1) \tag{4.51b}$$

$$\mathsf{V_{gzEBT}} = \max{}_{\mathtt{logexp}}(\mathsf{V_{gz0K}} - \frac{\mathsf{A_{VgEB}} * T_K^2}{T_K + T_{\mathsf{VgEB}}}, 0.05; 0.1) \tag{4.51c}$$

The function $\max{}_{\mathtt{logexp}}(x, x_0; a)$, which is defined in expression (4.197) on page 59, is used to set a lower bound of $0.05\mathrm{V}$ to the bandgaps $\mathsf{V_{gz0K}}$ and $\mathsf{V_{gzEBT}}$.

Expression (4.51c) models a material property and the parameters of this expression, $\mathsf{V_{gz0K}}$, $\mathsf{A_{VgEB}}$ and T_{VgEB}, are material constants. Values of these are tabulated in table 4. The default values in Mextram correspond to the silicon values tabulated in table 4.

Table 4: *Example values of the material constants for temperature dependence of the bandgap of various semiconducting materials (see relation 4.51c).*

material	$\mathsf{V_{gz0K}}(\mathrm{eV})$	$\mathsf{A_{VgEB}}(10^{-4}\mathrm{eV/K})$	$T_{\mathsf{VgEB}}(\mathrm{K})$
GaAs	1.519	5.405	204
Si	1.170	4.730	636
Ge	0.7437	4.774	235

Note that $\mathsf{A_{VgEB}}$ and T_{VgEB} are also model parameters of the Mextram model, but $\mathsf{V_{gz0K}}$ is not. In Mextram, $\mathsf{V_{gz0K}}$ is an internal model variable, the value of which is calculated according to expression (4.51b). The parameter $\mathsf{V_{gzEB}}$ of this expression is also a Mextram model parameter.

In practice, bandgap will depend on material composition (alloys, SiGe) and doping concentration. Therefore, in practice the actual values of the quantities tabulated in table 4 may deviate from the tabulated values. Therefore, and in anticipation of application of Mextram to transistors in different materials, the parameters $\mathsf{V_{gzEB}}$, $\mathsf{A_{VgEB}}$ and T_{VgEB} are accessible in Mextram as model parameters. Because the Zener effect is relatively insensitive to temperature however, we expect that the default values of these parameters will suffice in practice and no parameter extraction for these parameters will be needed.

The following T-scaling rules for the Zener current model do not introduce any new parameter:

$$\mathsf{N_{zEBT}} = \mathsf{N_{zEB}} \left(\frac{\mathsf{V_{gzEBT}}}{\mathsf{V_{gzEB}}} \right)^{3/2} \left(\frac{\mathsf{V_{d_ET}}}{\mathsf{V_{d_E}}} \right)^{\mathsf{p_E}-1} \tag{4.51d}$$

$$\mathsf{I_{zEBT}} = \mathsf{I_{zEB}} \left(\frac{\mathsf{V_{gzEBT}}}{\mathsf{V_{gzEB}}} \right)^{-1/2} \left(\frac{\mathsf{V_{d_ET}}}{\mathsf{V_{d_E}}} \right)^{2-\mathsf{p_E}} \exp(\mathsf{N_{zEB}} - \mathsf{N_{zEBT}}) \tag{4.51e}$$

Self-heating

$$\mathsf{R_{th,Tamb}} = \mathsf{R_{th}} \cdot \left(\frac{T_{\mathrm{amb}}}{T_{RK}} \right)^{\mathsf{A_{th}}} \tag{4.51f}$$

4.8 Description of currents

4.8.1 Main current

Ideal forward and reverse current:

$$I_f = \mathsf{I_{sT}}\, e^{\mathcal{V}_{\mathrm{B_2E_1}}/V_T} \tag{4.52}$$

$$I_r = \mathsf{I_{sT}}\, e^{V^*_{B_2C_2}/V_T} \tag{4.53}$$

The value of $V^*_{B_2C_2}$ is not always the same as the node voltage $\mathcal{V}_{\mathrm{B_2C_2}}$. The expression for $e^{V^*_{B_2C_2}/V_T}$ is given in Eqs. (4.109) and (4.111).

The Moll-Ross or integral charge-control relation is used to take high injection in the base into account. To avoid dividing by zero at punch-through in Eq. (4.57) the depletion charge term q_0 is modified. (Note that for SiGe transistors q_0^I might differ from q_0^Q, defined in Eq. (4.89). See Sec. 4.12).

$$q_0^I = 1 + \frac{V_{t_E}}{\mathsf{V_{erT}}} + \frac{V_{t_C}}{\mathsf{V_{efT}}} \tag{4.54}$$

$$q_1^I = \frac{q_0^I + \sqrt{(q_0^I)^2 + 0.01}}{2} \tag{4.55}$$

$$q_B^I = q_1^I \left(1 + \tfrac{1}{2}\, n_0 + \tfrac{1}{2}\, n_B\right) \tag{4.56}$$

$$I_N = \frac{I_f - I_r}{q_B^I} \tag{4.57}$$

The expressions for V_{t_E}, V_{t_C}, n_0, and n_B are given by Eqs. (4.117b), (4.133), (4.148), and (4.151), respectively.

4.8.2 Forward base currents

The total ideal base current is separated into a bulk and a sidewall component. The bulk component depends on the voltage $\mathcal{V}_{\mathrm{B_2E_1}}$ and the sidewall component on the voltage $\mathcal{V}_{\mathrm{B_1E_1}}$. The separation is given by the parameter $\mathsf{XI_{B_1}}$. (Note that I_{B_1} becomes more complicated when $\mathsf{X_{rec}} \neq 0$. See Sec. 4.12).

Bulk component:

$$I_{B_1} = (1 - \mathsf{XI_{B_1}})\, \frac{\mathsf{I_{sT}}}{\boldsymbol{\beta}_{\mathsf{fT}}} \left(e^{\mathcal{V}_{\mathrm{B_2E_1}}/V_T} - 1\right) \tag{4.58}$$

Sidewall component:

$$I^S_{B_1} = \mathsf{XI_{B_1}}\, \frac{\mathsf{I_{sT}}}{\boldsymbol{\beta}_{\mathsf{fT}}} \left(e^{\mathcal{V}_{\mathrm{B_1E_1}}/V_T} - 1\right) \tag{4.59}$$

The non-ideal base current is given by:

$$I_{B_2} = \mathsf{I_{BfT}} \left(e^{\mathcal{V}_{\mathrm{B_2E_1}}/\mathsf{m_{Lf}}V_T} - 1\right) + G_{\min}\, \mathcal{V}_{\mathrm{B_2E_1}} \tag{4.60}$$

See section 4.15 for a discussion about $G_{\min}$.

4.8.3 Reverse base currents

In Mextram the non-ideal reverse base current is

$$I_{B_3} = \mathsf{I_{BrT}}\ \frac{e^{\mathcal{V}_{\mathrm{B_1C_4}}/V_T} - 1}{e^{\mathcal{V}_{\mathrm{B_1C_4}}/2V_T} + e^{\mathsf{V_{Lr}}/2V_T}} + G_{\min}\ \mathcal{V}_{\mathrm{B_1C_4}} \tag{4.61}$$

See section 4.15 for a discussion about $G_{\min}$.

The substrate current (holes injected from base into the substrate or reversely, the main current of the parasitic PNP), is given by

$$I_{\mathrm{sub}} = \frac{2\,\mathsf{I_{SsT}}\ \left(e^{\mathcal{V}_{\mathrm{B_1C_4}}/V_T} - 1\right)}{1 + \sqrt{1 + 4\,\dfrac{\mathsf{I_{sT}}}{\mathsf{I_{ksT}}}\ e^{\mathcal{V}_{\mathrm{B_1C_4}}/V_T}}} \tag{4.62}$$

which includes high injection. Note that in this expression $4\,\mathsf{I_{sT}}/\mathsf{I_{ksT}}$ is used instead of $4\,\mathsf{I_{SsT}}/\mathsf{I_{ksT}}$ which simplifies parameter extraction [3].

In backwards compatibility mode ($\mathsf{I_{CSs}} < 0$), the current with substrate bias in forward is only included as a signal to the designer. In this mode, no physical meaning should be attached to I_{Sf}:

$$I_{\mathrm{Sf}} = \mathsf{I_{SsT}}\ \left(e^{\mathcal{V}_{\mathrm{SC_1}}/V_T} - 1\right) \tag{4.63}$$

For physical values of $\mathsf{I_{CSs}}$ ($\mathsf{I_{CSs}} \geq 0$), the substrate-collector current is described by an ideal diode model that has a physics based temperature scaling rule:

$$I_{\mathrm{Sf}} = \mathsf{I_{CSsT}}\ \left(e^{\mathcal{V}_{\mathrm{SC_1}}/V_T} - 1\right) \tag{4.64}$$

The extrinsic base current (electrons injected from collector to extrinsic base, similar to I_{B_1}) is given by

$$g_1 = \frac{4\,\mathsf{I_{sT}}}{\mathsf{I_{kT}}}\ e^{\mathcal{V}_{\mathrm{B_1C_4}}/V_T} \tag{4.65}$$

$$n_{B\mathrm{ex}} = \frac{g_1}{1 + \sqrt{1 + g_1}} \tag{4.66}$$

$$I_{\mathrm{ex}} = \frac{1}{\boldsymbol{\beta}_{\mathsf{iT}}}\ \left(\tfrac{1}{2}\,\mathsf{I_{kT}}\ n_{B\mathrm{ex}} - \mathsf{I_{sT}}\right) \tag{4.67}$$

4.8.4 Weak-avalanche current

In reverse mode ($I_{C_1C_2} \leq 0$) or hard saturation ($\mathcal{V}_{\mathrm{B_2C_1}} \geq \mathsf{V_{dCT}}$) both the avalanche current $I_{\mathrm{avl}} = 0$ and the generation factor G_{EM} are zero

$$I_{\mathrm{avl}} = 0\ ,\ G_{\mathrm{EM}} = 0 \tag{4.68}$$

In forward mode we have the following gradient of the electric field for zero bias

$$dEdx_0 = \frac{2\,\mathsf{V_{avl}}}{\mathsf{W_{avl}}^2} \tag{4.69}$$

The depletion layer thickness becomes

$$x_D = \sqrt{\frac{2}{dEdx_0}}\,\sqrt{\frac{\mathsf{V_{dcT}} - \mathcal{V}_{\mathrm{B_2C_1}}}{1 - I_{\mathrm{cap}}/\mathsf{I_{hc}}}} \tag{4.70}$$

The current I_{cap} will be given in Eq. (4.130).

The generation of avalanche current increases at high current levels. This is only taken into account when flag $\mathsf{EXAVL} = 1$.

When $\mathsf{EXAVL} = 0$, then the effective thickness of the epilayer is

$$W_{\mathrm{eff}} = \mathsf{W_{avl}} \tag{4.71}$$

When $\mathsf{EXAVL} = 1$, then

$$W_{\mathrm{eff}} = \mathsf{W_{avl}}\,\left(1 - \frac{x_i}{2\,W_{\mathrm{epi}}}\right)^2 \tag{4.72}$$

For either value of EXAVL the thickness over which the electric field is important is

$$W_D = \frac{x_D\,W_{\mathrm{eff}}}{\sqrt{x_D^2 + W_{\mathrm{eff}}^2}} \tag{4.73}$$

The average electric field and the field at the base-collector junction are

$$E_{\mathrm{av}} = \frac{\mathsf{V_{dcT}} - \mathcal{V}_{\mathrm{B_2C_1}}}{W_D} \tag{4.74}$$

$$E_0 = E_{\mathrm{av}} + \tfrac{1}{2}W_D\;dEdx_0\;\left(1 - \frac{I_{\mathrm{cap}}}{\mathsf{I_{hc}}}\right) \tag{4.75}$$

When $\mathsf{EXAVL} = 0$, then the maximum of the electric field is

$$E_M = E_0 \tag{4.76}$$

When $\mathsf{EXAVL} = 1$, then

$$SH_W = 1 + 2\,\mathsf{S_{fH}}\;\left(1 + 2\,\frac{x_i}{W_{\mathrm{epi}}}\right) \tag{4.77}$$

$$E_{fi} = \frac{1 + \mathsf{S_{fH}}}{1 + 2\,\mathsf{S_{fH}}} \tag{4.78}$$

$$E_W = E_{\rm av} - \tfrac{1}{2}\, W_D\; dEdx_0 \left(E_{fi} - \frac{I_{C_1C_2}}{\mathsf{I_{hc}}\; SH_W} \right) \tag{4.79}$$

$$E_M = \tfrac{1}{2} \left(E_W + E_0 + \sqrt{(E_W - E_0)^2 + 0.1\; E_{\rm av}^2\; I_{\rm cap}/\mathsf{I_{hc}}} \right) \tag{4.80}$$

The injection thickness $x_i/W_{\rm epi}$ is given in Eq. (4.106).

For either value of EXAVL the intersection point λ_D and the generation factor $G_{\rm EM}$ are

$$\lambda_D = \frac{E_M\; W_D}{2\,(E_M - E_{\rm av})} \tag{4.81}$$

$$G_{\rm EM} = \frac{A_n}{B_{n\rm T}}\; E_M\; \lambda_D \left\{ \exp\left[-\frac{B_{n\rm T}}{E_M} \right] - \exp\left[-\frac{B_{n\rm T}}{E_M} \left(1 + \frac{W_{\rm eff}}{\lambda_D} \right) \right] \right\} \tag{4.82}$$

When $E_M \simeq E_{\rm av}$ the expression for λ_D will diverge. Hence for $(1 - E_{\rm av}/E_M) < 10^{-7}$ we need to take the appropriate analytical limit and get:

$$G_{\rm EM} = A_n\; W_{\rm eff} \exp\left[-\frac{B_{n\rm T}}{E_M} \right] \tag{4.83}$$

The generation factor may not exceed 1 and may not exceed

$$G_{\rm max} = \frac{V_T}{I_{C_1C_2}\; (\mathsf{R_{BcT}} + R_{B_2})} + \frac{q_B^I}{\beta_{f\rm T}} + \frac{\mathsf{R_{ET}}}{\mathsf{R_{BcT}} + R_{B_2}} \tag{4.84}$$

The variable base resistance R_{B_2} is given by Eq. (4.92). The base charge terms q_B^I is given by Eq. (4.56). The current $I_{C_1C_2}$ is given by Eq. (4.98). The avalanche current then is

$$I_{\rm avl} = I_{C_1C_2}\; \frac{G_{\rm EM}\; G_{\rm max}}{G_{\rm EM}\; G_{\rm max} + G_{\rm EM} + G_{\rm max}} \tag{4.85}$$

4.8.5 Emitter-base Zener tunneling current

In Mextram 504.9, the contribution to the current across the emitter-base junction due to Zener tunneling effects is assumed to be always negligible in forward mode; hence $I_{\rm ztEB} = 0$ whenever $0 \le V_{B_2E_1}$. In reverse mode, $V_{B_2E_1} < 0$, it is modeled by the expressions below. Note that the transition at $V_{B_2E_1} = 0$ is non-trivial, yet the model for Zener tunneling current is C^∞: all derivatives of the Zener tunneling current $I_{\rm ztEB}$ are continuous everywhere, including $V_{B_2E_1} = 0$.

$$x_z = \frac{\mathcal{V}_{\rm B_2E_1}}{\mathsf{V_{dET}}} \tag{4.86a}$$

$$\tilde{E}_{0\mathrm{EB}} = \frac{1}{6\,(-x_z)^{2+\mathsf{p_E}}}\left(\mathsf{p_E}\left(1-{\mathsf{p_E}}^2-3x_z\,(\mathsf{p_E}-1)\right)-6x_z^2\,(\mathsf{p_E}-1+x_z)\right) \quad (4.86b)$$

$$D_{\mathrm{zEB}} = -\mathcal{V}_{\mathrm{B_2E_1}} - \frac{\mathsf{V_{gzEBT}}}{2^{2-\mathsf{p_E}}\,\mathsf{N_{zEBT}}}\,\tilde{E}_{0\mathrm{EB}}\left(1-\exp\left(\frac{2^{2-\mathsf{p_E}}\mathsf{N_{zEBT}}\,\mathcal{V}_{\mathrm{B_2E_1}}}{\mathsf{V_{gzEBT}}\,\tilde{E}_{0\mathrm{EB}}}\right)\right) \quad (4.87)$$

The Zener tunneling current I_{ztEB} is defined to be positive if it runs from node E_1 to node B_2.

$$I_{\mathrm{ztEB}} = \frac{\mathsf{I_{zEBT}}}{2^{1-\mathsf{p_E}}\,\mathsf{V_{d_ET}}}\,D_{\mathrm{zEB}}\,E_{0\mathrm{EB}}\exp\left(\mathsf{N_{zEBT}}\left(1-\frac{2^{1-\mathsf{p_E}}}{E_{0\mathrm{EB}}}\right)\right) \quad (4.88)$$

where $E_{0\mathrm{EB}}$ is as defined by expression (4.117a) on page 49.

4.8.6 Resistances

The parasitic resistances for the emitter ($\mathsf{R_{ET}}$), the base ($\mathsf{R_{BcT}}$) and the collector ($\mathsf{R_{CcT}}$, $\mathsf{R_{CblxT}}$ and $\mathsf{R_{CbliT}}$) depend only on temperature.

4.8.7 Variable base resistance

The variable part of the base resistance is modulated by the base charges and takes into account current crowding.

$$q_0^Q = 1 + \frac{V_{t_E}}{\mathsf{V_{erT}}} + \frac{V_{t_C}}{\mathsf{V_{efT}}} \quad (4.89)$$

$$q_1^Q = \frac{q_0^Q + \sqrt{(q_0^Q)^2 + 0.01}}{2} \quad (4.90)$$

$$q_B^Q = q_1^Q\,(1 + \tfrac{1}{2}\,n_0 + \tfrac{1}{2}\,n_B) \quad (4.91)$$

$$R_{B_2} = \frac{3\,\mathsf{R_{BvT}}}{q_B^Q} \quad (4.92)$$

$$I_{B_1B_2} = \frac{2V_T}{R_{B_2}}\left(e^{\mathcal{V}_{\mathrm{B_1B_2}}/V_T}-1\right) + \frac{\mathcal{V}_{\mathrm{B_1B_2}}}{R_{B_2}} \quad (4.93)$$

Note the correspondance and differences between R_{B_2} and I_N from Eq. (4.57).

4.8.8 Variable collector resistance: the epilayer model

This model of the epilayer resistance takes into account:
– The decrease in resistance due to carriers injected from the base if only the internal base-collector is forward biased (quasi-saturation) and if both the internal and external base-collector junctions are forward biased (hard saturation and reverse mode of operation).
– Ohmic current flow at low current densities.
– Space charge limited current flow at high current densities (Kirk effect; only in forward mode).

The current through the epilayer is given by

$$K_0 = \sqrt{1 + 4\, e^{(\mathcal{V}_{\mathrm{B_2C_2}} - \mathsf{V_{dCT}})/V_T}} \tag{4.94}$$

$$K_W = \sqrt{1 + 4\, e^{(\mathcal{V}_{\mathrm{B_2C_1}} - \mathsf{V_{dCT}})/V_T}} \tag{4.95}$$

$$p_W = \frac{2\, e^{(\mathcal{V}_{\mathrm{B_2C_1}} - \mathsf{V_{dCT}})/V_T}}{1 + K_W} \tag{4.96}$$

For numerical reasons: when $p_W < e^{-40}$ we take $p_W \rightarrow 0$.

$$E_c = V_T \left[K_0 - K_W - \ln\left(\frac{K_0 + 1}{K_W + 1} \right) \right] \tag{4.97}$$

$$I_{C_1C_2} = \frac{E_c + \mathcal{V}_{\mathrm{C_1C_2}}}{\mathsf{R_{CvT}}} \tag{4.98}$$

In reverse mode the node voltage difference $\mathcal{V}_{\mathrm{B_2C_2}}$ is the quantity that we use in further calculations. In forward mode the relation between the voltage difference $\mathcal{V}_{\mathrm{B_2C_2}}$ and the current $I_{C_1C_2}$ is not smooth enough. We will instead calculate $V^*_{B_2C_2}$ that is to be used in subsequent calculations. It has smoother properties than $\mathcal{V}_{\mathrm{B_2C_2}}$ itself. In forward mode the node voltage $\mathcal{V}_{\mathrm{C_2}}$ is *only* used for Eqs. (4.94) and (4.98).

For the rest of the quantities in the epilayer model a distinction must be made between forward and reverse mode.

Forward mode ($I_{C_1C_2} > 0$) The voltage and current at which quasi-saturation or Kirk effect start are given by

$$V_{qs}^{th} = \mathsf{V_{dCT}} + 2\, V_T \ln\left(\frac{I_{C_1C_2}\, \mathsf{R_{CvT}}}{2V_T} + 1 \right) - \mathcal{V}_{\mathrm{B_2C_1}} \tag{4.99}$$

$$V_{qs} = \tfrac{1}{2} \left(V_{qs}^{th} + \sqrt{(V_{qs}^{th})^2 + 4\, (0.1\, \mathsf{V_{dCT}})^2} \right) \tag{4.100}$$

$$I_{qs} = \frac{V_{qs}}{\mathsf{SCR_{Cv}}} \frac{V_{qs} + \mathsf{I_{hc}}\ \mathsf{SCR_{Cv}}}{V_{qs} + \mathsf{I_{hc}}\ \mathsf{R_{CvT}}} \tag{4.101}$$

From this we calculate

$$\alpha = \frac{1 + \mathsf{a_{x_i}}\ \ln\{1 + \exp[(I_{C_1C_2}/I_{qs} - 1)/\mathsf{a_{x_i}}]\}}{1 + \mathsf{a_{x_i}}\ \ln\{1 + \exp[-1/\mathsf{a_{x_i}}]\}} \tag{4.102}$$

We need to solve

$$\alpha\ I_{qs} = \frac{V_{qs}}{\mathsf{SCR_{Cv}}\ y_i^2} \frac{V_{qs} + \mathsf{SCR_{Cv}}\ \mathsf{I_{hc}}\ y_i}{V_{qs} + \mathsf{R_{CvT}}\ \mathsf{I_{hc}}} \tag{4.103}$$

which leads to

$$v = \frac{V_{qs}}{\mathsf{I_{hc}}\ \mathsf{SCR_{Cv}}} \tag{4.104}$$

$$y_i = \frac{1 + \sqrt{1 + 4\,\alpha\,v\,(1+v)}}{2\,\alpha\,(1+v)} \tag{4.105}$$

The injection thickness is given by

$$\frac{x_i}{W_{\mathrm{epi}}} = 1 - \frac{y_i}{1 + p_W y_i} \tag{4.106}$$

The hole density p_0^* at the base-collector junction is given by

$$g = \frac{I_{C_1C_2}\ \mathsf{R_{CvT}}}{2V_T} \frac{x_i}{W_{\mathrm{epi}}} \tag{4.107}$$

$$p_0^* = \frac{g-1}{2} + \sqrt{\left(\frac{g-1}{2}\right)^2 + 2g + p_W(p_W + g + 1)} \tag{4.108}$$

For numerical reasons: when $p_0^* < e^{-40}$ we take $p_0^* \to 0$.

$$e^{V^*_{B_2C_2}/V_T} = p_0^*(p_0^* + 1)\ e^{\mathsf{V_{dCT}}/V_T} \tag{4.109}$$

Reverse mode ($I_{C_1C_2} \le 0$) The hole density at the base-collector junction is given by

$$p_0^* = \frac{2\,e^{(\mathcal{V}_{\mathrm{B_2C_2}} - \mathsf{V_{dCT}})/V_T}}{1 + K_0} \tag{4.110}$$

$$e^{V^*_{B_2C_2}/V_T} = e^{\mathcal{V}_{\mathrm{B_2C_2}}/V_T} \tag{4.111}$$

The injection thickness is

$$\frac{x_i}{W_{\mathrm{epi}}} = \frac{E_c}{E_c + \mathcal{V}_{\mathrm{B_2C_2}} - \mathcal{V}_{\mathrm{B_2C_1}}} \tag{4.112}$$

Numerical problems might arise for $I_{C_1C_2} \simeq 0$. When $|\mathcal{V}_{\mathrm{C_1C_2}}| < 10^{-5}\, V_T$ or $|E_c| < e^{-40}\, V_T\, (K_0 + K_W)$ we approximate

$$p_{\mathrm{av}} = \frac{p_0^* + p_W}{2} \tag{4.113}$$

$$\frac{x_i}{W_{\mathrm{epi}}} = \frac{p_{\mathrm{av}}}{p_{\mathrm{av}} + 1} \tag{4.114}$$

4.9 Description of charges

4.9.1 Emitter depletion charges

The total base-emitter depletion capacitance is separated into a bulk and as sidewall component. The bulk component is located between nodes E_1 and B_2 and the sidewall component between nodes E_1 and B_1 (see Fig. 1)

The bulk component is

$$V_{FE} = \mathsf{V_{d_ET}} \left(1 - a_{j_E}^{-1/\mathsf{p_E}}\right) \tag{4.115}$$

$$V_{jE} = \mathcal{V}_{\mathrm{B_2E_1}} - 0.1\mathsf{V_{d_ET}} \ln\{1 + \exp[(\mathcal{V}_{\mathrm{B_2E_1}} - V_{FE})/0.1\mathsf{V_{d_ET}}]\} \tag{4.116}$$

$$E_{0}\mathrm{EB} = (1 - V_{jE}/\mathsf{V_{d_ET}})^{1-\mathsf{p_E}} \tag{4.117a}$$

$$V_{t_E} = \frac{\mathsf{V_{d_ET}}}{1-\mathsf{p_E}} \left[1 - E_{0}\mathrm{EB}\right] + a_{j_E}(\mathcal{V}_{\mathrm{B_2E_1}} - V_{jE}) \tag{4.117b}$$

$$Q_{t_E} = (1 - \mathsf{XC_{j_E}})\ \mathsf{C_{j_ET}}\ V_{t_E} \tag{4.118}$$

The sidewall component is

$$V_{jE}^{S} = \mathcal{V}_{\mathrm{B_1E_1}} - 0.1\mathsf{V_{d_ET}} \ln\{1 + \exp[(\mathcal{V}_{\mathrm{B_1E_1}} - V_{FE})/0.1\mathsf{V_{d_ET}}]\} \tag{4.119}$$

$$Q_{t_E}^{S} = \mathsf{XC_{j_E}}\ \mathsf{C_{j_ET}} \left(\frac{\mathsf{V_{d_ET}}}{1-\mathsf{p_E}} \left[1 - (1-V_{jE}^{S}/\mathsf{V_{d_ET}})^{1-\mathsf{p_E}}\right] + a_{j_E}(\mathcal{V}_{\mathrm{B_1E_1}} - V_{jE}^{S})\right) \tag{4.120}$$

4.9.2 Intrinsic collector depletion charge

In forward mode ($I_{C_1C_2} > 0$)

$$B_1 = \tfrac{1}{2}\mathsf{SCR_{Cv}}(I_{C_1C_2} - \mathsf{I_{hc}}) \tag{4.121}$$

$$B_2 = \mathsf{SCR_{Cv}}\ \mathsf{R_{CvT}}\ \mathsf{I_{hc}}\ I_{C_1C_2} \tag{4.122}$$

$$V_{x_i=0} = B_1 + \sqrt{B_1^2 + B_2} \tag{4.123}$$

In reverse mode ($I_{C_1C_2} \leq 0$)

$$V_{x_i=0} = \mathcal{V}_{\mathrm{C_1C_2}} \tag{4.124}$$

The junction voltage for the capacitance is given by

$$V_{\mathrm{junc}} = \mathcal{V}_{\mathrm{B_2C_1}} + V_{x_i=0} \tag{4.125}$$

The capacitance can now be calculated using

$$V_{ch} = \begin{cases} 0.1\ \mathsf{V_{dC}T} & \text{for } I_{C_1C_2} \leq 0 \\ \mathsf{V_{dC}T}\left(0.1 + 2\,\dfrac{I_{C_1C_2}}{I_{C_1C_2} + I_{qs}}\right) & \text{for } I_{C_1C_2} > 0 \end{cases} \tag{4.126}$$

$$b_{j_C} = \frac{a_{j_C} - \mathsf{X_{pT}}}{1 - \mathsf{X_{pT}}} \tag{4.127}$$

$$V_{FC} = \mathsf{V_{dC}T}\left(1 - b_{j_C}^{-1/\mathsf{pc}}\right) \tag{4.128}$$

$$V_{jC} = V_{\mathrm{junc}} - V_{ch}\ln\{1 + \exp[(V_{\mathrm{junc}} - V_{FC})/V_{ch}]\} \tag{4.129}$$

The current dependence is given by

$$I_{\mathrm{cap}} = \begin{cases} \dfrac{\mathsf{I_{hc}}\ I_{C_1C_2}}{\mathsf{I_{hc}} + I_{C_1C_2}} & \text{for } I_{C_1C_2} > 0 \\ I_{C_1C_2} & \text{for } I_{C_1C_2} \leq 0 \end{cases} \tag{4.130}$$

$$f_I = \left(1 - \frac{I_{\mathrm{cap}}}{\mathsf{I_{hc}}}\right)^{\mathsf{mC}} \tag{4.131}$$

The charge is now given by

$$V_{C_V} = \frac{\mathsf{V_{dC}T}}{1 - \mathsf{pC}}\left[1 - f_I\ (1 - V_{jC}/\mathsf{V_{dC}T})^{1-\mathsf{pC}}\right] + f_I\ b_{j_C}(V_{\mathrm{junc}} - V_{jC}) \tag{4.132}$$

$$V_{t_C} = (1 - \mathsf{X_{pT}})\ V_{C_V} + \mathsf{X_{pT}}\mathcal{V}_{\mathrm{B_2C_1}} \tag{4.133}$$

$$Q_{t_C} = \mathsf{XC_{jC}}\ \mathsf{C_{jC}T}\ V_{t_C} \tag{4.134}$$

4.9.3 Extrinsic collector depletion charges

The extrinsic collector depletion charge is partitioned between nodes C_1 and B_1 and nodes C_1 and B respectively, independent of the flag EXMOD.

$$V_{jC_{\rm ex}} = \mathcal{V}_{\rm B_1C_4} - 0.1\mathsf{V_{dC}T}\ln\{1+\exp[(\mathcal{V}_{\rm B_1C_4} - V_{FC})/0.1\mathsf{V_{dC}T}]\} \tag{4.135}$$

$$V_{\rm tex_V} = \frac{\mathsf{V_{dC}T}}{1-\mathsf{p_C}}\left[1-(1-V_{jC_{\rm ex}}/\mathsf{V_{dC}T})^{1-\mathsf{p_C}}\right] + b_{j_C}(\mathcal{V}_{\rm B_1C_4} - V_{jC_{\rm ex}}) \tag{4.136}$$

$$Q_{\rm tex} = \mathsf{C_{jC}T}\ \left[(1-\mathsf{X_{pT}})\ V_{\rm tex_V} + \mathsf{X_{pT}}\mathcal{V}_{\rm B_1C_4}\right](1-\mathsf{XC_{jC}})\ (1-\mathsf{X_{ext}}) \tag{4.137}$$

$$XV_{jC_{\rm ex}} = \mathcal{V}_{\rm BC_3} - 0.1\mathsf{V_{dC}T}\ln\{1+\exp[(\mathcal{V}_{\rm BC_3} - V_{FC})/0.1\mathsf{V_{dC}T}]\} \tag{4.138}$$

$$XV_{\rm tex_V} = \frac{\mathsf{V_{dC}T}}{1-\mathsf{p_C}}\left[1-(1-XV_{jC_{\rm ex}}/\mathsf{V_{dC}T})^{1-\mathsf{p_C}}\right] + b_{j_C}(\mathcal{V}_{\rm BC_3} - XV_{jC_{\rm ex}}) \tag{4.139}$$

$$XQ_{\rm tex} = \mathsf{C_{jC}T}\ \left[(1-\mathsf{X_{pT}})\ XV_{\rm tex_V} + \mathsf{X_{pT}}\mathcal{V}_{\rm BC_3}\right](1-\mathsf{XC_{jC}})\ \mathsf{X_{ext}} \tag{4.140}$$

4.9.4 Substrate depletion charge

$$V_{FS} = \mathsf{V_{dS}T}\left(1-a_{j_S}^{-1/\mathsf{p_S}}\right) \tag{4.141}$$

$$V_{jS} = \mathcal{V}_{\rm SC_1} - 0.1\mathsf{V_{dS}T}\ln\{1+\exp[(\mathcal{V}_{\rm SC_1} - V_{FS})/0.1\mathsf{V_{dS}T}]\} \tag{4.142}$$

$$Q_{t_S} = \mathsf{C_{jS}T}\ \left(\frac{\mathsf{V_{dS}T}}{1-\mathsf{p_S}}\left[1-(1-V_{jS}/\mathsf{V_{dS}T})^{1-\mathsf{p_S}}\right] + a_{j_S}(\mathcal{V}_{\rm SC_1} - V_{jS})\right) \tag{4.143}$$

4.9.5 Stored emitter charge

$$Q_{E0} = \tau_{\rm ET}\ \mathsf{I_{kT}}\left(\frac{\mathsf{I_{sT}}}{\mathsf{I_{kT}}}\right)^{1/\mathsf{m_\tau}} \tag{4.144}$$

$$Q_E = Q_{E0}\ \left(e^{\mathcal{V}_{\rm B_2E_1}/\mathsf{m_\tau}\,V_T} - 1\right) \tag{4.145}$$

4.9.6 Stored base charges

$$Q_{B0} = \tau_{\mathrm{BT}}\ \mathsf{I}_{\mathrm{kT}} \tag{4.146}$$

Base-emitter part

$$f_1 = \frac{4\,\mathsf{I}_{\mathrm{sT}}}{\mathsf{I}_{\mathrm{kT}}}\ e^{\mathcal{V}_{\mathrm{B_2E_1}}/V_T} \tag{4.147}$$

$$n_0 = \frac{f_1}{1+\sqrt{1+f_1}} \tag{4.148}$$

$$Q_{BE} = \tfrac{1}{2}\,Q_{B0}\ n_0\ q_1^Q \tag{4.149}$$

Base-collector part

$$f_2 = \frac{4\,\mathsf{I}_{\mathrm{sT}}}{\mathsf{I}_{\mathrm{kT}}}\ e^{V^*_{B_2C_2}/V_T} \tag{4.150}$$

$$n_B = \frac{f_2}{1+\sqrt{1+f_2}} \tag{4.151}$$

$$Q_{BC} = \tfrac{1}{2}\,Q_{B0}\ n_B\ q_1^Q \tag{4.152}$$

The expression for $e^{V^*_{B_2C_2}/V_T}$ is given in Eqs. (4.109) and (4.111).

4.9.7 Stored epilayer charge

$$Q_{\mathrm{epi0}} = \frac{4\,\tau_{\mathsf{epiT}}\ V_T}{\mathsf{R}_{\mathsf{CvT}}} \tag{4.153}$$

$$Q_{\mathrm{epi}} = \tfrac{1}{2}\ Q_{\mathrm{epi0}}\ \frac{x_i}{W_{\mathrm{epi}}}\ (p_0^* + p_W + 2) \tag{4.154}$$

4.9.8 Stored extrinsic charges

$$g_2 = 4\,e^{(\mathcal{V}_{\mathrm{B_1C_4}} - \mathsf{V}_{\mathsf{dCT}})/V_T} \tag{4.155}$$

$$p_{W\mathrm{ex}} = \frac{g_2}{1+\sqrt{1+g_2}} \tag{4.156}$$

$$Q_{\mathrm{ex}} = \frac{\tau_{\mathsf{RT}}}{\tau_{\mathsf{BT}} + \tau_{\mathsf{epiT}}}\ \left(\tfrac{1}{2}\,Q_{B0}\ n_{B\mathrm{ex}} + \tfrac{1}{2}\,Q_{\mathrm{epi0}}\ p_{W\mathrm{ex}}\right) \tag{4.157}$$

The electron density $n_{B\mathrm{ex}}$ is given in Eq. (4.66).

4.9.9 Overlap charges

The overlap capacitances C_{BEO} and C_{BCO} are constant.

4.10 Extended modelling of the reverse current gain EXMOD=1

4.10.1 Currents

The reverse currents $I_{\rm ex}$ and $I_{\rm sub}$ are redefined

$$I_{\rm ex} \rightarrow (1 - \mathsf{X_{ext}})\ I_{\rm ex} \tag{4.158}$$

$$I_{\rm sub} \rightarrow (1 - \mathsf{X_{ext}})\ I_{\rm sub} \tag{4.159}$$

The part $\mathsf{X_{ext}}$ of the reverse currents in the extrinsic transistor are connected to the external base node

$$Xg_1 = \frac{4\,\mathsf{I_{sT}}}{\mathsf{I_{kT}}}\ e^{\mathcal{V}_{\rm BC_3}/V_T} \tag{4.160}$$

$$Xn_{B\rm ex} = \frac{Xg_1}{1+\sqrt{1+Xg_1}} \tag{4.161}$$

$$XIM_{\rm ex} = \frac{\mathsf{X_{ext}}}{\mathsf{\beta_{riT}}}\ (\tfrac{1}{2}\,\mathsf{I_{kT}}\ Xn_{B\rm ex} - \mathsf{I_{sT}}) \tag{4.162}$$

$$XIM_{\rm sub} = \mathsf{X_{ext}}\ \frac{2\,\mathsf{I_{SsT}}\ \left(e^{\mathcal{V}_{\rm BC_3}/V_T}-1\right)}{1+\sqrt{1+4\,\dfrac{\mathsf{I_{sT}}}{\mathsf{I_{ksT}}}\ e^{\mathcal{V}_{\rm BC_3}/V_T}}} \tag{4.163}$$

To improve the convergency behaviour the diode-like currents in the branch B-C_1 are limited by a resistance of value $\mathsf{R_{CcT}}$:

$$V_{\rm ex} = V_T\ \left\{2 - \ln\left[\frac{\mathsf{X_{ext}}\ (\mathsf{I_{sT}}/\mathsf{\beta_{riT}} + \mathsf{I_{SsT}})\ \mathsf{R_{CcT}}}{V_T}\right]\right\} \tag{4.164}$$

$$VB_{\rm ex} = \tfrac{1}{2}\left[(\mathcal{V}_{\rm BC_3} - V_{\rm ex}) + \sqrt{(\mathcal{V}_{\rm BC_3} - V_{\rm ex})^2 + 0.0121}\right] \tag{4.165}$$

$$F_{\rm ex} = \frac{VB_{\rm ex}}{\mathsf{X_{ext}}\ (\mathsf{I_{sT}}/\mathsf{\beta_{riT}} + \mathsf{I_{SsT}})\ \mathsf{R_{CcT}} + (XIM_{\rm ex} + XIM_{\rm sub})\ \mathsf{R_{CcT}} + VB_{\rm ex}} \tag{4.166}$$

$$XI_{\rm ex} = F_{\rm ex}\ XIM_{\rm ex} \tag{4.167}$$

$$XI_{\rm sub} = F_{\rm ex}\ XIM_{\rm sub} \tag{4.168}$$

4.10.2 Charges

The charge $Q_{\rm ex}$ is redefined:

$$Q_{\rm ex} \rightarrow (1 - \mathsf{X_{ext}})\, Q_{\rm ex} \tag{4.169}$$

The charge in the branch B-C_3 is also limited by using $F_{\rm ex}$

$$Xg_2 = 4\, e^{(\mathcal{V}_{\rm BC_3} - \mathsf{V_{d_CT}})/V_T} \tag{4.170}$$

$$Xp_{W\rm ex} = \frac{Xg_2}{1 + \sqrt{1 + Xg_2}} \tag{4.171}$$

$$XQ_{\rm ex} = F_{\rm ex}\, \mathsf{X_{ext}}\, \frac{\tau_{\rm RT}}{\tau_{\rm BT} + \tau_{\rm epiT}}\, \left(\tfrac{1}{2}\, Q_{B0}\, Xn_{B\rm ex} + \tfrac{1}{2}\, Q_{\rm epi0}\, Xp_{W\rm ex}\right) \tag{4.172}$$

4.11 Distributed high-frequency effects in the intrinsic base $\mathsf{EXPHI}{=}1$

Distributed high-frequency effects are modelled, in first order approximation, both in lateral direction (current crowding) and in vertical direction (excess phase-shift). The distributed effects are an optional part of the Mextram model and can be switched on and off by a flag (on: $\mathsf{EXPHI} = 1$ and off: $\mathsf{EXPHI} = 0$).

The high-frequency current crowding is modelled by

$$Q_{B_1B_2} = \tfrac{1}{5}\, \mathcal{V}_{\rm B_1B_2}\, \left(\frac{{\rm d}Q_{t_E}}{{\rm d}\mathcal{V}_{\rm B_2E_1}} + \tfrac{1}{2}\, Q_{B0}\, q_1^Q\, \frac{{\rm d}n_0}{{\rm d}\mathcal{V}_{\rm B_2E_1}} + \frac{{\rm d}Q_E}{{\rm d}\mathcal{V}_{\rm B_2E_1}}\right) \tag{4.173}$$

For simplicity reasons only the forward depletion and diffusion charges are taken into account. (Note that the second term is the derivative of $Q_{BE} = \frac{1}{2} Q_{B0}\, q_1^Q\, n_0$, but with the derivative of q_1^Q neglected).

In vertical direction (excess phase-shift) base-charge partitioning is used. For simplicity reasons it is only implemented for the forward base charge (Q_{BE}) and for high level injection. Now Q_{BE} from Eq. (4.149) and Q_{BC} from Eq. (4.152) are redefined according to

$$Q_{BC} \rightarrow \tfrac{1}{3}\, Q_{BE} + Q_{BC} \tag{4.175}$$

$$Q_{BE} \rightarrow \tfrac{2}{3}\, Q_{BE} \tag{4.176}$$

4.12 Heterojunction features

The most important difference between SiGe and pure Si transistors is the functional difference between hole charges and Gummel number. When the Ge concentration has a non-zero slope ($\mathsf{dE_g} \neq 0$) we redefine the q_0^I describing the Early effect for the currents (the q_0^Q remains unchanged):

$$q_0^I \rightarrow \frac{\exp\left(\left[\frac{V_{t_E}}{\mathsf{V_{erT}}}+1\right]\ \frac{\mathsf{dE_{gT}}}{V_T}\right)-\exp\left(\frac{-V_{t_C}}{\mathsf{V_{efT}}}\ \frac{\mathsf{dE_{gT}}}{V_T}\right)}{\exp\left(\frac{\mathsf{dE_{gT}}}{V_T}\right)-1} \tag{4.177}$$

Another feature that might be needed for SiGe transistors is recombination in the base. This changes the forward ideal base current (when $\mathsf{X_{rec}} \neq 0$)

$$\begin{aligned} I_{B_1} \rightarrow \frac{\mathsf{I_{sT}}}{\beta_{\mathrm{fT}}}\left(1-\mathsf{XI_{B_1}}\right)\Bigg[&\left(1-\mathsf{X_{rec}}\right)\ \left(e^{\mathcal{V}_{\mathrm{B_2E_1}}/V_T}-1\right) \\ &+\mathsf{X_{rec}}\left(e^{\mathcal{V}_{\mathrm{B_2E_1}}/V_T}+e^{V^*_{B_2C_2}/V_T}-2\right)\left(1+\frac{V_{t_C}}{\mathsf{V_{efT}}}\right)\Bigg] \end{aligned} \tag{4.178}$$

The last term also describes Auger recombination in high injection.

4.13 Noise model

For noise analysis noise current sources are added to the small-signal equivalent circuit. In these equations f represents the operation frequency of the transistor and Δf is the bandwidth. When Δf is taken as $1\,\mathrm{Hz}$, a noise density is obtained.

Thermal noise:

$$\overline{iN_{R_E}^2} = \frac{4\,kT_K}{\mathsf{R_{ET}}}\,\Delta f \tag{4.179}$$

$$\overline{iN_{R_{Bc}}^2} = \frac{4\,kT_K}{\mathsf{R_{BcT}}}\,\Delta f \tag{4.180}$$

$$\overline{iN_{R_{Cc}}^2} = 4\,kT_K\,\mathsf{G_{CcT}}\,\Delta f \tag{4.181a}$$

$$\overline{iN_{\mathsf{R_{Cblx}}}^2} = 4\,kT_K\,\mathsf{G_{CblxT}}\,\Delta f \tag{4.181b}$$

$$\overline{iN_{\mathsf{R_{Cbli}}}^2} = 4\,kT_K\,\mathsf{G_{CbliT}}\,\Delta f \tag{4.181c}$$

For the variable part of the base resistance a different formula is used, taking into account the effect of current crowding on noise behaviour [23]

$$\overline{iN_{R_{Bv}}^2} = \frac{4\,kT_K}{R_{B_2}}\,\frac{4\,e^{\mathcal{V}_{\mathrm{B_1B_2}}/V_T}+5}{3}\,\Delta f \tag{4.182}$$

Correlation between base and collector current noise sources due to avalanche [25] ¶

$$\overline{iN_B\;iN_C^*} = -\mathsf{K_{avl}}\cdot 2qI_{\mathrm{avl}}\cdot(2+2G_{\mathrm{EM}})\,\Delta f \tag{4.183}$$

Collector current shot noise, including avalanche contribution

$$\overline{iN_C^2} = 2q\,\frac{I_f+I_r}{q_B^I}\,\Delta f + \mathsf{K_{avl}}\cdot 2qI_{\mathrm{avl}}\cdot(3+2G_{\mathrm{EM}})\,\Delta f \tag{4.184}$$

Forward base current shot noise, $1/f$-noise, and avalanche contribution

$$\overline{iN_B^2} = \left\{2q\,\left(|I_{B_1}|+|I_{B_2}|+|I_{\mathrm{ZtEB}}|\right)+\frac{\mathsf{K_f}}{f}\,(1-\mathsf{XI_{B_1}})\,\left(\frac{|I_{B_1}|}{1-\mathsf{XI_{B_1}}}\right)^{\mathsf{A_f}}\right.$$
$$\left.+\frac{\mathsf{K_{fN}}}{f}\,|I_{B_2}|^{2(\mathsf{m_{Lf}}-1)+\mathsf{A_f}(2-\mathsf{m_{Lf}})}\right\}\Delta f + \mathsf{K_{avl}}\cdot 2qI_{\mathrm{avl}}\cdot(1+2G_{\mathrm{EM}})\,\Delta f \tag{4.185}$$

¶In the formulation as given the noise due to the avalanche current uses a correlation between two noise sources. In some simulators it is not possible or not easy to have correlated noise sources. An equivalent implementation of the noise due to the avalanche current is then as follows. The noise source $\overline{iN_B\;iN_C^*}$ is not being used. Instead, a noise source between node B_2 and node C_2 is added, having $\overline{iN_{\mathrm{avl}}^2} = \mathsf{K_{avl}}\cdot 4qI_{\mathrm{avl}}\cdot(1+G_{\mathrm{EM}})\Delta f$. The part due to avalanche in the collector current noise source is changed to $\overline{iN_C^2} = \cdots + \mathsf{K_{avl}}\cdot 2qI_{\mathrm{avl}}\Delta f$. The part due to avalanche in the base current noise source is changed to $\overline{iN_B^2} = \cdots - \mathsf{K_{avl}}\cdot 2qI_{\mathrm{avl}}\Delta f$ (note the '$-$'-sign). The disadvantage of this implementation is that $\overline{iN_B^2}$ can actually become negative! One should check that the simulator is able to handle this.

Emitter-base sidewall current shot noise and $1/f$-noise

$$\overline{iN_{BS}^2} = \left\{ 2q\ |I_{B_1}^S| + \frac{\mathsf{K_f}}{f}\ \mathsf{XI_{B_1}}\ \left(\frac{|I_{B_1}^S|}{\mathsf{XI_{B_1}}} \right)^{\mathsf{A_f}} \right\}\ \Delta f \tag{4.186}$$

Reverse base current shot noise and $1/f$-noise

$$\overline{iN_{B_3}^2} = \left\{ 2q\ |I_{B_3}| + \frac{\mathsf{K_f}}{f}\ |I_{B_3}|^{\mathsf{A_f}} \right\}\ \Delta f \tag{4.187}$$

Extrinsic current shot noise and $1/f$-noise.
When $\mathsf{EXMOD} = 0$ we have

$$\overline{iN_{I_{\rm ex}}^2} = \left\{ 2q\ |I_{\rm ex}| + \frac{\mathsf{K_f}}{f}\ |I_{\rm ex}|^{\mathsf{A_f}} \right\}\ \Delta f \tag{4.188}$$

When $\mathsf{EXMOD} = 1$ we have

$$\overline{iN_{I_{\rm ex}}^2} = \left\{ 2q\ |I_{\rm ex}| + \frac{\mathsf{K_f}}{f}\ (1{-}\mathsf{X_{ext}})\ \left(\frac{|I_{\rm ex}|}{1{-}\mathsf{X_{ext}}} \right)^{\mathsf{A_f}} \right\}\ \Delta f \tag{4.189}$$

$$\overline{iN_{XI_{\rm ex}}^2} = \left\{ 2q\ |XI_{\rm ex}| + \frac{\mathsf{K_f}}{f}\ \mathsf{X_{ext}}\ \left(\frac{|XI_{\rm ex}|}{\mathsf{X_{ext}}} \right)^{\mathsf{A_f}} \right\}\ \Delta f \tag{4.190}$$

Substrate current shot noise (between nodes B_1 and S, resp. B and S)

$$\overline{iN_{I_{\rm sub}}^2} = 2q\ |I_{\rm sub}|\ \Delta f \tag{4.191}$$

$$\overline{iN_{XI_{\rm sub}}^2} = 2q\ |XI_{\rm sub}|\ \Delta f \tag{4.192}$$

4.14 Self-heating

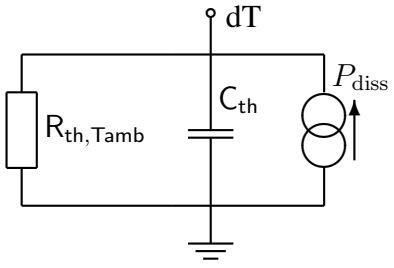

Material	$\mathsf{A_{th}}$
Si	1.3
Ge	1.25
GaAs	1.25
AlAs	1.37
InAs	1.1
InP	1.4
GaP	1.4
SiO_2	0.7

Figure 2: *On the left, the self-heating network. Note that for increased flexibility the node dT should be available to the user. On the right are parameter values that can be used for* $\mathsf{A_{th}}$.

For self-heating an extra network is introduced, see Fig. 2. It contains the self-heating resistance $\mathsf{R_{th,Tamb}}$ and capacitance $\mathsf{C_{th}}$, both connected between ground and the temperature node dT. The value of the voltage $\mathcal{V}_{\rm dT}$ at the temperature node gives the increase in local temperature. The dissipation is given by

$$\begin{aligned} P_{\rm diss} = {} & I_N\,(\mathcal{V}_{\rm B_2E_1} - V^*_{B_2C_2}) + I_{C_1C_2}\,(V^*_{B_2C_2} - \mathcal{V}_{\rm B_2C_1}) - I_{\rm avl}\,V^*_{B_2C_2} \\ & + \mathcal{V}^2_{\rm EE_1}/\mathsf{R_{ET}} + \mathcal{V}^2_{\rm BB_1}/\mathsf{R_{BcT}} \\ & + \mathcal{V}^2_{\rm CC_3}\,\mathsf{G_{CcT}} + \mathcal{V}^2_{\rm C_3C_4}\,\mathsf{G_{CblxT}} + \mathcal{V}^2_{\rm C_4C_1}\,\mathsf{G_{CbliT}} \\ & + I_{B_1B_2}\,\mathcal{V}_{\rm B_1B_2} + (I_{B_1} + I_{B_2} - I_{\rm ztEB})\mathcal{V}_{\rm B_2E_1} + I^S_{B_1}\,\mathcal{V}_{\rm B_1E_1} \\ & + (I_{\rm ex} + I_{B_3})\,\mathcal{V}_{\rm B_1C_4} + XI_{\rm ex}\,\mathcal{V}_{\rm BC_3} \\ & + I_{\rm sub}\mathcal{V}_{\rm B_1S} + XI_{\rm sub}\mathcal{V}_{\rm BS} - I_{\rm Sf}\,\mathcal{V}_{\rm C_1S} \end{aligned} \tag{4.193}$$

Note that the effect of the parameter DTA and dynamic selfheating as discussed here are independent [4, 28], see Sec. 2.6.2. To use a more complicated self-heating network, one can increase $\mathsf{R_{th}}$ to very large values, make $\mathsf{C_{th}}$ zero, and add the wanted self-heating network externally to the node dT. Examples of how to use thermal networks are given in Ref. [28].

For the value of $\mathsf{A_{th}}$ we recommend using values from literature that describe the temperature scaling of the thermal conductivity. For the most important materials, the values are given in Figure 2, which is largely based on Ref. [29], see also [30].

Please note that taking $\mathsf{C_{th}} = 0$ in the self-heating model is *incorrect* for AC simulations (and hence also for transient simulations). The reason is that $\mathsf{C_{th}} = 0$ means that self-heating is infinitely fast. In reality, however, self-heating is much slower than the relevant time scales in most applications. Therefore, for simulations always a non-zero thermal capacitance should be used, even when the thermal capacitance has not been extracted. Since in practice the thermal time delay is of the order of 1 µs, a reasonable estimate for the thermal capitance can be given by $\mathsf{C_{th}} = 1\,\mu{\rm s}/\mathsf{R_{th}}$.

4.15 Implementation issues

Minimal conductance We have added a constant conductance $G_{\min}$ to the forward and reverse non-ideal base currents. These are needed in circuit simulators to improve convergence. We do not need them to describe the transistor. Nevertheless, their influence can be seen on some characteristics. For implementation testing and comparison it is therefore important to give $G_{\min}$ the prescribed value. Otherwise, when the circuit simulator permits it, $G_{\min}$ can be given another value. $G_{\min}$ is not included in the operating point information.

Transition functions In several places in the code a transition function is used, like the `hyp`-functions and the `log-exp`-functions. These functions are the smoothed versions of the functions `min` and `max`. These functions must be programmed in a numerical stable way. This can be done in several ways. Here we only give the basic formulations.

For the depletion charges we use the function

$$\min{}_{\texttt{logexp}}(x, x_0; a) = x - a\ \ln\{1 + \exp[(x - x_0)/a]\} \tag{4.194}$$

In the implementation this is coded as

$$\min{}_{\texttt{logexp}}(x, x_0; a) = \begin{cases} x - a\ \ln\{1 + \exp[(x - x_0)/a]\} & \text{for } x < x_0 \\ x_0 - a\ \ln\{1 + \exp[(x_0 - x)/a]\} & \text{for } x \geq x_0 \end{cases} \tag{4.195}$$

In the epilayer model we calculate α using

$$\max{}_{\texttt{logexp}}(x, x_0; a) = x_0 + a\ \ln\{1 + \exp[(x - x_0)/a]\} \tag{4.196}$$

In the implementation this is coded as

$$\max{}_{\texttt{logexp}}(x, x_0; a) = \begin{cases} x_0 + a\ \ln\{1 + \exp[(x - x_0)/a]\} & \text{for } x < x_0 \\ x + a\ \ln\{1 + \exp[(x_0 - x)/a]\} & \text{for } x \geq x_0 \end{cases} \tag{4.197}$$

The same is used for the temperature scaling of the diffusion voltages. Real hyperbolic functions are used for the calculation of $q_1^{Q,I}$, V_{qs}, and $V_{B\text{ex}}$:

$$\max{}_{\texttt{hyp}}(x, x_0; \epsilon) = \tfrac{1}{2}\left[\sqrt{(x - x_0)^2 + 4\epsilon^2} + x + x_0\right] \tag{4.198}$$

In the implementation this can be coded as

$$\max{}_{\texttt{hyp}}(x, x_0; \epsilon) = \begin{cases} x_0 + \dfrac{2\epsilon^2}{\sqrt{(x - x_0)^2 + 4\epsilon^2} + x_0 - x} & \text{for } x < x_0 \\ x + \dfrac{2\epsilon^2}{\sqrt{(x - x_0)^2 + 4\epsilon^2} + x - x_0} & \text{for } x \geq x_0 \end{cases} \tag{4.199}$$

One can also make a difference between the cases $|x| < 2\epsilon$ and $|x| > 2\epsilon$ to improve the stability.

Some derivatives For some of the equations the derivatives can be simplified by using some math. For instance, for n_0 we have

$$n_0 = \frac{f_1}{1+\sqrt{1+f_1}} = \sqrt{1+f_1} - 1 \tag{4.200a}$$

For the implementation of n_0 we need the first expression, especially when f_1 is small. But for the derivative we can take the second expression. The same holds for

$$n_B = \frac{f_2}{1+\sqrt{1+f_2}} = \sqrt{1+f_2} - 1 \tag{4.200b}$$

$$n_{B\mathrm{ex}} = \frac{g_1}{1+\sqrt{1+g_1}} = \sqrt{1+g_1} - 1 \tag{4.200c}$$

$$Xn_{B\mathrm{ex}} = \frac{Xg_1}{1+\sqrt{1+Xg_1}} = \sqrt{1+Xg_1} - 1 \tag{4.200d}$$

$$p_{W\mathrm{ex}} = \frac{g_2}{1+\sqrt{1+g_2}} = \sqrt{1+g_2} - 1 \tag{4.200e}$$

$$Xp_{W\mathrm{ex}} = \frac{Xg_2}{1+\sqrt{1+Xg_2}} = \sqrt{1+Xg_2} - 1 \tag{4.200f}$$

For the epilayer model we have similar equations, where again the second expression can be used for calculating derivatives:

$$p_W = \frac{2\,e^{(\mathcal{V}_{\mathrm{B_2C_1}}-\mathsf{V}_{\mathrm{d_CT}})/V_T}}{1+K_W} = \tfrac{1}{2}\,(K_W - 1) \tag{4.200g}$$

$$p_0^* = \frac{2\,e^{(\mathcal{V}_{\mathrm{B_2C_2}}-\mathsf{V}_{\mathrm{d_CT}})/V_T}}{1+K_0} = \tfrac{1}{2}\,(K_0 - 1) \tag{4.200h}$$

The latter is needed only in reverse mode.

Numerical stability of p_0^* For any root of a quadratic equation there are two ways of writing the solution. These differ in their numerical stability. Therefore, for p_0^*, we implement:

$$p_0^* = \begin{cases} \dfrac{g-1}{2} + \sqrt{\left(\dfrac{g-1}{2}\right)^2 + 2g + p_W(p_W+g+1)}, & \text{for } g > 1 \\ \dfrac{2g + p_W(p_W+g+1)}{\dfrac{1-g}{2} + \sqrt{\left(\dfrac{1-g}{2}\right)^2 + 2g + p_W(p_W+g+1)}}, & \text{for } g < 1 \end{cases} \tag{4.201}$$

4.16 Embedding of PNP transistors

Although NPN transistors are the most used bipolar transistors it is also necessary to be able to describe PNP-transistors. The equations given above are only for NPN transistors. It is however easy to map a PNP-device with its bias conditions onto an NPN model. To do this we need three steps:
• The model uses the following internal voltages:

$$\mathcal{V}_{\mathrm{B_2C_1}},\ \mathcal{V}_{\mathrm{B_2C_2}},\ \mathcal{V}_{\mathrm{B_2E_1}},\ \mathcal{V}_{\mathrm{B_1E_1}},\ \mathcal{V}_{\mathrm{B_1B_2}},\ \mathcal{V}_{\mathrm{B_1C_1}},\ \mathcal{V}_{\mathrm{BC_1}},\ \mathcal{V}_{\mathrm{SC_1}}$$

For a PNP the sign of these voltages must be changed ($V \rightarrow -V$). The value of $\mathcal{V}_{\mathrm{dT}}$ does *not* change sign.
• Calculate the currents, charges and noise densities with the equations for the NPN transistor. Note that the parameters are still like those for an NPN. For instance all currents like $\mathsf{I_s}$ must be taken positive.
• Change the sign of all resulting currents ($I \rightarrow -I$)

$$I_N,\ I_{B_1B_2},\ I_{C_1C_2},\ I_{\mathrm{avl}},\ I_{B_1},\ I^S_{B_1},\ I_{B_2},\ I_{\mathsf{ztEB}},\ I_{B_3},\ I_{\mathrm{ex}},\ XI_{\mathrm{ex}},\ I_{\mathrm{sub}},\ XI_{\mathrm{sub}},\ I_{\mathrm{Sf}}$$

and charges ($Q \rightarrow -Q$)

$$Q_E,\ Q_{t_E},\ Q_{t_C},\ Q_{BE},\ Q_{BC},\ Q_{\mathrm{epi}},\ Q_{B_1B_2},\ Q_{\mathrm{ex}},\ XQ_{\mathrm{ex}},\ Q_{\mathrm{tex}},\ XQ_{\mathrm{tex}},\ Q_{t_S},\ Q_{BEO},\ Q_{BCO}$$

The noise current densities do not change sign. The power dissipation term P_{diss} and the thermal charge $\mathsf{C_{th}} \cdot V_{dT}$ do not change sign. The following derivatives *do* need an extra sign:

$$\frac{\partial P_{\mathrm{diss}}}{\partial \mathcal{V}_{\mathrm{B_2E_1}}}, \qquad \text{etc.}$$

All other derivatives $\partial I/\partial V$ and $\partial Q/\partial V$ do not need an extra sign.

Furthermore, note that the constants A_n and B_n for the avalanche model are different for NPN's and for PNP's.

4.17 Distribution of the collector resistance

The buried layer resistances were introduced in Mextram 504.7, in a backwards compatibe way. This implies that the default values of these resistances is zero. Because values of $0\,\Omega$ thus are allowed for resistances $\mathsf{R_{Cblx}}$ and $\mathsf{R_{Cbli}}$, the lower clipping value of the resistances is zero and very small values of the resistances $\mathsf{R_{Cblx}}$ and $\mathsf{R_{Cbli}}$ are formally allowed. Resistance values very close to zero are known to form a potential threat to convergence however. In order to exclude the possibility that the resistances of the buried layer take such small values during the convergence process due to temperature effects, the lower clipping value for the temperature coefficient $\mathsf{A_{Cbl}}$ of the resistances $\mathsf{R_{Cblx}}$ and $\mathsf{R_{Cbli}}$ has been set to zero.

In case one of both of the $\mathsf{R_{Cblx}}$ and $\mathsf{R_{Cbli}}$ resistances vanish, the corresponding node (C_3 and or C_4) effectively disappears from the equivalent circuit. Hence the circuit topology depends on parameter values. Special attention has to be paid to this in implementation of the model.

4.18 Operating point information

The operating point information is a list of quantities that describe the internal state of the transistor. When a circuit simulator is able to provide these, it might help the designer understand the behaviour of the transistor and the circuit. All of these values have the sign that belongs to NPN-transistors (so normally I_C and $\mathcal{V}_{\mathrm{B_2E_1}}$ will be positive, even for a PNP transistor).

The full list of operating point information consists of four parts. First the external collector current, base current and current gain are given. Next we have all the branch biases, the currents and the charges. Then we have, as usual, the elements that can be used if a full small-signal equivalent circuit is needed. These are all the derivatives of the charges and currents. At last, and possibly the most informative, we have given approximations to the small-signal model which together form a hybrid-π model with similar behaviour as the full Mextram model. In addition the cut-off frequency is included.

Note that $G_{\min}$ is not included in the expressions of the operating point information (see section 4.15).

The external currents and current gain:

I_E	External DC emitter current
I_C	External DC collector current
I_B	External DC base current
I_S	External DC substrate current
β_{dc}	External DC current gain I_C/I_B

External voltage differences:

V_{BE}	External base-emitter voltage
V_{BC}	External base-collector voltage
V_{CE}	External collector-emitter voltage
V_{SE}	External substrate-emitter voltage
V_{BS}	External base-substrate voltage
V_{SC}	External substrate-collector voltage

Since we have 5 internal nodes we need 5 voltage differences to describe the bias at each internal node, given the external biases. We take those that are the most informative for the internal state of the transistor:

$\mathcal{V}_{\mathrm{B_2E_1}}$	Internal base-emitter bias
$\mathcal{V}_{\mathrm{B_2C_2}}$	Internal base-collector bias
$\mathcal{V}_{\mathrm{B_2C_1}}$	Internal base-collector bias including epilayer
$\mathcal{V}_{\mathrm{B_1C_1}}$	External base-collector bias without parasitic resistances
$\mathcal{V}_{\mathrm{C_4C_1}}$	Bias over intrinsic buried layer
$\mathcal{V}_{\mathrm{C_3C_4}}$	Bias over extrinsic buried layer
$\mathcal{V}_{\mathrm{E_1E}}$	Bias over emitter resistance

The actual currents are:

I_N	Main current

$I_{C_1C_2}$	Epilayer current
$I_{B_1B_2}$	Pinched-base current
I_{B_1}	Ideal forward base current
$I_{B_1}^S$	Ideal side-wall base current
I_{ztEB}	Zener tunneling current in emitter-base junction
I_{B_2}	Non-ideal forward base current
I_{B_3}	Non-ideal reverse base current
I_{avl}	Avalanche current
I_{ex}	Extrinsic reverse base current
XI_{ex}	Extrinsic reverse base current
I_{sub}	Substrate current
XI_{sub}	Substrate current
I_{Sf}	Substrate-Collector current
I_{R_E}	Current through emitter resistance
$I_{R_{Bc}}$	Current through constant base resistance
$I_{R_{Cblx}}$	Current through extrinsic buried layer resistance
$I_{R_{Cbli}}$	Current through intrinsic buried layer resistance
$I_{R_{Cc}}$	Current through collector contact resistance

The actual charges are:

Q_E	Emitter charge or emitter neutral charge
Q_{t_E}	Base-emitter depletion charge
$Q_{t_E}^S$	Sidewall base-emitter depletion charge
Q_{BE}	Base-emitter diffusion charge
Q_{BC}	Base-collector diffusion charge
Q_{t_C}	Base-collector depletion charge
Q_{epi}	Epilayer diffusion charge
$Q_{B_1B_2}$	AC current crowding charge
Q_{tex}	Extrinsic base-collector depletion charge
XQ_{tex}	Extrinsic base-collector depletion charge
Q_{ex}	Extrinsic base-collector diffusion charge
XQ_{ex}	Extrinsic base-collector diffusion charge
Q_{t_S}	Collector-substrate depletion charge

The small-signal equivalent circuit contains the following conductances. In the terminology we use the notation A_x, A_y, and A_z to denote derivatives of the quantity A to some voltage difference. We use x for base-emitter biases, y is for derivatives w.r.t. $\mathcal{V}_{\mathrm{B_2C_2}}$ and z is used for all other base-collector biases. The subindex π is used for base-emitter base currents, μ is used for base-collector base currents, Rbv for derivatives of $I_{B_1B_2}$ and Rcv for derivatives of $I_{C_1C_2}$.

Quantity	Equation	Description
g_x	$\partial I_N/\partial \mathcal{V}_{\mathrm{B_2E_1}}$	Forward transconductance
g_y	$\partial I_N/\partial \mathcal{V}_{\mathrm{B_2C_2}}$	Reverse transconductance
g_z	$\partial I_N/\partial \mathcal{V}_{\mathrm{B_2C_1}}$	Reverse transconductance
g_π^S	$\partial I_{B_1}^S/\partial \mathcal{V}_{\mathrm{B_1E_1}}$	Conductance sidewall b-e junction
$g_{\pi,x}$	$\partial(I_{B_1}+I_{B_2}-I_{\mathrm{ztEB}})/\partial \mathcal{V}_{\mathrm{B_2E_1}}$	Conductance floor b-e junction
$g_{\pi,y}$	$\partial I_{B_1}/\partial \mathcal{V}_{\mathrm{B_2C_2}}$	Early effect on recombination base current
$g_{\pi,z}$	$\partial I_{B_1}/\partial \mathcal{V}_{\mathrm{B_2C_1}}$	Early effect on recombination base current
$g_{\mu,x}$	$-\partial I_{\mathrm{avl}}/\partial \mathcal{V}_{\mathrm{B_2E_1}}$	Early effect on avalanche current limiting

$g_{\mu,y}$	$-\partial I_{\rm avl}/\partial \mathcal{V}_{\rm B_2C_2}$	Conductance of avalanche current
$g_{\mu,z}$	$-\partial I_{\rm avl}/\partial \mathcal{V}_{\rm B_2C_1}$	Conductance of avalanche current
$g_{\mu\rm ex}$	$\partial(I_{\rm ex}+I_{B_3}/\partial \mathcal{V}_{\rm B_1C_4}$	Conductance extrinsic b-c junction
$Xg_{\mu\rm ex}$	$\partial XI_{\rm ex}/\partial \mathcal{V}_{\rm BC_3}$	Conductance extrinsic b-c junction
$g_{Rcv,y}$	$\partial I_{C_1C_2}/\partial \mathcal{V}_{\rm B_2C_2}$	Conductance of epilayer current
$g_{Rcv,z}$	$\partial I_{C_1C_2}/\partial \mathcal{V}_{\rm B_2C_1}$	Conductance of epilayer current
r_{bv}	$1/(\partial I_{B_1B_2}/\partial \mathcal{V}_{\rm B_1B_2})$	Base resistance
$g_{Rbv,x}$	$\partial I_{B_1B_2}/\partial \mathcal{V}_{\rm B_2E_1}$	Early effect on base resistance
$g_{Rbv,y}$	$\partial I_{B_1B_2}/\partial \mathcal{V}_{\rm B_2C_2}$	Early effect on base resistance
$g_{Rbv,z}$	$\partial I_{B_1B_2}/\partial \mathcal{V}_{\rm B_2C_1}$	Early effect on base resistance
R_E	$\mathsf{R_{ET}}$	Emitter resistance
R_{Bc}	$\mathsf{R_{BcT}}$	Constant base resistance
R_{Cc}	$\mathsf{R_{CcT}}$	Collector contact resistance
R_{Cblx}	$\mathsf{R_{CblxT}}$	Extrinsic buried layer resistance
R_{Cbli}	$\mathsf{R_{CbliT}}$	Intrinsic buried layer resistance
g_S	$\partial I_{\rm sub}/\partial \mathcal{V}_{\rm B_1C_1}$	Conductance parasitic PNP transistor
Xg_S	$\partial XI_{\rm sub}/\partial \mathcal{V}_{\rm BC_1}$	Conductance parasitic PNP transistor
$g_{\rm Sf}$	$\partial I_{\rm Sf}/\partial \mathcal{V}_{\rm SC_1}$	Conductance Substrate-Collector current

The small-signal equivalent circuit contains the following capacitances

Quantity	Equation	Description
C_{BE}^S	$\partial Q_{t_E}^S/\partial \mathcal{V}_{\rm B_1E_1}$	Capacitance sidewall b-e junction
$C_{BE,x}$	$\partial(Q_{t_E}+Q_{BE}+Q_E)/\partial \mathcal{V}_{\rm B_2E_1}$	Capacitance floor b-e junction
$C_{BE,y}$	$\partial Q_{BE}/\partial \mathcal{V}_{\rm B_2C_2}$	Early effect on b-e diffusion charge
$C_{BE,z}$	$\partial Q_{BE}/\partial \mathcal{V}_{\rm B_2C_1}$	Early effect on b-e diffusion charge
$C_{BC,x}$	$\partial Q_{BC}/\partial \mathcal{V}_{\rm B_2E_1}$	Early effect on b-c diffusion charge
$C_{BC,y}$	$\partial(Q_{t_C}+Q_{BC}+Q_{\rm epi})/\partial \mathcal{V}_{\rm B_2C_2}$	Capacitance floor b-c junction
$C_{BC,z}$	$\partial(Q_{t_C}+Q_{BC}+Q_{\rm epi})/\partial \mathcal{V}_{\rm B_2C_1}$	Capacitance floor b-c junction
$C_{BC\rm ex}$	$\partial(Q_{\rm tex}+Q_{\rm ex})/\partial \mathcal{V}_{\rm B_1C_4}$	Capacitance extrinsic b-c junction
$XC_{BC\rm ex}$	$\partial(XQ_{\rm tex}+XQ_{\rm ex})/\partial \mathcal{V}_{\rm BC_3}$	Capacitance extrinsic b-c junction
$C_{B_1B_2}$	$\partial Q_{B_1B_2}/\partial \mathcal{V}_{\rm B_1B_2}$	Capacitance AC current crowding
$C_{B_1B_2,x}$	$\partial Q_{B_1B_2}/\partial \mathcal{V}_{\rm B_2E_1}$	Cross-capacitance AC current crowding
$C_{B_1B_2,y}$	$\partial Q_{B_1B_2}/\partial \mathcal{V}_{\rm B_2C_2}$	Cross-capacitance AC current crowding
$C_{B_1B_2,z}$	$\partial Q_{B_1B_2}/\partial \mathcal{V}_{\rm B_2C_1}$	Cross-capacitance AC current crowding
C_{t_S}	$\partial Q_{t_S}/\partial \mathcal{V}_{\rm SC_1}$	Capacitance s-c junction

The full small-signal circuit is in practice not very useful, since it is difficult to do hand-calculations with it. We therefore include the elements of an approximate small-signal model, shown in Fig. 3. This model contains the following elements:

g_m	Transconductance
β	Current amplification
g_{out}	Output conductance
g_μ	Feedback transconductance
R_E	Emitter resistance (already given above)
r_B	Base resistance
r_C	Collector resistance

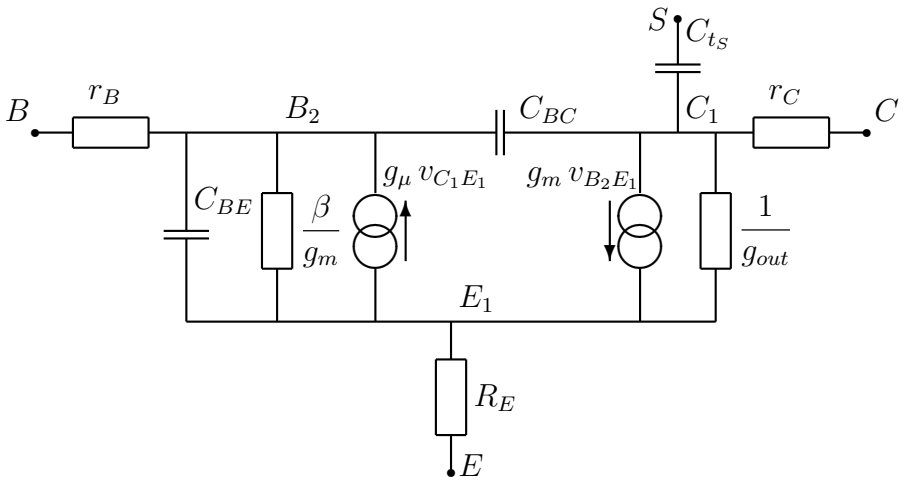

Figure 3: *Small-signal equivalent circuit describing the approximate behaviour of the Mextram model. The actual forward Early voltage can be found as* $V_{eaf} = I_C/g_{out} - \mathcal{V}_{\rm CE}$. *which can be different from the parameter value* $\mathsf{V_{ef}}$, *especially when* $\mathsf{dE_g} \neq 0$.

C_{BE}	Base-emitter capacitance
C_{BC}	Base-collector capacitance
C_{t_S}	Collector-substrate capacitance (already given above)

We make a few assumptions by making this approximation. It is meant to work in forward mode. For use in reverse mode or for the equivalent hybrid-π version of the circuit we refer to Ref. [2]. To keep the model simple, the base-emitter and base-collector capacitances are a sum of various contributions that are in the full model between different nodes. The elements that have not been defined before can be calculated from the small signal parameters of the full model. As help variables we use

$$\frac{\mathrm{d}y}{\mathrm{d}x} = \frac{g_x - g_{\mu,x}}{g_{Rcv,y} + g_{\mu,y} - g_y} \tag{4.202}$$

$$\frac{\mathrm{d}y}{\mathrm{d}z} = \frac{g_z - g_{Rcv,z} - g_{\mu,z}}{g_{Rcv,y} + g_{\mu,y} - g_y} \tag{4.203}$$

$$g_\pi = g_\pi^S + g_{\pi,x} + g_{\mu,x} + g_{\pi,z} + g_{\mu,z} + (g_{\pi,y} + g_{\mu,y}) \left[\frac{\mathrm{d}y}{\mathrm{d}x} + \frac{\mathrm{d}y}{\mathrm{d}z}\right] \tag{4.204}$$

The quantities in the small-signal circuit then are:

$$g_m = \frac{g_{Rcv,y}(g_x - g_{\mu,x} + g_z - g_{\mu,z}) - (g_{Rcv,z})(g_y - g_{\mu,y})}{g_{Rcv,y} + g_{\mu,y} - g_y} \tag{4.205}$$

$$\beta = g_m/g_\pi \tag{4.206}$$

$$g_{out} = \frac{(g_y - g_{\mu,y})g_{Rcv,z} - (g_z - g_{\mu,z})g_{Rcv,y}}{g_{Rcv,y} + g_{\mu,y} - g_y} \tag{4.207}$$

$$g_\mu = g_{\pi,z} + g_{\mu,z} + (g_{\pi,y} + g_{\mu,y})\frac{\mathrm{d}y}{\mathrm{d}z} + g_{\mu\mathrm{ex}} + Xg_{\mu\mathrm{ex}} \tag{4.208}$$

$$r_B = \mathsf{R_{BcT}} + r_{bv} \tag{4.209}$$

$$r_C = \mathsf{R_{CcT}} + \mathsf{R_{CblxT}} + \mathsf{R_{CbliT}} \tag{4.210}$$

$$C_{BE} = C_{BE,x} + C^S_{BE} + C_{BC,x} + (C_{BE,y} + C_{BC,y})\,\frac{\mathrm{d}y}{\mathrm{d}x} + \mathsf{C_{BEO}} \tag{4.211}$$

$$C_{BC} = (C_{BE,y} + C_{BC,y})\,\frac{\mathrm{d}y}{\mathrm{d}z} + C_{BC,z} + C_{BC\mathrm{ex}} + XC_{BC\mathrm{ex}} + \mathsf{C_{BCO}} \tag{4.212}$$

Note that we added the overlap capacitances to the internal capacitances for simplicity.

Apart from the small signal approximated hybrid-π model, we would also like to have a rather good estimate of f_T, the cut-off frequency. We neglect the substrate current, but we now do take into account that the capacitances have different positions in the equivalent circuit. The derivation [2] is based on $1/(2\pi f_T) = \mathrm{d}Q/\mathrm{d}I_C$ for constant V_{CE}. The

formulas used to calculate f_T are:

$$\gamma_x = (g_{\pi,x} + g_{\mu,x} - g_{Rbv,x})\, r_{bv} \tag{4.213}$$
$$\gamma_y = (g_{\pi,y} + g_{\mu,y} - g_{Rbv,y})\, r_{bv} \tag{4.214}$$
$$\gamma_z = (g_{\pi,z} + g_{\mu,z} - g_{Rbv,z})\, r_{bv} \tag{4.215}$$
$$g_{Bf,x} = g_{\pi,x} + g_\pi^S\,(1+\gamma_x) \tag{4.216}$$
$$g_{Bf,y} = g_{\pi,y} + g_\pi^S\,\gamma_y \tag{4.217}$$
$$g_{Bf,z} = g_{\pi,z} + g_\pi^S\,\gamma_z \tag{4.218}$$
$$\alpha = \frac{1+\left[g_{Rcv,y}\frac{\mathrm{d}y}{\mathrm{d}x}\right] r_C + \left[g_x{+}g_{Bf,x}{+}(g_y{+}g_{Bf,y})\frac{\mathrm{d}y}{\mathrm{d}x}\right] \mathsf{R_{ET}}}{1-\left[g_{Rcv,z}{+}g_{Rcv,y}\frac{\mathrm{d}y}{\mathrm{d}z}\right] r_C - \left[g_z{+}g_{Bf,z}{+}(g_y+g_{Bf,y})\frac{\mathrm{d}y}{\mathrm{d}z}\right] \mathsf{R_{ET}}} \tag{4.219}$$
$$r_x = \left[g_{Rcv,y}\frac{\mathrm{d}y}{\mathrm{d}x} + \alpha\,\left(g_{Rcv,z} + g_{Rcv,y}\frac{\mathrm{d}y}{\mathrm{d}z}\right)\right]^{-1} \tag{4.220}$$
$$r_z = \alpha\, r_x \tag{4.221}$$
$$r_y = \frac{1-g_{Rcv,z}r_z}{g_{Rcv,y}} \tag{4.222}$$
$$r_{b1b2} = \gamma_x\, r_x + \gamma_y\, r_y + \gamma_z\, r_z \tag{4.223}$$
$$r_{\mathrm{ex}} = r_z + r_{b1b2} - \mathsf{R_{CbliT}} \tag{4.224}$$
$$\begin{aligned} Xr_{\mathrm{ex}} = {} & r_{\mathrm{ex}}{+}\mathsf{R_{BcT}}\left[(g_{Bf,x}{+}g_{\mu,x})\, r_x + (g_{Bf,y}{+}g_{\mu,y})\, r_y\right. \\ & \left.{+}(g_{Bf,z}{+}g_{\mu,z})\, r_z\right] - \mathsf{R_{CbliT}} - \mathsf{R_{CblxT}} \end{aligned} \tag{4.225}$$
$$\begin{aligned} \tau_T = {} & C_{BE}^S\,(r_x + r_{b1b2}) + (C_{BE,x} + C_{BC,x})\, r_x + (C_{BE,y} + C_{BC,y})\, r_y \\ & + (C_{BE,z} + C_{BC,z})\, r_z + C_{BC\mathrm{ex}}\, r_{\mathrm{ex}} + XC_{BC\mathrm{ex}}\, Xr_{\mathrm{ex}} \\ & + (\mathsf{C_{BEO}} + \mathsf{C_{BCO}})\,(Xr_{\mathrm{ex}} - \mathsf{R_{CcT}}) \end{aligned} \tag{4.226}$$

Apart from the cut-off frequency we also have some other quantities to describe the internal state of the model:

f_T	$1/(2\pi\,\tau_T)$	Good approximation for cut-off frequency
I_{qs}		Current at onset of quasi-saturation
x_i/W_{epi}		Thickness of injection layer
$V^*_{B_2C_2}$		Physical value of internal base-collector bias

Related to self-heating we have the following extra quantities

P_{diss}	Dissipation
T_K	Actual temperature

5 Going from 503 to 504

In general it is possible to do Mextram 504 simulations using Mextram 503 parameters as input, without losing much accuracy, even though Mextram 503 is not fully backward compatible with Mextram 504. Most of the Mextram 503 model equations have been modified to some extent. So even when the model parameters are not changed, like for the three depletion capacitances, the simulation results may differ slightly as a function of bias. To do Mextram 504 simulations with Mextram 503 parameters as input, we have developed a procedure to convert Mextram 503 parameters to Mextram 504 parameters. In this section we describe this conversion. These conversion rules have been checked over bias and temperature for transistors in several processes. A Pstar input deck is available upon request that contains all the conversion rules explained in this section.

5.1 Overview

The Mextram 503 model contains 62 parameters while Mextram 504 contains 75 parameters in total. In Mextram 504 new parameters are introduced for the Early effect, avalanche multiplication, the non-ideal base current, transit times, temperature scaling rules and self-heating. There are 22 new parameters and 9 parameters have been removed. The parameter τ_{NE} is renamed to τ_E for consistency reasons. In Table 5 below we have given an overview of the parameters that are new in Mextram 504 and those that have been removed compared to Mextram 503.

The value of some parameters can directly be given, as has been done in the table. For those parameters that do not have a fixed value we give the conversion rules below. Some of the parameters that are present in both Mextram 503 and Mextram 504 have to be changed slightly for use in Mextram 504. These are I_{Bf} for the non-ideal forward base current and the temperature parameters V_{g_B} and V_{gs}.

Table 5: *Overview of the new parameters in Mextram 504 and the parameters removed compared to Mextram 503. For some of the parameters we have already given the value that should be used when converting from Mextram 503 to Mextram 504.*

Part of the model	New	Removed
Early Voltages	V_{er}	Q_{B0}
	V_{ef}	
Built-in field of the base		η
Non-ideal base current	m_{Lf}	V_{Lf}
Avalanche model	W_{avl}	AVL
	V_{avl}	E_{fi}
Epilayer model	$a_{x_i} = 0.3$	
Overlap capacitances	$C_{BEO} = 0$	
	$C_{BCO} = 0$	
Transit times	τ_B	
	τ_{epi}	
	τ_R	

Part of the model	New	Removed
Self-heating	$\mathsf{R_{th}} = 0$ $\mathsf{C_{th}} = 0$ $\mathsf{A_{th}} = 0$	
SiGe modelling	$\mathsf{dE_g} = 0$ $\mathsf{X_{rec}} = 0$	
Noise modelling	$\mathsf{K_{avl}} = 0$	
Temperature model:		
Emitter resistance	$\mathsf{A_E} = 0$	
Base width	$\mathsf{A_{Q_{B0}}}$	$\mathsf{N_A}$ $\mathsf{V_I}$
Forward current gain	$\mathsf{dV_{g\beta f}}$	$\mathsf{V_{g_E}}$
Reverse current gain	$\mathsf{dV_{g\beta r}} = 0$	
Emitter transit time	$\mathsf{dV_{g\tau_E}}$	
Non-ideal base currents		$\mathsf{E_R}$
Total	22	9

For the conversion rules a few quantities have to be given beforehand. These are the breakdown voltage $\mathrm{BV_{ceo}}$ for the avalanche model and the calibration temperature T_{cal} for the temperature rules. Since some of the temperature rules have been changed it is not possible to get exactly the same results for Mextram 503 and Mextram 504 for all temperatures. The calibration temperature T_{cal} is used below as the temperature where the Mextram 503 and the Mextram 504 temperature rules give the same result. A good value for T_{cal} is $100^{\circ}\mathrm{C}$, which is in general not too close to the temperature at which parameter extraction has been done but which gives a reasonable temperature range.

5.2 Temperature scaling

The Mextram 503 temperature scaling rules have been evaluated and many of them have been slightly adapted. This results in minor changes of the related parameters. We will calibrate the new model at a certain temperature T_{cal}. For the equations we need the following definitions, that closely follow the definitions in Sec. 4

$$T_{RK} = T_{\mathrm{ref}} + 273.15 \tag{5.1}$$

$$T_K = T_{\mathrm{cal}} + 273.15 \tag{5.2}$$

$$t_N = \frac{T_K}{T_{RK}} \tag{5.3}$$

$$V_T = \left(\frac{k}{q}\right) T_K \tag{5.4}$$

$$V_{T_R} = \left(\frac{k}{q}\right) T_{RK} \tag{5.5}$$

$$\frac{1}{V_{\Delta T}} = \frac{1}{V_T} - \frac{1}{V_{T_R}} \tag{5.6}$$

The temperature dependence of the neutral base charge $\mathsf{Q_{B0}}$ in Mextram 503 is quite complicated due to the base width modulation and therefore many parameters are involved (e.g. $\mathsf{V_{g_B}}$, $\mathsf{V_{g_C}}$, $\mathsf{N_A}$, and $\mathsf{V_l}$). We removed $\mathsf{Q_{B0}}$ from the parameter list. However, the temperature dependent ratio $\mathsf{Q_{B0T}}/\mathsf{Q_{B0}}$ is still needed in the model. We simplify it by using a power law $\mathsf{Q_{B0T}}/\mathsf{Q_{B0}} = t_N^{\mathsf{A_{Q_{B0}}}}$ with parameter $\mathsf{A_{Q_{B0}}}$. To determine this parameter we must repeat a part of the Mextram 503 temperature model:

$$\mathsf{V_{d_ET}} = -3\,V_T\,\ln t_N + \mathsf{V_{d_E}}\,t_N + (1-t_N)\,\mathsf{V_{g_B}} \tag{5.7}$$

$$\mathsf{V_{d_CT}} = -3\,V_T\,\ln t_N + \mathsf{V_{d_C}}\,t_N + (1-t_N)\,\mathsf{V_{g_C}} \tag{5.8}$$

$$\mathsf{C_{j_ET}} = \mathsf{C_{j_E}}\left(\frac{\mathsf{V_{d_E}}}{\mathsf{V_{d_ET}}}\right)^{\mathsf{p_E}} \tag{5.9}$$

$$\mathsf{C_{j_CT}} = \mathsf{C_{j_C}}\left[(1-\mathsf{X_p})\left(\frac{\mathsf{V_{d_C}}}{\mathsf{V_{d_CT}}}\right)^{\mathsf{p_C}} + \mathsf{X_p}\right] \tag{5.10}$$

$$\mathsf{X_{pT}} = \mathsf{X_p}\,\frac{\mathsf{C_{j_C}}}{\mathsf{C_{j_CT}}} \tag{5.11}$$

$$Q_E = \frac{1-\mathsf{XC_{j_E}}}{1-\mathsf{p_E}}\,\mathsf{C_{j_E}}\,\mathsf{V_{d_E}} \tag{5.12}$$

$$Q_C = \left(\frac{1-\mathsf{X_p}}{1-\mathsf{p_C}} + \mathsf{X_p}\right)\,\mathsf{XC_{j_C}}\,\mathsf{C_{j_C}}\,\mathsf{V_{d_C}} \tag{5.13}$$

$$g_i = 2\cdot\left[1+\sqrt{1+\frac{\mathsf{N_A}\,\exp\left(\mathsf{V_l}/V_{TR}\right)}{6.04\cdot 10^{14}\,T_{RK}^{1.5}}}\right]^{-1} \tag{5.14}$$

$$Q_{\mathrm{imp}} = \left(\mathsf{Q_{B0}} + Q_E + Q_C\right)/g_i \tag{5.15}$$

$$Q_{E\mathrm{T}} = \frac{1-\mathsf{XC_{j_E}}}{1-\mathsf{p_E}}\,\mathsf{C_{j_ET}}\,\mathsf{V_{d_ET}} \tag{5.16}$$

$$Q_{C\mathrm{T}} = \left(\frac{1-\mathsf{X_{pT}}}{1-\mathsf{p_C}} + \mathsf{X_{pT}}\right)\,\mathsf{XC_{j_C}}\,\mathsf{C_{j_CT}}\,\mathsf{V_{d_CT}} \tag{5.17}$$

$$g_{i\mathrm{T}} = 2\cdot\left[1+\sqrt{1+\frac{\mathsf{N_A}\,\exp\left(\mathsf{V_l}/V_T\right)}{6.04\cdot 10^{14}\,T_K^{1.5}}}\right]^{-1} \tag{5.18}$$

$$\mathsf{Q_{B0T}} = g_{i\mathrm{T}}\,Q_{\mathrm{imp}} - Q_{E\mathrm{T}} - Q_{C\mathrm{T}} \tag{5.19}$$

Finally the base charge temperature coefficient becomes

$$\mathsf{A_{Q_{B0}}} = \frac{\ln(\mathsf{Q_{B0T}}/\mathsf{Q_{B0}})}{\ln t_N} \tag{5.20}$$

Next the parameters $\mathsf{V_{g_B}}$ of the collector saturation current $\mathsf{I_s}$ and $\mathsf{V_{g_S}}$ of the substrate saturation current $\mathsf{I_{Ss}}$ are adapted. This is done by demanding that the temperature rules for Mextram 503 and Mextram 504 lead to the same saturation currents at temperature T_{cal}. This leads to

$$\mathsf{V_{g_B}}^{(504)} = \mathsf{V_{g_B}}^{(503)} + V_{\Delta T}\,(0.2 + 0.5\,\mathsf{A_B} - \mathsf{A_{Q_{B0}}})\,\ln t_N \tag{5.21}$$

$$\mathsf{V_{g_S}}^{(504)} = \mathsf{V_{g_S}}^{(503)} + V_{\Delta T}\,(0.5 - 2\,\mathsf{A_S})\,\ln t_N \tag{5.22}$$

In the same way we demand that the forward current gain of both models is the same at the calibration temperature. This leads to

$$\mathsf{dV_{g\beta f}} = \mathsf{V_{g_B}}^{(503)} - \mathsf{V_{g_E}} + V_{\Delta T}\ (0.5\,\mathsf{A_B} - \mathsf{A_{Q_{B0}}} - 0.03)\ \ln t_N \tag{5.23}$$

Parameter $\mathsf{V_{g_E}}$ is removed from the list. The last bandgap voltage difference we need to define is that of the emitter transit time. Again we demand that the emitter transit time is the same for both models at the calibration temperature, but we simplify the case where $\mathsf{m_\tau} \neq 1$

$$\mathsf{dV_{g\tau_E}} = \mathsf{V_{g_j}} - \mathsf{V_{g_B}}^{(503)}/\mathsf{m_\tau} \tag{5.24}$$

5.3 Early effect

In Mextram 503 the parameters $\mathsf{Q_{B0}}$ and $\mathsf{XC_{jC}}$ are used to define the forward and reverse Early voltage. In Mextram 504 we directly have the Early voltages $\mathsf{V_{ef}}$ and $\mathsf{V_{er}}$ as parameters. The advantage is that the correlation of the Early effect with parameter $\mathsf{XC_{jE}}$ is removed and that $\mathsf{XC_{jC}}$ can be used solely to distribute the base-collector junction capacitance. In Mextram 504 the parameters $1 - \mathsf{XC_{jE}}$ and $\mathsf{XC_{jC}}$ are defined as the fraction of the base-emitter and base-collector depletion capacitance underneath the emitter and have to be obtained from geometrical scaling rules. Parameter $\mathsf{Q_{B0}}$ is removed from the list. The conversion rules for the new parameters are:

$$\mathsf{V_{er}} = \frac{\mathsf{Q_{B0}}}{(1 - \mathsf{XC_{jE}})\ \mathsf{C_{jE}}} \tag{5.25}$$

$$\mathsf{V_{ef}} = \frac{\mathsf{Q_{B0}}}{\mathsf{XC_{jC}}\ \mathsf{C_{jC}}} \tag{5.26}$$

These parameters are the Early voltages at zero base-emitter and base-collector bias. The real forward Early voltage increases with $\mathcal{V}_{\mathrm{BE}}$ and $\mathcal{V}_{\mathrm{BC}}$ and its maximum is usually about 2 times higher than the parameter value.

5.4 Avalanche multiplication

In Mextram 504 the avalanche multiplication model is basically the same as that of Mextram 503. The modelling of the base-collector depletion layer width W_D with collector voltage is simplified. In Mextram 503 the bias dependency of W_D with collector voltage and current is given by the base-collector depletion charge model. Therefore avalanche multiplication is apart from the avalanche parameter AVL also dependent on parameters $\mathsf{X_p}$ and $\mathsf{p_C}$ of the base-collector capacitance model. $\mathsf{X_p}$ and $\mathsf{p_C}$ define the increase of the avalanche current (slope) with collector voltage and they are average values of the total base-collector junction capacitance. Avalanche currents are generated only in the base-collector region underneath the emitter and $\mathsf{X_p}$ and $\mathsf{p_C}$ may be different there due to a selective implanted collector, additional implants in the extrinsic base regions or the sidewall base-collector junction capacitance. In Mextram 504 we take the effective thickness

$\mathsf{W_{avl}}$ and punch through voltage $\mathsf{V_{avl}}$ (defined by the dope and thickness) of the epilayer underneath the emitter as parameters. A relatively simple model of a one-sided step junction is used to calculate W_D as a function of collector voltage and current. In this way we decouple the avalanche model parameters from the base-collector capacitance model parameters. To calculate the new parameters $\mathsf{W_{avl}}$ and $\mathsf{V_{avl}}$ from the Mextram 503 parameter set we have to calibrate the avalanche current at a certain collector voltage. A suitable voltage is the collector-emitter breakdown voltage $\mathrm{BV_{ceo}}$. This is the voltage where the base current becomes zero with increasing collector voltage. Because this voltage is slightly bias and temperature dependent it has to be given as an input. At this given collector voltage the maximum electric field, and therefore the calculated avalanche current, will be made the same for both models. In Mextram 503 the gradient of the electric field $\partial E/\partial x$ under the condition $I_c \ll \mathsf{I_{hc}}$ and the depletion layer thickness W_D as a function of collector voltage are:

$$\frac{\partial E}{\partial x} = 2\,\mathsf{V_{dc}}\,\left(\frac{B_n}{\mathsf{AVL}}\right)^2 \tag{5.27}$$

$$f_c = \frac{1-\mathsf{X_p}}{(1+\mathrm{BV_{ceo}}/\mathsf{V_{dc}})^{\mathsf{pc}}} + \mathsf{X_p} \tag{5.28}$$

$$W_D = \frac{\mathsf{AVL}}{B_n\; f_c} \tag{5.29}$$

In Mextram 504 the depletion layer thickness x_D using the same bias condition is:

$$x_D = \sqrt{\frac{2\;(\mathsf{V_{dc}}+\mathrm{BV_{ceo}})}{\partial E/\partial x}} \tag{5.30}$$

The depletion layer thickness has to be the same in both models and therefore W_D also equals $x_D\;\mathsf{W_{avl}}/\sqrt{x_D^2+\mathsf{W_{avl}}^2}$. This leads to

$$\mathsf{W_{avl}} = \frac{x_D\;W_D}{\sqrt{x_D^2-W_D^2}} \tag{5.31}$$

$$\mathsf{V_{avl}} = \frac{\partial E}{\partial x}\;\frac{\mathsf{W_{avl}}^2}{2} \tag{5.32}$$

In the improbable case that the equation for $\mathsf{W_{avl}}$ leads to numerical problems ($x_D < W_D$) either the parameter set is unphysical or the process is not optimized. In both cases one needs to give a physical value for $\mathsf{W_{avl}}$ by hand.

5.5 Non-ideal forward base current

The non-ideal base current I_{B_2} has, in Mextram 503, a cross-over voltage $\mathsf{V_{Lf}}$ where the slope $1/m = V_T\;\partial \ln I_{B_2}/\partial \mathcal{V}_{\mathrm{BE}}$ decreases from 1 to $1/2$. In most cases $\mathsf{V_{Lf}}$ is small and in the bias range of interest the slope of I_{B_2} is constant (1/2). With this model it is difficult to

describe a steady increasing gain over several decades. To be more flexible in this sense we introduce in Mextram 504 a constant non-ideality factor $\mathsf{m_{Lf}}$. To keep the number of parameters the same we remove $\mathsf{V_{Lf}}$. In the conversion we define two base-emitter voltages where the non-ideal base current of both models are the same

$$V_1 = 0.45 \tag{5.33}$$

$$V_2 = 0.75 \tag{5.34}$$

$$I_1 = \mathsf{I_{Bf}}^{(503)} \frac{\exp(V_1/V_{T_R}) - 1}{\exp\left(V_1/2\,V_{T_R}\right) + \exp\left(\mathsf{V_{Lf}}/2\,V_{T_R}\right)} \tag{5.35}$$

$$I_2 = \mathsf{I_{Bf}}^{(503)} \frac{\exp(V_2/V_{T_R}) - 1}{\exp\left(V_2/2\,V_{T_R}\right) + \exp\left(\mathsf{V_{Lf}}/2\,V_{T_R}\right)} \tag{5.36}$$

$$\mathsf{m_{Lf}} = \frac{V_2 - V_1}{V_{T_R}\,\ln\left(I_2/I_1\right)} \tag{5.37}$$

$$\mathsf{I_{Bf}}^{(504)} = \frac{I_2}{\exp\left(V_2/\mathsf{m_{Lf}}\,V_{T_R}\right) - 1} \tag{5.38}$$

When $\mathsf{V_{Lf}} \lesssim 0.3$ we have $\mathsf{m_{Lf}} = 2$ and $\mathsf{I_{Bf}}^{(504)} = \mathsf{I_{Bf}}^{(503)}$.

5.6 Transit times

In Mextram 503 we have only the emitter transit time τ_{NE} (renamed to τ_{E} in Mextram 504) as parameter. All other transit times, like for the base and collector, are calculated from DC parameters. In Mextram 504 we introduce transit times for the base, collector and reverse mode. They can easily be calculated from the Mextram 503 parameter set.

$$\tau_{\mathsf{B}} = \frac{\mathsf{Q_{B0}}}{\mathsf{I_k}} \tag{5.39}$$

$$\tau_{\mathsf{epi}} = \frac{\mathsf{I_s}\;\mathsf{Q_{B0}}\;{\mathsf{R_{Cv}}}^2 \exp\left(\mathsf{V_{d_C}}/V_{T_R}\right)}{4\,V_{T_R}^2} \tag{5.40}$$

$$\tau_{\mathsf{R}} = \left(\tau_{\mathsf{B}} + \tau_{\mathsf{epi}}\right)\;\frac{1 - \mathsf{XC_{jC}}}{\mathsf{XC_{jC}}} \tag{5.41}$$

Because the cut-off frequency f_T is sensitive to many parameters in some cases it might be necessary to correct a transit time (e.g. τ_{E} or τ_{B}). This can be done by tuning the top of the f_T.

6 Numerical examples

In this section we provide some numerical examples, based on Pstar 4.2. These results can be used to check the correctness of a model implementation. More numerical examples can be generated using the solver on the web [1]. Here we used the values of the default parameter set given in Sec. 4.3, but with $\mathsf{dE_g} = 0.01$ and $\mathsf{X_{rec}} = 0.1$, to include also the SiGe expressions. Some flags were changed as indicated in the tables. Self-heating is not included, unless specifically stated. Substrate currents below $1\,\mathrm{fA}$ were disregarded.

6.1 Forward Gummel plot

In this example the base voltage is swept from 0.4 to $1.2\,\mathrm{V}$, with emitter and substrate voltages at $0\,\mathrm{V}$ and the collector voltage at $1\,\mathrm{V}$.

Device temperature $T = 25°\mathrm{C}$

$\mathcal{V}_{\mathrm{BE}}\,(\mathrm{V})$	$I_C\,(\mathrm{A})$	$I_B\,(\mathrm{A})$	$I_{\mathrm{sub}}\,(\mathrm{A})$
0.40	$1.0474 \cdot 10^{-10}$	$7.0562 \cdot 10^{-12}$	—
0.50	$4.8522 \cdot 10^{-09}$	$7.4371 \cdot 10^{-11}$	—
0.60	$2.2402 \cdot 10^{-07}$	$1.7371 \cdot 10^{-09}$	—
0.70	$1.0254 \cdot 10^{-05}$	$7.1660 \cdot 10^{-08}$	—
0.80	$4.2490 \cdot 10^{-04}$	$3.1412 \cdot 10^{-06}$	—
0.90	$5.5812 \cdot 10^{-03}$	$5.2923 \cdot 10^{-05}$	—
1.00	$1.5882 \cdot 10^{-02}$	$2.7185 \cdot 10^{-04}$	$-7.3559 \cdot 10^{-14}$
1.10	$2.7384 \cdot 10^{-02}$	$7.8543 \cdot 10^{-04}$	$-6.8642 \cdot 10^{-10}$
1.20	$3.8631 \cdot 10^{-02}$	$1.6447 \cdot 10^{-03}$	$-5.5645 \cdot 10^{-06}$

Device temperature $T = 100°\mathrm{C}$

$\mathcal{V}_{\mathrm{BE}}\,(\mathrm{V})$	$I_C\,(\mathrm{A})$	$I_B\,(\mathrm{A})$	$I_{\mathrm{sub}}\,(\mathrm{A})$
0.40	$8.0045 \cdot 10^{-08}$	$5.9427 \cdot 10^{-10}$	—
0.50	$1.6985 \cdot 10^{-06}$	$9.9748 \cdot 10^{-09}$	—
0.60	$3.5649 \cdot 10^{-05}$	$2.0657 \cdot 10^{-07}$	—
0.70	$6.6588 \cdot 10^{-04}$	$4.1113 \cdot 10^{-06}$	—
0.80	$5.2130 \cdot 10^{-03}$	$4.3737 \cdot 10^{-05}$	$-4.0795 \cdot 10^{-14}$
0.90	$1.3673 \cdot 10^{-02}$	$2.2102 \cdot 10^{-04}$	$-1.2225 \cdot 10^{-10}$
1.00	$2.3552 \cdot 10^{-02}$	$6.7151 \cdot 10^{-04}$	$-7.9106 \cdot 10^{-07}$
1.10	$3.2388 \cdot 10^{-02}$	$2.1960 \cdot 10^{-03}$	$-6.6654 \cdot 10^{-04}$
1.20	$3.5243 \cdot 10^{-02}$	$8.2877 \cdot 10^{-03}$	$-3.8786 \cdot 10^{-03}$

Device temperature $T = 25°\mathrm{C}$, with self-heating

$\mathcal{V}_{\mathrm{BE}}\,(\mathrm{V})$	$I_C\,(\mathrm{A})$	$I_B\,(\mathrm{A})$	$I_{\mathrm{sub}}\,(\mathrm{A})$	$T_K(°\mathrm{C})$
0.80	$4.2781 \cdot 10^{-04}$	$3.1619 \cdot 10^{-06}$	—	25.129
0.90	$5.7715 \cdot 10^{-03}$	$5.5125 \cdot 10^{-05}$	—	26.746
1.00	$1.6471 \cdot 10^{-02}$	$2.9026 \cdot 10^{-04}$	$-2.4797 \cdot 10^{-13}$	30.028
1.10	$2.8246 \cdot 10^{-02}$	$8.4606 \cdot 10^{-04}$	$-5.4441 \cdot 10^{-09}$	33.753
1.20	$3.9449 \cdot 10^{-02}$	$1.8510 \cdot 10^{-03}$	$-7.5766 \cdot 10^{-05}$	37.501

6.2 Reverse Gummel plot

In this example again the base voltage is swept from 0.4 to $1.2\,\mathrm{V}$, but now with collector and substrate voltages at $0\,\mathrm{V}$ and the emitter voltage at $1\,\mathrm{V}$.

Device temperature $T = 25°\mathrm{C}$, EXMOD $= 1$

$\mathcal{V}_{\mathrm{BC}}\,(\mathrm{V})$	$I_E\,(\mathrm{A})$	$I_B\,(\mathrm{A})$	$I_{\mathrm{sub}}\,(\mathrm{A})$
0.40	$1.6687 \cdot 10^{-10}$	$2.9777 \cdot 10^{-10}$	$-2.7723 \cdot 10^{-10}$
0.50	$7.7698 \cdot 10^{-09}$	$1.4499 \cdot 10^{-08}$	$-1.3590 \cdot 10^{-08}$
0.60	$3.6108 \cdot 10^{-07}$	$7.0890 \cdot 10^{-07}$	$-6.6504 \cdot 10^{-07}$
0.70	$1.5810 \cdot 10^{-05}$	$3.2360 \cdot 10^{-05}$	$-3.0260 \cdot 10^{-05}$
0.80	$3.9318 \cdot 10^{-04}$	$5.9320 \cdot 10^{-04}$	$-5.2275 \cdot 10^{-04}$
0.90	$2.2197 \cdot 10^{-03}$	$2.5994 \cdot 10^{-03}$	$-1.9150 \cdot 10^{-03}$
1.00	$4.8747 \cdot 10^{-03}$	$5.8002 \cdot 10^{-03}$	$-3.5480 \cdot 10^{-03}$
1.10	$7.6813 \cdot 10^{-03}$	$9.6108 \cdot 10^{-03}$	$-5.2096 \cdot 10^{-03}$
1.20	$1.0540 \cdot 10^{-02}$	$1.3724 \cdot 10^{-02}$	$-6.9400 \cdot 10^{-03}$

Device temperature $T = 100°\mathrm{C}$, EXMOD $= 1$

$\mathcal{V}_{\mathrm{BC}}\,(\mathrm{V})$	$I_E\,(\mathrm{A})$	$I_B\,(\mathrm{A})$	$I_{\mathrm{sub}}\,(\mathrm{A})$
0.40	$1.2362 \cdot 10^{-07}$	$2.5885 \cdot 10^{-07}$	$-2.4907 \cdot 10^{-07}$
0.50	$2.5916 \cdot 10^{-06}$	$5.7085 \cdot 10^{-06}$	$-5.4918 \cdot 10^{-06}$
0.60	$4.7158 \cdot 10^{-05}$	$9.9629 \cdot 10^{-05}$	$-9.5155 \cdot 10^{-05}$
0.70	$4.7495 \cdot 10^{-04}$	$6.7806 \cdot 10^{-04}$	$-6.1741 \cdot 10^{-04}$
0.80	$1.8123 \cdot 10^{-03}$	$2.0214 \cdot 10^{-03}$	$-1.6608 \cdot 10^{-03}$
0.90	$3.7155 \cdot 10^{-03}$	$3.9952 \cdot 10^{-03}$	$-2.9251 \cdot 10^{-03}$
1.00	$5.7889 \cdot 10^{-03}$	$6.3542 \cdot 10^{-03}$	$-4.2443 \cdot 10^{-03}$
1.10	$7.9240 \cdot 10^{-03}$	$8.9302 \cdot 10^{-03}$	$-5.6007 \cdot 10^{-03}$
1.20	$1.0097 \cdot 10^{-02}$	$1.1632 \cdot 10^{-02}$	$-6.9964 \cdot 10^{-03}$

Device temperature $T = 25°\mathrm{C}$, EXMOD $= 0$

$\mathcal{V}_{\mathrm{BC}}\,(\mathrm{V})$	$I_E\,(\mathrm{A})$	$I_B\,(\mathrm{A})$	$I_{\mathrm{sub}}\,(\mathrm{A})$
0.40	$1.6687 \cdot 10^{-10}$	$2.9777 \cdot 10^{-10}$	$-2.7723 \cdot 10^{-10}$
0.50	$7.7698 \cdot 10^{-09}$	$1.4499 \cdot 10^{-08}$	$-1.3590 \cdot 10^{-08}$
0.60	$3.6094 \cdot 10^{-07}$	$7.0873 \cdot 10^{-07}$	$-6.6488 \cdot 10^{-07}$
0.70	$1.5544 \cdot 10^{-05}$	$3.1916 \cdot 10^{-05}$	$-2.9848 \cdot 10^{-05}$
0.80	$3.2428 \cdot 10^{-04}$	$5.1459 \cdot 10^{-04}$	$-4.5927 \cdot 10^{-04}$
0.90	$1.5972 \cdot 10^{-03}$	$1.8906 \cdot 10^{-03}$	$-1.5217 \cdot 10^{-03}$
1.00	$3.5189 \cdot 10^{-03}$	$3.7361 \cdot 10^{-03}$	$-2.7309 \cdot 10^{-03}$
1.10	$5.6544 \cdot 10^{-03}$	$5.7762 \cdot 10^{-03}$	$-3.9166 \cdot 10^{-03}$
1.20	$7.8552 \cdot 10^{-03}$	$7.9157 \cdot 10^{-03}$	$-5.0659 \cdot 10^{-03}$

6.3 Output characteristics

In these two examples the base current is kept constant at $10\,\mu\mathrm{A}$. The collector current is swept from 0 to $20\,\mathrm{mA}$ (note the two different step sizes of the collector current). Emitter and substrate are grounded. In the second example extended avalanche is switched on which makes the collector-emitter voltage decrease again when $I_C > 8\,\mathrm{mA}$. This decrease is not observed in the first example.

Device temperature $T = 25°\mathrm{C}$, EXAVL $= 0$

$I_C\,(\mathrm{A})$	$\mathcal{V}_{\mathrm{CE}}\,(\mathrm{V})$	$\mathcal{V}_{\mathrm{BE}}\,(\mathrm{V})$	$I_{\mathrm{sub}}\,(\mathrm{A})$
$0.0 \cdot 10^{+00}$	$4.8992 \cdot 10^{-03}$	$6.7332 \cdot 10^{-01}$	$-9.3489 \cdot 10^{-06}$
$5.0 \cdot 10^{-04}$	$1.5574 \cdot 10^{-01}$	$8.0558 \cdot 10^{-01}$	$-5.7683 \cdot 10^{-06}$
$1.0 \cdot 10^{-03}$	$2.1013 \cdot 10^{-01}$	$8.2659 \cdot 10^{-01}$	$-2.0019 \cdot 10^{-06}$
$1.5 \cdot 10^{-03}$	$9.8664 \cdot 10^{+00}$	$8.3759 \cdot 10^{-01}$	—
$2.0 \cdot 10^{-03}$	$1.1711 \cdot 10^{+01}$	$8.4755 \cdot 10^{-01}$	—
$4.0 \cdot 10^{-03}$	$1.3321 \cdot 10^{+01}$	$8.7643 \cdot 10^{-01}$	—
$6.0 \cdot 10^{-03}$	$1.3922 \cdot 10^{+01}$	$8.9793 \cdot 10^{-01}$	—
$8.0 \cdot 10^{-03}$	$1.4297 \cdot 10^{+01}$	$9.1636 \cdot 10^{-01}$	—
$1.0 \cdot 10^{-02}$	$1.4575 \cdot 10^{+01}$	$9.3309 \cdot 10^{-01}$	—
$1.2 \cdot 10^{-02}$	$1.4802 \cdot 10^{+01}$	$9.4877 \cdot 10^{-01}$	—
$1.4 \cdot 10^{-02}$	$1.5003 \cdot 10^{+01}$	$9.6378 \cdot 10^{-01}$	—
$1.6 \cdot 10^{-02}$	$1.5208 \cdot 10^{+01}$	$9.7854 \cdot 10^{-01}$	—
$1.8 \cdot 10^{-02}$	$1.5414 \cdot 10^{+01}$	$9.9306 \cdot 10^{-01}$	—
$2.0 \cdot 10^{-02}$	$1.5612 \cdot 10^{+01}$	$1.0073 \cdot 10^{+00}$	—

Device temperature $T = 25°\mathrm{C}$, EXAVL $= 1$

$I_C\,(\mathrm{A})$	$\mathcal{V}_{\mathrm{CE}}\,(\mathrm{V})$	$\mathcal{V}_{\mathrm{BE}}\,(\mathrm{V})$	$I_{\mathrm{sub}}\,(\mathrm{A})$
$0.0 \cdot 10^{+00}$	$4.8992 \cdot 10^{-03}$	$6.7332 \cdot 10^{-01}$	$-9.3489 \cdot 10^{-06}$
$5.0 \cdot 10^{-04}$	$1.5574 \cdot 10^{-01}$	$8.0558 \cdot 10^{-01}$	$-5.7683 \cdot 10^{-06}$
$1.0 \cdot 10^{-03}$	$2.1013 \cdot 10^{-01}$	$8.2659 \cdot 10^{-01}$	$-2.0019 \cdot 10^{-06}$
$1.5 \cdot 10^{-03}$	$9.7462 \cdot 10^{+00}$	$8.3761 \cdot 10^{-01}$	—
$2.0 \cdot 10^{-03}$	$1.1520 \cdot 10^{+01}$	$8.4758 \cdot 10^{-01}$	—
$4.0 \cdot 10^{-03}$	$1.2909 \cdot 10^{+01}$	$8.7650 \cdot 10^{-01}$	—
$6.0 \cdot 10^{-03}$	$1.3240 \cdot 10^{+01}$	$8.9805 \cdot 10^{-01}$	—
$8.0 \cdot 10^{-03}$	$1.3256 \cdot 10^{+01}$	$9.1653 \cdot 10^{-01}$	—
$1.0 \cdot 10^{-02}$	$1.3073 \cdot 10^{+01}$	$9.3337 \cdot 10^{-01}$	—
$1.2 \cdot 10^{-02}$	$1.2748 \cdot 10^{+01}$	$9.4923 \cdot 10^{-01}$	—
$1.4 \cdot 10^{-02}$	$1.2354 \cdot 10^{+01}$	$9.6479 \cdot 10^{-01}$	—
$1.6 \cdot 10^{-02}$	$1.1927 \cdot 10^{+01}$	$9.8009 \cdot 10^{-01}$	—
$1.8 \cdot 10^{-02}$	$1.1497 \cdot 10^{+01}$	$9.9506 \cdot 10^{-01}$	—
$2.0 \cdot 10^{-02}$	$1.1103 \cdot 10^{+01}$	$1.0098 \cdot 10^{+00}$	—

Device temperature $T = 25°\mathrm{C}$, EXAVL $= 0$, with self-heating

$I_C\,(\mathrm{A})$	$\mathcal{V}_{\mathrm{CE}}\,(\mathrm{V})$	$\mathcal{V}_{\mathrm{BE}}\,(\mathrm{V})$	$I_{\mathrm{sub}}\,(\mathrm{A})$	$T_K(°\mathrm{C})$
$0.0 \cdot 10^{+00}$	$4.8992 \cdot 10^{-03}$	$6.7331 \cdot 10^{-01}$	$-9.3489 \cdot 10^{-06}$	25.002
$5.0 \cdot 10^{-04}$	$1.5576 \cdot 10^{-01}$	$8.0554 \cdot 10^{-01}$	$-5.7687 \cdot 10^{-06}$	25.026
$1.0 \cdot 10^{-03}$	$2.1016 \cdot 10^{-01}$	$8.2650 \cdot 10^{-01}$	$-2.0036 \cdot 10^{-06}$	25.066
$1.5 \cdot 10^{-03}$	$9.6837 \cdot 10^{+00}$	$8.3146 \cdot 10^{-01}$	—	29.360
$2.0 \cdot 10^{-03}$	$1.1676 \cdot 10^{+01}$	$8.3782 \cdot 10^{-01}$	—	32.008
$4.0 \cdot 10^{-03}$	$1.3370 \cdot 10^{+01}$	$8.5510 \cdot 10^{-01}$	—	41.046
$6.0 \cdot 10^{-03}$	$1.4032 \cdot 10^{+01}$	$8.6521 \cdot 10^{-01}$	—	50.261
$8.0 \cdot 10^{-03}$	$1.4471 \cdot 10^{+01}$	$8.7219 \cdot 10^{-01}$	—	59.733
$1.0 \cdot 10^{-02}$	$1.4816 \cdot 10^{+01}$	$8.7738 \cdot 10^{-01}$	—	69.452
$1.2 \cdot 10^{-02}$	$1.5116 \cdot 10^{+01}$	$8.8139 \cdot 10^{-01}$	—	79.419
$1.4 \cdot 10^{-02}$	$1.5396 \cdot 10^{+01}$	$8.8458 \cdot 10^{-01}$	—	89.667
$1.6 \cdot 10^{-02}$	$1.5698 \cdot 10^{+01}$	$8.8735 \cdot 10^{-01}$	—	100.35
$1.8 \cdot 10^{-02}$	$1.6014 \cdot 10^{+01}$	$8.8966 \cdot 10^{-01}$	—	111.48
$2.0 \cdot 10^{-02}$	$1.6339 \cdot 10^{+01}$	$8.9147 \cdot 10^{-01}$	—	123.04

6.4 Small-signal characteristics

In the next example the cut-off frequency f_T is calculated. The emitter and substrate are at $0\,\mathrm{V}$ and the collector is at $1\,\mathrm{V}$. The DC base voltage is swept and the amplitude of the AC base voltage is $1\,\mathrm{mV}$. We give the absolute values of the small-signal base and collector currents, as well as $f_T = f \cdot i_C/i_B$ with $f = 1\,\mathrm{GHz}$.

Device temperature $T = 25°\mathrm{C}$

$\mathcal{V}_{\mathrm{BE}}\,(\mathrm{V})$	$\lvert i_C\rvert\,(\mathrm{A})$	$\lvert i_B\rvert\,(\mathrm{A})$	$f_T\,(\mathrm{Hz})$
0.70	$5.9997 \cdot 10^{-07}$	$1.3075 \cdot 10^{-06}$	$4.5887 \cdot 10^{+08}$
0.72	$9.6236 \cdot 10^{-07}$	$1.3790 \cdot 10^{-06}$	$6.9789 \cdot 10^{+08}$
0.74	$1.8469 \cdot 10^{-06}$	$1.4944 \cdot 10^{-06}$	$1.2359 \cdot 10^{+09}$
0.76	$3.7588 \cdot 10^{-06}$	$1.6993 \cdot 10^{-06}$	$2.2120 \cdot 10^{+09}$
0.78	$7.6130 \cdot 10^{-06}$	$2.0818 \cdot 10^{-06}$	$3.6568 \cdot 10^{+09}$
0.80	$1.4783 \cdot 10^{-05}$	$2.7966 \cdot 10^{-06}$	$5.2861 \cdot 10^{+09}$
0.82	$2.6511 \cdot 10^{-05}$	$4.0416 \cdot 10^{-06}$	$6.5596 \cdot 10^{+09}$
0.84	$4.2265 \cdot 10^{-05}$	$6.0608 \cdot 10^{-06}$	$6.9735 \cdot 10^{+09}$
0.86	$5.7134 \cdot 10^{-05}$	$9.8903 \cdot 10^{-06}$	$5.7768 \cdot 10^{+09}$
0.88	$5.9762 \cdot 10^{-05}$	$1.6082 \cdot 10^{-05}$	$3.7161 \cdot 10^{+09}$
0.90	$5.6033 \cdot 10^{-05}$	$2.0063 \cdot 10^{-05}$	$2.7928 \cdot 10^{+09}$
0.92	$5.3789 \cdot 10^{-05}$	$2.2275 \cdot 10^{-05}$	$2.4148 \cdot 10^{+09}$
0.94	$5.1755 \cdot 10^{-05}$	$2.3876 \cdot 10^{-05}$	$2.1677 \cdot 10^{+09}$
0.96	$4.9648 \cdot 10^{-05}$	$2.5173 \cdot 10^{-05}$	$1.9722 \cdot 10^{+09}$
0.98	$4.7568 \cdot 10^{-05}$	$2.6275 \cdot 10^{-05}$	$1.8104 \cdot 10^{+09}$
1.00	$4.5599 \cdot 10^{-05}$	$2.7232 \cdot 10^{-05}$	$1.6745 \cdot 10^{+09}$

Device temperature $T = 100°\mathrm{C}$

$\mathcal{V}_{\mathrm{BE}}\,(\mathrm{V})$	$\lvert i_C\rvert\,(\mathrm{A})$	$\lvert i_B\rvert\,(\mathrm{A})$	$f_T\,(\mathrm{Hz})$
0.70	$1.7942 \cdot 10^{-05}$	$3.1922 \cdot 10^{-06}$	$5.6205 \cdot 10^{+09}$
0.72	$2.7792 \cdot 10^{-05}$	$4.5464 \cdot 10^{-06}$	$6.1129 \cdot 10^{+09}$
0.74	$3.8727 \cdot 10^{-05}$	$7.2524 \cdot 10^{-06}$	$5.3399 \cdot 10^{+09}$
0.76	$4.3039 \cdot 10^{-05}$	$1.2464 \cdot 10^{-05}$	$3.4532 \cdot 10^{+09}$
0.78	$3.9912 \cdot 10^{-05}$	$1.6559 \cdot 10^{-05}$	$2.4103 \cdot 10^{+09}$
0.80	$3.7841 \cdot 10^{-05}$	$1.8771 \cdot 10^{-05}$	$2.0159 \cdot 10^{+09}$
0.82	$3.6295 \cdot 10^{-05}$	$2.0316 \cdot 10^{-05}$	$1.7865 \cdot 10^{+09}$
0.84	$3.4742 \cdot 10^{-05}$	$2.1556 \cdot 10^{-05}$	$1.6117 \cdot 10^{+09}$
0.86	$3.3203 \cdot 10^{-05}$	$2.2614 \cdot 10^{-05}$	$1.4683 \cdot 10^{+09}$
0.88	$3.1741 \cdot 10^{-05}$	$2.3545 \cdot 10^{-05}$	$1.3481 \cdot 10^{+09}$
0.90	$3.0392 \cdot 10^{-05}$	$2.4380 \cdot 10^{-05}$	$1.2466 \cdot 10^{+09}$
0.92	$2.9166 \cdot 10^{-05}$	$2.5134 \cdot 10^{-05}$	$1.1604 \cdot 10^{+09}$
0.94	$2.8062 \cdot 10^{-05}$	$2.5826 \cdot 10^{-05}$	$1.0866 \cdot 10^{+09}$
0.96	$2.7097 \cdot 10^{-05}$	$2.6497 \cdot 10^{-05}$	$1.0226 \cdot 10^{+09}$
0.98	$2.6416 \cdot 10^{-05}$	$2.7340 \cdot 10^{-05}$	$9.6623 \cdot 10^{+08}$
1.00	$2.6804 \cdot 10^{-05}$	$2.9323 \cdot 10^{-05}$	$9.1407 \cdot 10^{+08}$

6.5 Y-parameters

In the last example we show the two-port Y-parameters as a function of frequency f. The transistor is biased around the top of the f_T: $\mathcal{V}_{\mathrm{B}} = 0.85\,\mathrm{V}$, $\mathcal{V}_{\mathrm{C}} = 2.0\,\mathrm{V}$ and both emitter and substrate are grounded. In the first data set (two tables) the distributed high frequency effects are switched on. In the second set they are switched off.

Device temperature $T = 25°\mathrm{C}$, $\mathsf{EXPHI} = 1$

$f\,(\mathrm{Hz})$	$\mathrm{Re}\,Y_{11}\,(\mathrm{S})$	$\mathrm{Im}\,Y_{11}\,(\mathrm{S})$	$\mathrm{Re}\,Y_{21}\,(\mathrm{S})$	$\mathrm{Im}\,Y_{21}\,(\mathrm{S})$
$1.0 \cdot 10^{+06}$	$4.4048 \cdot 10^{-04}$	$6.5967 \cdot 10^{-06}$	$5.2977 \cdot 10^{-02}$	$-1.5626 \cdot 10^{-05}$
$2.0 \cdot 10^{+06}$	$4.4048 \cdot 10^{-04}$	$1.3193 \cdot 10^{-05}$	$5.2977 \cdot 10^{-02}$	$-3.1251 \cdot 10^{-05}$
$5.0 \cdot 10^{+06}$	$4.4051 \cdot 10^{-04}$	$3.2984 \cdot 10^{-05}$	$5.2977 \cdot 10^{-02}$	$-7.8128 \cdot 10^{-05}$
$1.0 \cdot 10^{+07}$	$4.4062 \cdot 10^{-04}$	$6.5967 \cdot 10^{-05}$	$5.2976 \cdot 10^{-02}$	$-1.5626 \cdot 10^{-04}$
$2.0 \cdot 10^{+07}$	$4.4107 \cdot 10^{-04}$	$1.3193 \cdot 10^{-04}$	$5.2975 \cdot 10^{-02}$	$-3.1251 \cdot 10^{-04}$
$5.0 \cdot 10^{+07}$	$4.4421 \cdot 10^{-04}$	$3.2979 \cdot 10^{-04}$	$5.2967 \cdot 10^{-02}$	$-7.8117 \cdot 10^{-04}$
$1.0 \cdot 10^{+08}$	$4.5542 \cdot 10^{-04}$	$6.5932 \cdot 10^{-04}$	$5.2939 \cdot 10^{-02}$	$-1.5617 \cdot 10^{-03}$
$2.0 \cdot 10^{+08}$	$5.0016 \cdot 10^{-04}$	$1.3165 \cdot 10^{-03}$	$5.2827 \cdot 10^{-02}$	$-3.1180 \cdot 10^{-03}$
$5.0 \cdot 10^{+08}$	$8.0909 \cdot 10^{-04}$	$3.2542 \cdot 10^{-03}$	$5.2053 \cdot 10^{-02}$	$-7.7020 \cdot 10^{-03}$
$1.0 \cdot 10^{+09}$	$1.8549 \cdot 10^{-03}$	$6.2581 \cdot 10^{-03}$	$4.9432 \cdot 10^{-02}$	$-1.4776 \cdot 10^{-02}$
$2.0 \cdot 10^{+09}$	$5.3061 \cdot 10^{-03}$	$1.0865 \cdot 10^{-02}$	$4.0788 \cdot 10^{-02}$	$-2.5405 \cdot 10^{-02}$
$5.0 \cdot 10^{+09}$	$1.5819 \cdot 10^{-02}$	$1.4624 \cdot 10^{-02}$	$1.4542 \cdot 10^{-02}$	$-3.2040 \cdot 10^{-02}$

Device temperature $T = 25°\mathrm{C}$, EXPHI $= 1$

f (Hz)	$\mathrm{Re}\, Y_{12}$ (S)	$\mathrm{Im}\, Y_{12}$ (S)	$\mathrm{Re}\, Y_{22}$ (S)	$\mathrm{Im}\, Y_{22}$ (S)
$1.0 \cdot 10^{+06}$	$-7.5618 \cdot 10^{-08}$	$-3.7249 \cdot 10^{-07}$	$1.4843 \cdot 10^{-05}$	$1.7837 \cdot 10^{-06}$
$2.0 \cdot 10^{+06}$	$-7.5710 \cdot 10^{-08}$	$-7.4497 \cdot 10^{-07}$	$1.4844 \cdot 10^{-05}$	$3.5675 \cdot 10^{-06}$
$5.0 \cdot 10^{+06}$	$-7.6354 \cdot 10^{-08}$	$-1.8624 \cdot 10^{-06}$	$1.4846 \cdot 10^{-05}$	$8.9186 \cdot 10^{-06}$
$1.0 \cdot 10^{+07}$	$-7.8655 \cdot 10^{-08}$	$-3.7248 \cdot 10^{-06}$	$1.4853 \cdot 10^{-05}$	$1.7837 \cdot 10^{-05}$
$2.0 \cdot 10^{+07}$	$-8.7860 \cdot 10^{-08}$	$-7.4497 \cdot 10^{-06}$	$1.4880 \cdot 10^{-05}$	$3.5674 \cdot 10^{-05}$
$5.0 \cdot 10^{+07}$	$-1.5228 \cdot 10^{-07}$	$-1.8623 \cdot 10^{-05}$	$1.5072 \cdot 10^{-05}$	$8.9184 \cdot 10^{-05}$
$1.0 \cdot 10^{+08}$	$-3.8227 \cdot 10^{-07}$	$-3.7242 \cdot 10^{-05}$	$1.5757 \cdot 10^{-05}$	$1.7836 \cdot 10^{-04}$
$2.0 \cdot 10^{+08}$	$-1.3006 \cdot 10^{-06}$	$-7.4448 \cdot 10^{-05}$	$1.8493 \cdot 10^{-05}$	$3.5662 \cdot 10^{-04}$
$5.0 \cdot 10^{+08}$	$-7.6569 \cdot 10^{-06}$	$-1.8549 \cdot 10^{-04}$	$3.7464 \cdot 10^{-05}$	$8.8993 \cdot 10^{-04}$
$1.0 \cdot 10^{+09}$	$-2.9387 \cdot 10^{-05}$	$-3.6667 \cdot 10^{-04}$	$1.0278 \cdot 10^{-04}$	$1.7689 \cdot 10^{-03}$
$2.0 \cdot 10^{+09}$	$-1.0395 \cdot 10^{-04}$	$-7.0484 \cdot 10^{-04}$	$3.3293 \cdot 10^{-04}$	$3.4647 \cdot 10^{-03}$
$5.0 \cdot 10^{+09}$	$-3.9478 \cdot 10^{-04}$	$-1.5393 \cdot 10^{-03}$	$1.3617 \cdot 10^{-03}$	$8.0768 \cdot 10^{-03}$

Device temperature $T = 25°\mathrm{C}$, EXPHI $= 0$

f (Hz)	$\mathrm{Re}\, Y_{11}$ (S)	$\mathrm{Im}\, Y_{11}$ (S)	$\mathrm{Re}\, Y_{21}$ (S)	$\mathrm{Im}\, Y_{21}$ (S)
$1.0 \cdot 10^{+06}$	$4.4048 \cdot 10^{-04}$	$6.5941 \cdot 10^{-06}$	$5.2977 \cdot 10^{-02}$	$-1.4779 \cdot 10^{-05}$
$2.0 \cdot 10^{+06}$	$4.4048 \cdot 10^{-04}$	$1.3188 \cdot 10^{-05}$	$5.2977 \cdot 10^{-02}$	$-2.9559 \cdot 10^{-05}$
$5.0 \cdot 10^{+06}$	$4.4051 \cdot 10^{-04}$	$3.2971 \cdot 10^{-05}$	$5.2977 \cdot 10^{-02}$	$-7.3897 \cdot 10^{-05}$
$1.0 \cdot 10^{+07}$	$4.4063 \cdot 10^{-04}$	$6.5941 \cdot 10^{-05}$	$5.2976 \cdot 10^{-02}$	$-1.4779 \cdot 10^{-04}$
$2.0 \cdot 10^{+07}$	$4.4108 \cdot 10^{-04}$	$1.3188 \cdot 10^{-04}$	$5.2975 \cdot 10^{-02}$	$-2.9558 \cdot 10^{-04}$
$5.0 \cdot 10^{+07}$	$4.4426 \cdot 10^{-04}$	$3.2966 \cdot 10^{-04}$	$5.2968 \cdot 10^{-02}$	$-7.3887 \cdot 10^{-04}$
$1.0 \cdot 10^{+08}$	$4.5561 \cdot 10^{-04}$	$6.5905 \cdot 10^{-04}$	$5.2942 \cdot 10^{-02}$	$-1.4771 \cdot 10^{-03}$
$2.0 \cdot 10^{+08}$	$5.0090 \cdot 10^{-04}$	$1.3159 \cdot 10^{-03}$	$5.2837 \cdot 10^{-02}$	$-2.9492 \cdot 10^{-03}$
$5.0 \cdot 10^{+08}$	$8.1369 \cdot 10^{-04}$	$3.2526 \cdot 10^{-03}$	$5.2112 \cdot 10^{-02}$	$-7.2866 \cdot 10^{-03}$
$1.0 \cdot 10^{+09}$	$1.8731 \cdot 10^{-03}$	$6.2525 \cdot 10^{-03}$	$4.9656 \cdot 10^{-02}$	$-1.3988 \cdot 10^{-02}$
$2.0 \cdot 10^{+09}$	$5.3743 \cdot 10^{-03}$	$1.0835 \cdot 10^{-02}$	$4.1541 \cdot 10^{-02}$	$-2.4106 \cdot 10^{-02}$
$5.0 \cdot 10^{+09}$	$1.6073 \cdot 10^{-02}$	$1.4339 \cdot 10^{-02}$	$1.6744 \cdot 10^{-02}$	$-3.0715 \cdot 10^{-02}$

Device temperature $T = 25°\mathrm{C}$, EXPHI $= 0$

f (Hz)	$\mathrm{Re}\, Y_{12}$ (S)	$\mathrm{Im}\, Y_{12}$ (S)	$\mathrm{Re}\, Y_{22}$ (S)	$\mathrm{Im}\, Y_{22}$ (S)
$1.0 \cdot 10^{+06}$	$-7.5618 \cdot 10^{-08}$	$-3.7248 \cdot 10^{-07}$	$1.4843 \cdot 10^{-05}$	$1.7832 \cdot 10^{-06}$
$2.0 \cdot 10^{+06}$	$-7.5710 \cdot 10^{-08}$	$-7.4497 \cdot 10^{-07}$	$1.4844 \cdot 10^{-05}$	$3.5665 \cdot 10^{-06}$
$5.0 \cdot 10^{+06}$	$-7.6354 \cdot 10^{-08}$	$-1.8624 \cdot 10^{-06}$	$1.4846 \cdot 10^{-05}$	$8.9162 \cdot 10^{-06}$
$1.0 \cdot 10^{+07}$	$-7.8656 \cdot 10^{-08}$	$-3.7248 \cdot 10^{-06}$	$1.4852 \cdot 10^{-05}$	$1.7832 \cdot 10^{-05}$
$2.0 \cdot 10^{+07}$	$-8.7861 \cdot 10^{-08}$	$-7.4496 \cdot 10^{-06}$	$1.4879 \cdot 10^{-05}$	$3.5665 \cdot 10^{-05}$
$5.0 \cdot 10^{+07}$	$-1.5229 \cdot 10^{-07}$	$-1.8623 \cdot 10^{-05}$	$1.5064 \cdot 10^{-05}$	$8.9160 \cdot 10^{-05}$
$1.0 \cdot 10^{+08}$	$-3.8229 \cdot 10^{-07}$	$-3.7242 \cdot 10^{-05}$	$1.5724 \cdot 10^{-05}$	$1.7831 \cdot 10^{-04}$
$2.0 \cdot 10^{+08}$	$-1.3006 \cdot 10^{-06}$	$-7.4447 \cdot 10^{-05}$	$1.8360 \cdot 10^{-05}$	$3.5653 \cdot 10^{-04}$
$5.0 \cdot 10^{+08}$	$-7.6569 \cdot 10^{-06}$	$-1.8548 \cdot 10^{-04}$	$3.6649 \cdot 10^{-05}$	$8.8981 \cdot 10^{-04}$
$1.0 \cdot 10^{+09}$	$-2.9382 \cdot 10^{-05}$	$-3.6662 \cdot 10^{-04}$	$9.9701 \cdot 10^{-05}$	$1.7693 \cdot 10^{-03}$
$2.0 \cdot 10^{+09}$	$-1.0383 \cdot 10^{-04}$	$-7.0445 \cdot 10^{-04}$	$3.2297 \cdot 10^{-04}$	$3.4701 \cdot 10^{-03}$
$5.0 \cdot 10^{+09}$	$-3.9076 \cdot 10^{-04}$	$-1.5358 \cdot 10^{-03}$	$1.3402 \cdot 10^{-03}$	$8.1198 \cdot 10^{-03}$

Acknowledgements

For the development of the model we have had valuable discussions with Dr. Henk C. de Graaff.

For testing it we leaned heavily on measurements of Ramon Havens and on the benchmarking effort of the Compact Model Council (CMC). For the implementation we made use of the modelkit features of Pstar made by ED&T. We especially thank Jos Peters for creating the many executables we needed. For their feedback we thank the members of the implementation team, Michiel Stoutjesdijk, Kees van Velthooven, Rob Heeres, Jan Symons and Jan-Hein Egbers. A final acknowledgement is made to Dick Klaassen and Reinout Woltjer for their continuous support of this work.

October 2004, J.P.

We would like to express gratitude to:

– Dr. H.C. de Graaff, for continued discussions on device physics and the foundations of the Mextram model.

– Dr. D.B.M. Klaassen, Dr. A.J. Scholten (NXP Semiconductors), Prof. J. Burghartz and Dr. L.C.N. de Vreede (Delft University of Technology) for their support to the Mextram model.

– Dr. S. Mijalković, Dr. H.C. Wu and K. Buisman (Delft Univ.) for their extensive work on implementation of Mextram in the Verilog-A language and to L. Lemaitre (Freescale) for advice on this work.

– to G. Coram (Analog Devices) for extensive support on the development of the Verilog-A implementation.

March 2008, RvdT.

Acknowledgements are due to the GEIA/ Compact Model Council for countinuous support of Mextram.

Furthermore we would like to express gratitude to:

– Marjan Driessen, Jos Dohmen and Jos Peeters (NXP Semiconductors) for detailed feedback on the Mextram documentation and the Verilog-A implementation,

– Geoffrey Coram (Analog Devices) for continued discussions on Verilog-A implementation matters,

– Paul Humphries (Analog Devices Inc.) for fruitful discussions,

– Colin McAndrew (Freescale), Rob Jones (IBM), Teresa Cruz Ravelo (NXP Semiconductors), Rick Poore (Agilent), Doug Weiser (Texas Instruments Inc.) and Jos Dohmen (NXP) for advice on development of Mextram support for the CMC QA toolkit, and vice versa,

June 2009, RvdT.

At Delft University, the following have contributed to the development of the Mextram model as a student and member of the Mextram development team:

- Vladimir Milovanovic [31]
- Daniel Vidal

January 2010, RvdT.

References

[1] For the most recent model descriptions, source code, and documentation, see the web-site www.nxp.com/models.

[2] J. C. J. Paasschens, W. J. Kloosterman, and R. van der Toorn, "Model derivation of Mextram 504. The physics behind the model," Unclassified Report NL-UR 2002/806, Philips Nat.Lab., 2002. See Ref. [1].

[3] J. C. J. Paasschens, W. J. Kloosterman, and R. J. Havens, "Parameter extraction for the bipolar transistor model Mextram, level 504," Unclassified Report NL-UR 2001/801, Philips Nat.Lab., 2001. See Ref. [1].

[4] J. C. J. Paasschens and R. van der Toorn, "Introduction to and usage of the bipolar transistor model Mextram," Unclassified Report NL-UR 2002/823, Philips Nat.Lab., 2002. See Ref. [1].

[5] H. K. Gummel and H. C. Poon, "An integral charge control model of bipolar transistors," *Bell Sys. Techn. J.*, vol. May-June, pp. 827–852, 1970.

[6] J. L. Moll and I. M. Ross, "The dependence of transistor parameters on the distribution of base layer resistivity," *Proc. IRE*, vol. 44, pp. 72–78, Jan. 1956.

[7] H. K. Gummel, "A charge control relation for bipolar transistors," *Bell Sys. Techn. J.*, vol. January, pp. 115–120, 1970.

[8] The term 'integral charge control model' was introduced by Gummel and Poon [5]. Their 'integral' means the combination of Gummel's new charge control relation [7] and conventional charge control theory, such "that parameters for the ac response also shape the dc characteristics" [5]. Unfortunately, nowadays the term 'integral charge control relation' (ICCR) is used to refer to Gummel's new charge control relation only, and not to the model by Gummel and Poon.

[9] E. O. Kane, "Theory of tunneling," *Journal of Applied Physics*, vol. 32, pp. 83–91, January 1961.

[10] G. A. M. Hurkx, "On the modelling of tunneling currents in reverse-biased p-n junctions," *Solid-State Electronics*, vol. 32, no. 8, pp. 665–668, 1989.

[11] J. L. Moll, *Physics of Semiconductors*. New York: McGraw-Hill, 1964.

[12] A. J. Scholten, G. D. Smit, M. Durand, R. van Langevelde, and D. B. Klaassen, "The physical background of JUNCAP2," *IEEE Trans. Elec. Dev.*, vol. 53, pp. 2098–2107, September 2006.

[13] M. P. J. G. Versleijen, "Distributed high frequency effects in bipolar transistors," in *Proc. of the Bipolar Circuits and Technology Meeting*, pp. 85–88, 1991.

[14] G. M. Kull, L. W. Nagel, S. Lee, P. Lloyd, E. J. Prendergast, and H. Dirks, "A unified circuit model for bipolar transistors including quasi-saturation effects," *IEEE Trans. Elec. Dev.*, vol. ED-32, no. 6, pp. 1103–1113, 1985.

[15] H. C. de Graaff and W. J. Kloosterman, "Modeling of the collector epilayer of a bipolar transistor in the Mextram model," *IEEE Trans. Elec. Dev.*, vol. ED-42, pp. 274–282, Feb. 1995.

[16] J. C. J. Paasschens, W. J. Kloosterman, R. J. Havens, and H. C. de Graaff, "Improved modeling of ouput conductance and cut-off frequency of bipolar transistors," in *Proc. of the Bipolar Circuits and Technology Meeting*, pp. 62–65, 2000.

[17] J. C. J. Paasschens, W. J. Kloosterman, R. J. Havens, and H. C. de Graaff, "Improved compact modeling of ouput conductance and cutoff frequency of bipolar transistors," *IEEE J. of Solid-State Circuits*, vol. 36, pp. 1390–1398, 2001.

[18] W. J. Kloosterman and H. C. de Graaff, "Avalanche multiplication in a compact bipolar transistor model for circuit simulation," *IEEE Trans. Elec. Dev.*, vol. ED-36, pp. 1376–1380, 1989.

[19] W. J. Kloosterman, J. C. J. Paasschens, and R. J. Havens, "A comprehensive bipolar avalanche multiplication compact model for circuit simulation," in *Proc. of the Bipolar Circuits and Technology Meeting*, pp. 172–175, 2000.

[20] A. G. Chynoweth, "Ionization rates for electrons and holes in silicon," *Physical Review*, vol. 109, pp. 1537–1540, 1958.

[21] R. van der Toorn, J. J. Dohmen, and O. Hubert, "Distribution of the collector resistance of planar bipolar transistors: Impact on small signal characteristics and compact modelling," in *Proc. Bipolar/BiCMOS Circuits and Technology Meeting*, no. 07CH37879, pp. 184–187, IEEE, 2007.

[22] J. C. J. Paasschens, S. Harmsma, and R. van der Toorn, "Dependence of thermal resistance on ambient and actual temperature," in *Proc. of the Bipolar Circuits and Technology Meeting*, pp. 96–99, 2004.

[23] J. C. J. Paasschens, "Compact modeling of the noise of a bipolar transistor under DC and AC current crowding conditions," *IEEE Trans. Elec. Dev.*, vol. 51, pp. 1483–1495, 2004.

[24] H. C. de Graaff, W. J. Kloosterman, J. A. M. Geelen, and M. C. A. M. Koolen, "Experience with the new compact Mextram model for bipolar transistors," in *Proc. of the Bipolar Circuits and Technology Meeting*, pp. 246–249, 1989.

[25] J. C. J. Paasschens and R. de Kort, "Modelling the excess noise due to avalanche multiplication in (heterojunction) bipolar transistors," in *Proc. of the Bipolar Circuits and Technology Meeting*, pp. 108–111, 2004.

[26] W. J. Kloosterman, J. A. M. Geelen, and D. B. M. Klaassen, "Efficient parameter extraction for the Mextram model," in *Proc. of the Bipolar Circuits and Technology Meeting*, pp. 70–73, 1995.

[27] W. J. Kloosterman, J. C. J. Paasschens, and D. B. M. Klaassen, "Improved extraction of base and emitter resistance from small signal high frequency admittance measurements," in *Proc. of the Bipolar Circuits and Technology Meeting*, pp. 93–96, 1999.

[28] J. C. J. Paasschens, "Usage of thermal networks of compact models. Some tips for non-specialists," Technical Note PR-TN 2004/00528, Philips Nat.Lab., 2004.

[29] V. Palankovski, R. Schultheis, and S. Selberherr, "Simulation of power heterojunction bipolar transistor on gallium arsenide," *IEEE Trans. Elec. Dev.*, vol. 48, pp. 1264–1269, 2001. Note: the paper uses $\alpha = 1.65$ for Si, but $\alpha = 1.3$ gives a better fit; also, κ_{300} for GaAs is closer to 40 than to the published value of 46 (Palankovski, personal communication).

[30] S. M. Sze, *Physics of Semiconductor Devices*. Wiley, New York, 2 ed., 1981.

[31] V. Milovanovic, R. van der Toorn, P. Humphries, D. P. Vidal, and A. Vafanejad, "Compact model of zener tunneling current in bipolar transistors featuring a smooth transistion to zero forward bias current," in *Proc. of the Bipolar Circuits and Technology Meeting*, IEEE, 2009.

